ASPECTS OF LAMINAR FREE CONVECTION FROM A VERTICAL PLATE

A T H E S I S

-by-

J. GRYZAGORIDIS (BSc., MSc., Pr. Eng..)

Submitted to the Department of Mechanical Engineering of the University of CapeTown as the requirement for the degree of

Doctor of Philosophy

1972.

ACKNOWLEDGEMENTS

The author wishes to thank the many people who assisted in this study.

The physical labours of Mr. W.K. Bettesworth, M.A. Bettesworth, J. Busbridge, J.R. Gordon, in the construction of the apparatus, are greatly appreciated.

Thanks are extended to Mr. R.M. Stegen, Dr. C.P. Burger, Dr. J.B. Thuren, and Professor P. Metcalf, for their patience and advice during the course of this study.

Special thanks are extended to Dr. W.P. Boyle for his invaluable advice, patience and understanding in his capacity as supervisor of this thesis.

The financial assistance of the University of Cape Town Staff Research Fund is gratefully acknowledged, as is the assistance with typing given by Mrs. L.E. Edwards.

- ABSTRACT -

The thesis is comprised of a number of aspects pertaining to the phenomenon of laminar free convection from a vertical plate. A survey of literature is presented which brings out the fact, that the phenomenon although it has been investigated to a large extent, still gives rise to widespread dispute and uncertainties which need careful examination.

An analytical approach is presented showing that the hydrodynamic boundary layer is equal to the thermal boundary layer. In the past it was simply assumed to be so, in order to limit the computations, and the assumption was justified by the excellent agreement between calculations and experimental data.

An analysis is presented showing the analogy existing between the Grashof and Reynolds numbers, as it is expected in the case of low velocities and considerable temperature differences. i.e. in free convection.

An extensive experimental investigation pertaining to average heat transfer rates from a vertical plate at low Grashof numbers is presented and provides the necessary evidence in a much disputed region. It is shown conclusively that as far as average heat transfer rates are concerned, the agreement with the already accepted relationship can be extended to Grashof numbers as low as 10.

The author's feelings that the Nusselt-Grashof numbers relationship for local heat rates, near the leading edge, is not universal, have been proven correct by the results obtained in a further experimental investigation. This aspect has also been a point of dispute by various investigators as it is evident from the

literature/ .....

literature survey.

An analytical approach covering the aspect of non-uniform temperature plate and its effects on the temperature profiles and boundary layer is presented, indicating that the temperature profiles are similar to those for a uniform temperature plate and that the boundary layer thickness is still proportional to the distance from the leading edge of the plate, raised to the quarter power. These conclusions are substantiated by data that the author has obtained by experiment.

Finally, a novel approach to convective phenomena is presented. The convective process is related to a diffusion process and thus examined in a microscopic scale. This approach, rather new in the field of convective heat transfer, does not replace any of the existing theories or methods, however it does enrich our knowledge of the phenomenon, by yielding expressions for the Buoyancy Diffusion Coefficient, buoyancy force and acceleration. An experimental investigation has shown that the use of the Buoyancy Diffusion Coefficient near the surface of a vertical plate yielded correct heat transfer rates as predicted by the existing theories.

In summary, the author, by presenting this thesis is claiming the following contributions to the field of free-convective heat transfer from a vertical plate:

i. Proof that the thermal boundary layer is <u>equal</u> to the hydrodynamic one.

ii. Proof that in the case of free convection from a vertical plate there exists an analogy between the Grashof and Reynolds numbers. That the condition of $Re^2 = C\ Gr$ <u>is satisfied</u> and using the existing solution for the velocity profiles, which have been verified by experiment, it was

possible to/ .....

possible to solve for the Constant C.

iii. Experimental data extending the validity of the existing relationship for average heat transfer rates in a disputed region, i.e. at low Grashof numbers.

iv. Experimental evidence that the Grashof-Nusselt numbers relationship is not universal near the leading edge of a vertical plate.

v. An analytical investigation supported by experimental data dealing with the effects of variable plate temperature on the boundary layer and temperature profiles. The results of these are at variance with previous investigations.

vi. A novel approach to convective phenomena which although not replacing the existing theories, does enrich our knowledge. Furthermore the derivation of the Buoyancy Diffusion Coefficient using Brownian motion theory, is verified by experiment.

TABLE OF CONTENTS

Page

Nomenclature 1

Preface 4

Chapter I.

Survey of previous investigations of free convection from a vertical plate 7

Chapter II.

Theoretical Background:

a - Boundary layer considerations 24

b - Analogy between forced and free convection 36

c - A note on the equation of motion for natural convection from a vertical plate 40

d - The effect of variable wall temperature on the boundary layer of a vertical plate 43

e - Buoyancy Diffusion Coefficient 46

Chapter III.

Experimental Apparatus, Instrumentation and Procedure in obtaining average heat transfer rates at low Grashof numbers 50

Chapter IV.

Results of the investigation for average heat transfer rates at low Grashof numbers 64

Chapter V.

Experimental Apparatus, Instrumentation, Procedure and Results of the investigation for local heat rates near the leading edge of a vertical plate 82

Chapter VI.

Experimental Apparatus, Instrumentation, Procedure and Results of the investigation for the effects of variable wall temperature on the boundary layer of a vertical plate 96

Chapter VII.

Application of the Buoyancy Diffusion Coefficient 110

Chapter VIII/ .....

Chapter VIII. Page

Discussion and Conclusions.

1. On the Order of Magnitude of δ and δ_T 116

2. On the Analogy with Forced Convection..... 117

3. On the Average Heat Transfer Rates at Low Grashof Numbers 118

4. On the Local Heat Transfer Rates near the Leading Edge 121

5. On the Effects of Variable Wall Temperature on the Boundary Layer 122

6. On the Buoyancy Diffusion Coefficient 125

Appendix A.

Dimensional Analysis of Properties 131

Appendix B.

Emissivity 138

Appendix C.

Sample Calculations and Selected Data 142

References 149

NOMENCLATURE

Symbol	Description	Units
A	Plate's surface area.	ft^2
C_p	Specific heat at constant pressure.	$Btu/lbm\,^oF$
g	Local acceleration of gravity.	ft/sec^2.
Gr_x	Local Grashof number $(\rho^2 \frac{\beta g \Delta T x^3}{\mu^2})$	Dimensionless.
$\overline{Gr}_L$	Grashof number based on the plate's height. $(\rho^2 \frac{\beta g \Delta T L^3}{\mu^2})$	Dimensionless.
h_c	Local free-convective heat transfer coefficient.	$Btu/hr\ ft^2\ ^oF$
$\overline{h}_c$	Average free convective heat transfer coefficient.	$Btu/hr\ ft^2\ ^oF$
h_r	Radiation heat transfer coefficient.	$Btu/hr\ ft^2\ ^oF$
k	Thermal conductivity of the fluid.	$Btu/hr\ ft\ ^oF$
L	Characteristic dimension of the vertical plate (height)	ft
m,n,p,r	Denote exponent	Dimensionless
Nu_x	Local Nusselt number $(\frac{h_c x}{k})$	Dimensionless
$\overline{Nu}$	Average Nusselt number $(\frac{h_c L}{k})$	Dimensionless
P	Pressure of the fluid	lbf/ft^2
Pr	Prandtl number $(\frac{C_p \mu}{k})$	Dimensionless
Q_{net}	Net heat transfer rate between a hot body and a fluid	Btu/hr
Q_c	Heat transfer by convection	Btu/hr

Q_r/ .....

Symbol	Description	Units
Q_r	Heat transfer by radiation	Btu/hr
R	Ideal gas constant	ft lbf/lbm ^{o}R
T_f	Film temperature	^{o}F or ^{o}R
T_r	Reference temperature	^{o}F or ^{o}R
T_w	Temperature of the plate	^{o}F or ^{o}R
T_∞	Bulk fluid temperature	^{o}F or ^{o}R
T_c	Temperature of the chamber walls	^{o}R
u	Combined unit surface conductance	Btu/hr ft^2 ^{o}F
U	Fluid velocity in the x direction	ft/sec.
v	Fluid velocity in the y direction	ft/sec.
x	Distance along the height of the plate	ft.
y	Distance perpendicular to the plate	ft.

GREEK SYMBOLS

Symbol	Description	Units
α	Thermal diffusivity, $\frac{k}{\rho C_p}$	ft^2/hr
β	Temperature coefficient of volume expansion.	$1/{}^{o}R$
δ	Hydrodynamic Boundary layer thickness.	ft.
δ_t	Thermal Boundary layer thickness.	ft.
ϵ	Emissivity.	Dimensionless
η	Similarity variable.	Dimensionless
θ	Temperature difference. $(T-T_\infty)$	${}^{o}F$
λ	Ratio of thermal to hydrodynamic Boundary layer thickness.	Dimensionless
μ	Absolute viscosity.	lbm/ft.sec.
ν	Kinematic viscosity.	$ft^2/sec.$
ρ	Mass density.	lbm/ft^3.
σ	Stefan-Boltzman constant.	Btu/hr $ft^2 {}^{o}R^4$.
τ_w	Shear stress at the wall.	lbf/ft^2.

∂	Denotes partial differential.

ASPECTS OF LAMINAR FREE CONVECTION FROM A VERTICAL PLATE

PREFACE

Free - or natural - convection flow arises, for instance, when a heated object is placed in a fluid which is at rest, and the density of which varies with temperature.

The transfer of heat between the solid boundary and the fluid takes place by a combination of conduction and mass transport induced by the resulting density gradients. If the boundary is at a temperature higher than that of the fluid, heat flows first by conduction from the solid to the fluid. The internal energy of the fluid is increased, decreasing the density of the fluid, and is carried away by the resulting motion.

From a survey of the literature, it is evident that many experimentors have studied the phenomenon of heat transfer by free convection from cylinders, spheres and flat plates. These are relatively simple geometries with which to work, and the fact that spheres <u>are</u> geometrically similar - as, for all practical purposes, are long cylinders also - has aided the correlation of data from different sources.

However, in the case of flat plates which are not inherently geometrically similar, the work has not been sufficiently complete or well enough organized to permit very extensive or general correlation, although some progress has been made recently in that direction.

There are four general methods for the evaluation of convective heat transfer:

i. Experiments, with procedure organized by techniques of dimensional analysis.

ii/ .....

ii. Exact mathematical solution of the boundary layer equations.

iii. Approximate analysis of the boundary layer by integral methods.

iv. The analogy between heat-mass and momentum transfer.

Each of the above-mentioned methods has its merits when dealing with different aspects of the phenomenon of free convection from a vertical flat plate, however none is sufficiently general to cover all the aspects with sufficient and accurate information.

It will be shown later that experimentors need to be familiar with all these methods in order to cover a variety of aspects of the phenomenon.

For example, dimensional analysis is particularly useful in those cases in which the exact differential expression of the physical laws involved or the solutions of such expressions are not known. With a little effort a partial solution to nearly any problem is obtained. On the other hand a complete solution is not obtained, nor is the inner mechanism of a phenomenon revealed.

Of course the analytical methods of approach are particularly attractive to experimentors. Using a differential control volume the equations of motion and heat transfer can be derived, describing the process at any point in the boundary layer; knowing the physical boundary conditions and employing similarity variables these partial differential equations may be transformed to ordinary differential equations and thus obtain a solution. However it is not always possible to apply a similarity variable, in which case the solution of these partial differential equations becomes extremely difficult.

In order/ .....

In order to circumvent these difficulties an approximate analysis which simplifies the mathematical manipulations can be employed. This involves writing the differential equations for a fixed control volume or aggregate of particles in the boundary layer, known as integral methods. In cases where exact solutions are available, they agree with satisfactory accuracy with the solution obtained by the approximate method.

Finally, the similarities in the differential equations for momentum, energy and mass transfer have permitted the prediction of solutions among transfer phenomena for which limited quantitative data are available. This method renders itself particularly useful in the case of turbulent flow.

This investigation deals with a number of aspects of the phenomenon of laminar free-convection from a vertical plate which have either received very little attention, are under dispute or have not been investigated conclusively.

/ .....

CHAPTER I.

A survey of Previous Investigations into the Free Convection From a Vertical Flat Plate.

A survey of the heat transfer literature has shown that the phenomenon of free-convection from a vertical plate has been investigated both analytically and experimentally.

Students of heat transfer and practising engineers are presented with the empirical relationship

$$\overline{Nu} = 0.555\ (Gr.Pr.)^{\frac{1}{4}} \qquad (1.1)$$

which is a power-law that best fits the experimental data gathered through the years. Textbooks such as Kreith's [1] and Schlichting's [2] present equation 1.1, which is widely accepted as universal for the range of $10^5 < Gr.Pr. < 10^9$. Still another expression is given by Boelter [3]

$$\overline{Nu} = 0.600\ (Gr.Pr.)^{\frac{1}{4}} \qquad (1.1a)$$

as being an approximate solution. However below the range of $Gr.Pr. = 10^5$ this power-law relationship is widely disputed by a number of investigators, [4] [5] [6] [7].

Equation 1.1 is in very good agreement with the solution of the boundary layer equation governing the phenomenon of free convection from a vertical plate, however the solution is only valid in the immediate vicinity of a semi-infinite surface, that is, when boundary layer flow is exhibited, and for large Grashof numbers. For finite and moderate Grashof values it appears that some refinements should be made to the boundary layer solution. In subsequent paragraphs some attempts to refine the boundary layer solution by other investigators will be presented.

Some Aspects/ .....

Some Aspects of the Phenomenon of Free Convection from a Vertical Flat Plate.

a. Velocity and Temperature Distributions.

One of the most significant contributions to the problem of laminar free convection from a heated vertical plate comes from E. Pohlhausen [8] who in 1921 solved for the velocity and temperature distributions from the continuity, hydrodynamic, and conduction equations. (See fig. 1.1 and 1.2)

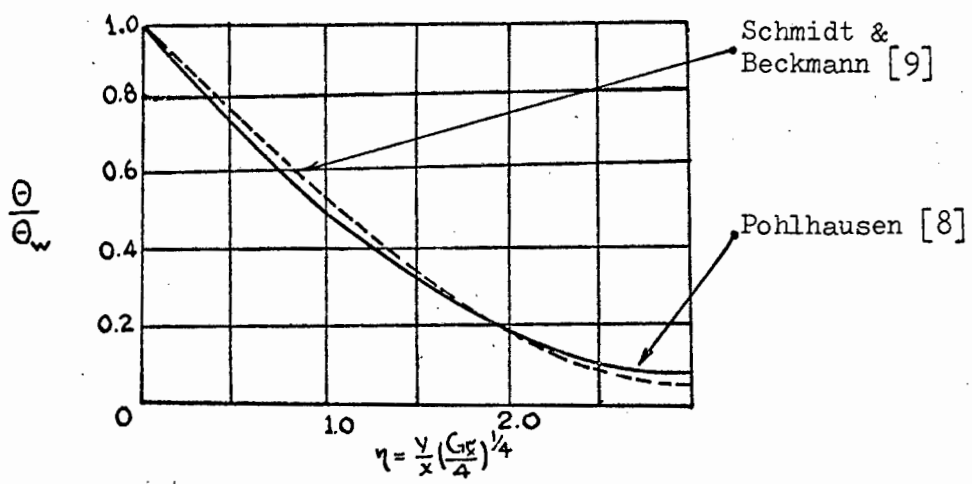

Fig. 1.1 Temperature Profiles (from [2]).

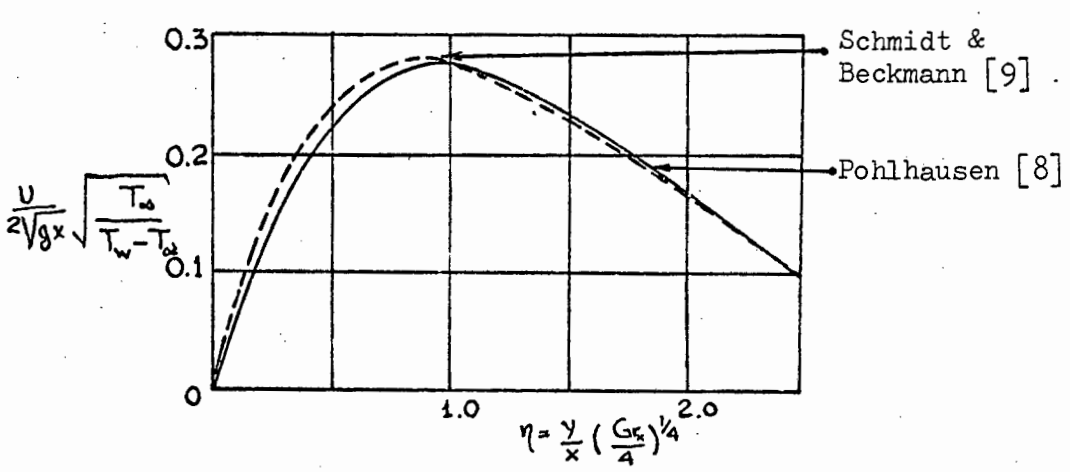

Fig. 1.2 Velocity Profiles (from [2]).

In 1930 E. Schmidt and W. Beckmann [9] carried out experiments measuring the velocity and temperature profiles in the boundary layer of a vertical heated plate, and their data is in excellent agreement with the theoretical solutions by Pohlhausen [8].

(See Figures/ .....

(see Figures 1.1 and 1.2). They also derived analytically an expression for local Nusselt numbers

$$Nu_x = 0.360\ (Gr_x)^{\frac{1}{4}} \qquad (1.2)$$

for air having a Prandtl number of 0.74.

The above expression when integrated over the entire length of the plate, yields an average Nusselt number of

$$\overline{Nu} = 0.516\ (Gr.Pr.)^{\frac{1}{4}} \qquad (1.3)$$

which is in very good agreement with the empirical power-law relationship (Eq. 1.1).

b. Uniform heat flux and uniform wall temperature.

The heated vertical surface has been assumed as being at uniform temperature. This assumption is not valid of course, because as the boundary layer grows proportionally to the length of the plate the resistance to heat flow increases; consequently the early part of the plate will be at a lower temperature than the latter. In other words physically there is a temperature gradient along the height of the plate. If conditions of uniform wall temperature are assumed, when the plate is electrically heated, a representative temperature of the surface of the plate must be determined in order to evaluate an average Nusselt number.

In 1956 a theoretical analysis by Sparrow and Gregg [10] yielded a solution of the boundary layer equations for a vertical plate having uniform heat flux. Their results show that when an average Nusselt number is calculated for a plate with uniform heat flux using the temperature difference halfway along the height, the results are remarkably close to those obtained when using a uniform temperature plate. For the range $0.1 > Pr > 100$ the ratio of Nusselt numbers calculated using uniform heat flux to the ones using uniform wall temperature was on the average 1.1.

c. Representative/ ...

c. Representative temperature level inside the boundary layer.

Previous investigators have used the properties involved in dimensionless parameters, evaluated at the plate's surface temperature, the bulk fluid temperature, or the film temperature defined as

$$T_f = 0.5\ (T_w + T_\infty) \qquad (1.4)$$

the latter being most widely used.

The above-mentioned representative temperatures have been chosen arbitrarily, that is, without any analysis of the variation of properties within the boundary layer. However, in 1961 Sparrow and Gregg [11] recommended a representative temperature rule given by

$$T_r = T_w - 0.38\ (T_w - T_\infty) \qquad (1.5)$$

which is based on a variable property analysis and on the comparison to constant property solutions. The error in the heat transfer rate predicted from the constant property solution by using a representative temperature given by equation (1.5) is at the most 0.6 per cent over the entire range $\frac{1}{4} < \frac{T_w}{T_\infty} < 4$. It is also indicated that when an ideal gas is assumed the coefficient of thermal expansion (β) should be taken at the bulk fluid temperature (T_∞).

d. The effect of enclosure around a vertical heated plate.

In order to investigate a wide range of Grashof numbers, when dealing with a gas such as air, the variation is sought by manipulating three of the variables appearing in the Grashof number

$$Gr = \rho^2\ \frac{\beta g\ \Delta T\ L^3}{\mu^2}$$

that is, the density of the fluid, the temperature difference between the plate and the fluid or the plate's length. At low Grashof numbers the thermal boundary layer thickness on the plate

increases/ .....

increases considerably. Pohlhausen [8] was the first one to indicate this aspect, and in 1957 J.J. Mahoney [12] performed a mathematical analysis using a three-dimensional boundary layer, showing that while convection is negligible in comparison with conduction near the body at very low Grashof numbers, it becomes as important at distances from the body of the order of Gr^{-n} where n varies between $\frac{1}{3}$ and $\frac{1}{4}$ with the body shape. Whenever the size of the thermal boundary layer thickness is large in comparison with all the dimensions of the body the use of the conduction equation yields correct heat transfer rates. If however the boundary layer thickness is small compared to the body dimensions the heat transfer is adequately calculated from the two-dimensional convection solution. It has been shown [8] [12] that the boundary layer thickness increases considerably at small Grashof numbers, and if a large variation of the Grashof number is sought an enclosure must be employed, where the pressure can be manipulated thus changing the fluid's density. Care should be taken that there should be no interference of the boundary layer with the surface of the enclosure. For the same reason care should be taken when determining the bulk fluid's temperature, ensuring that the measuring device is not within the boundary layer.

e. <u>The effects of slip on the laminar free-convective flow</u>.

Seeking variation of the Grashof number in the low range through density changes, low pressures are employed. When the pressure is very low it cannot be assumed that when the fluid flows over a body it attains, at the body surface, the local velocity and temperature of the body, and slip flow may then exist. In 1965 P.H. Oosthuizen [13] devised a method which attempted to predict approximately the effects of very small amounts of slip on laminar free convective flow over a vertical plate,

the main/ ....

the main aim being to try to indicate the circumstances under which slip effects become appreciable. Rather than predicting very accurately the magnitude of these effects he was able to show departure from the boundary layer solution, that is from his analysis, the predicted Nusselt numbers fall below those indicated by the power-law relationship equation (1.1).

f. Attempts to refine the boundary layer solution.

The first attempt to refine the boundary layer solution appears in a paper by Yang and Jerger [4]. In a perturbation analysis carried only to first order, they show departure from the classical solution as indicated in Fig. (1.3) Although they show good agreement in the velocity distribution with Schmidt and Beckmann [9] their predicted Nusselt numbers fall below those of the classical solution. The reason for this discrepancy lies in the fact that Yang and Jerger [4] have failed to take into account the effect ahead of the leading edge of the plate. In 1965 Suriano, Yang and Donlon [5] in another theoretical investigation introduced the leading edge effects. Their argument was that the pressure in the vicinity of the leading edge of the plate is less than the bulk fluid's pressure. This will induce a flow field outside the leading edge of the boundary layer producing higher energy transport rate and consequently higher Nusselt numbers than those predicted by Yang and Jerger [4].

They [5] performed a perturbation analysis with the Grashof number itself taken as the perturbation parameter and produced results tending towards Nusselt numbers as shown in Figure (1.3).

In contrast to the above-mentioned perturbation solution in 1968 W.T. Kierkus [14] performed a

perturbation/ .....

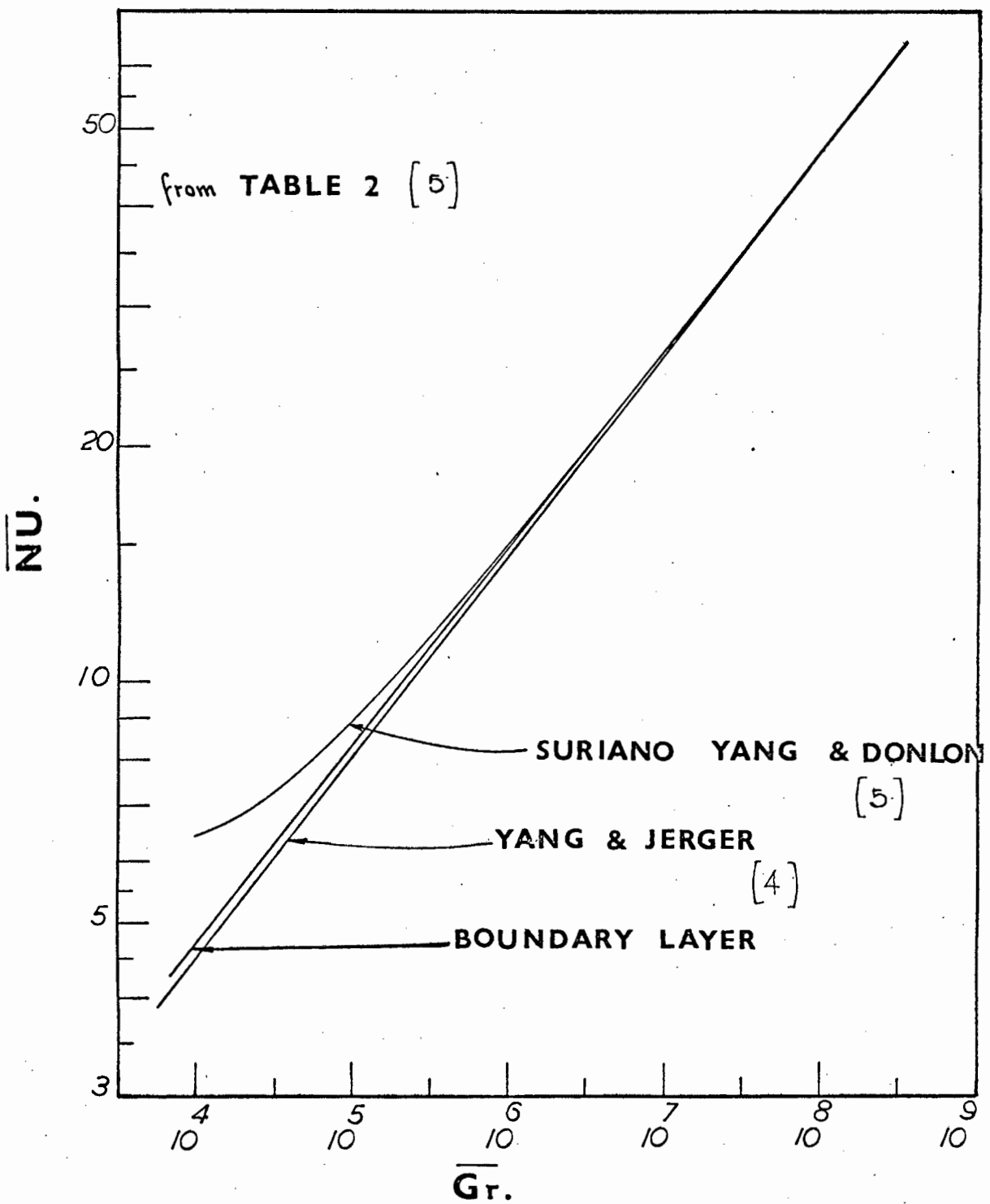
50
20
10
5
3
$\overline{NU}$.
from TABLE 2 [5]
SURIANO YANG & DONLON
[5]
YANG & JERGER
[4]
BOUNDARY LAYER
10^4
10^5
10^6
10^7
10^8
10^9
$\overline{Gr}$.

FIGURE 1-3

perturbation analysis for two dimensional laminar free-convection about an inclined isothermal plate, for angles of 0, $\pm$ 15°, $\pm$ 30°, $\pm$ 45°, using the classical boundary layer solution as the zeroeth order approximation. Both velocity and temperature distributions for Prandtl number of 0.7 are in very good agreement with Schmidt and Beckmann [9] (see Figure 1.4).

Suriano and Yang [6] in 1968 presented another attempt to refine the boundary layer solution for low Grashof numbers using a finite difference scheme, solving the hydrodynamic and energy equations for steady laminar free convection about a heated isothermal vertical plate. They stated that in the low Grashof number range the energy transfer is predominately by heat conduction; while convection prevails in the upper range. They presented a table of their results for Prandtl number of 0.72 and compared them with existing data. (See Fig 1.5).

g. Experimental data.

Detailed experimental data for the entire range of Grashof numbers were presented in 1936 by O.A. Saunders [7] who, employing a vacuum chamber where the density of the air could be reduced, was able to reach very low Grashof numbers. In addition to the vacuum chamber he employed four different plates of 22.9, 7.6, 2.5 and 0.325-cm height. Using the two larger plates he obtained the data for the high Grashof number range where excellent agreement is observed with the power law relationship (Eq.1.1). In contrast when he used the smaller plates a marked departure was observed.

Figure 1.6/ .....

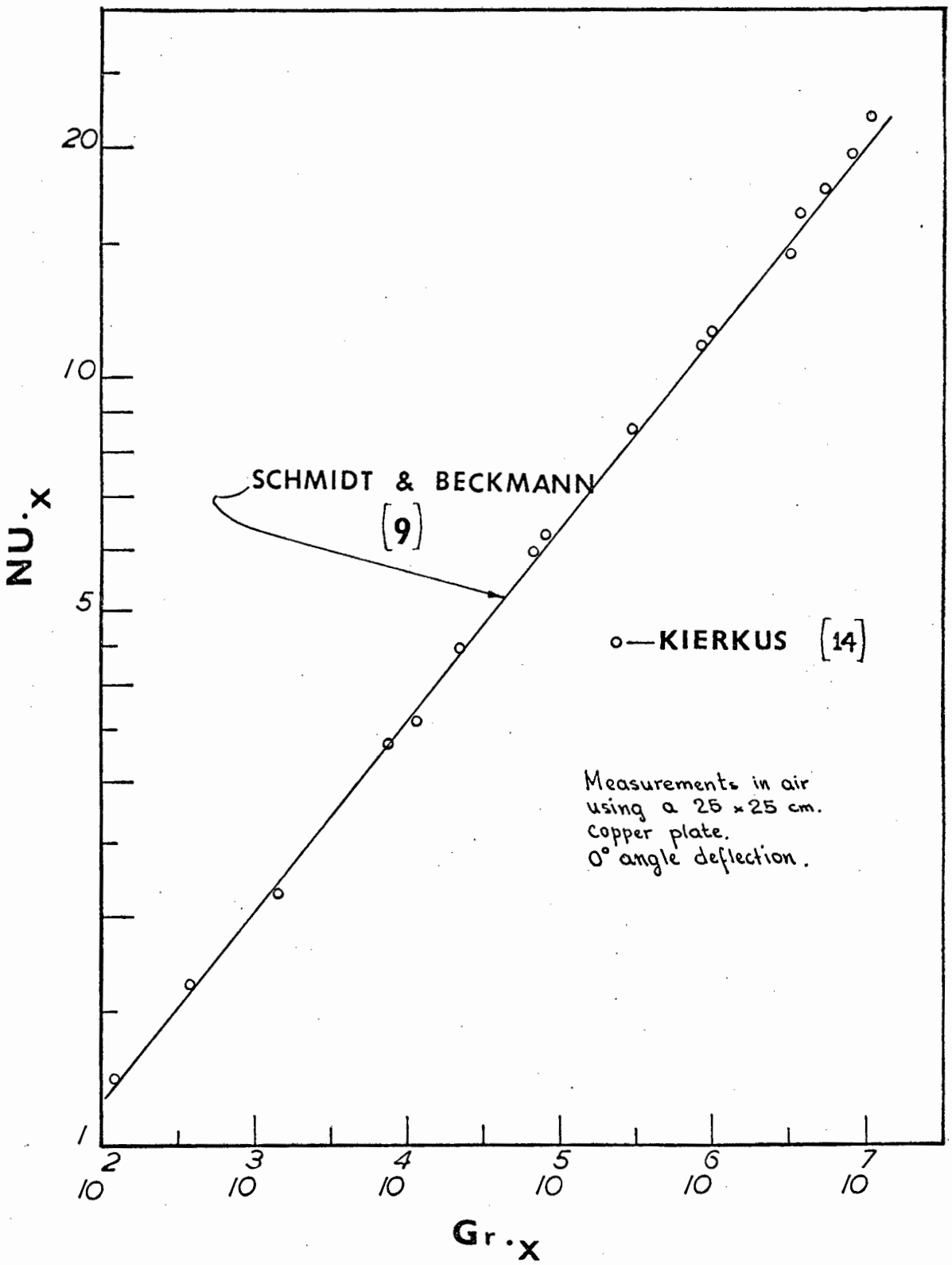
20
10
5
1
NU.x
SCHMIDT & BECKMANN
[9]
o—KIERKUS [14]
Measurements in air
using a 25 x 25 cm.
copper plate.
0° angle deflection.
10^2
10^3
10^4
10^5
10^6
10^7
Gr.x

FIGURE 1-4

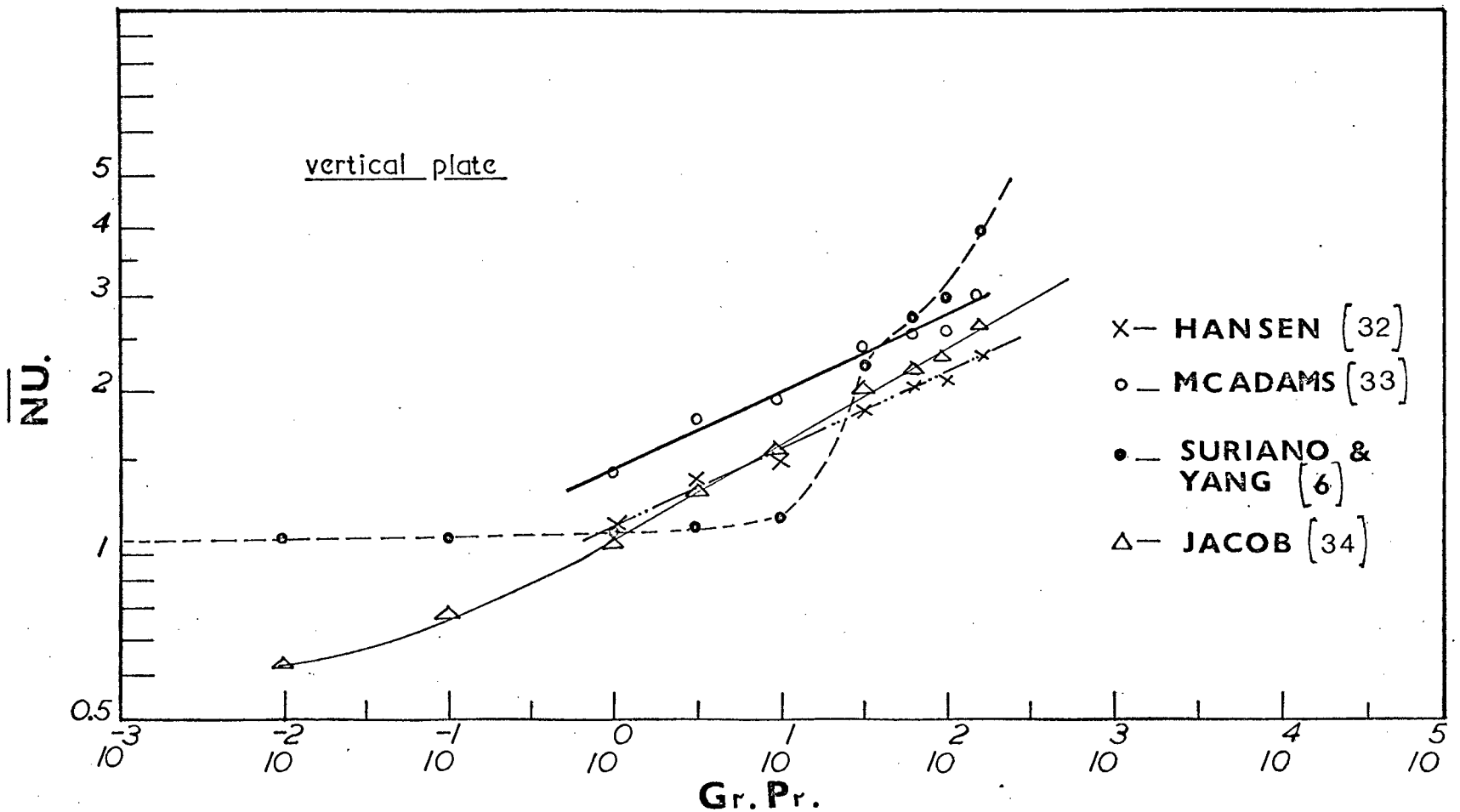
vertical plate
$\overline{Nu}$.
5
4
3
2
1
0.5
10^{-3}
10^{-2}
10^{-1}
10^{0}
10^{1}
10^{2}
10^{3}
10^{4}
10^{5}
Gr. Pr.
X— HANSEN [32]
o— MCADAMS [33]
•— SURIANO & YANG [6]
Δ— JACOB [34]

FIGURE 1-5

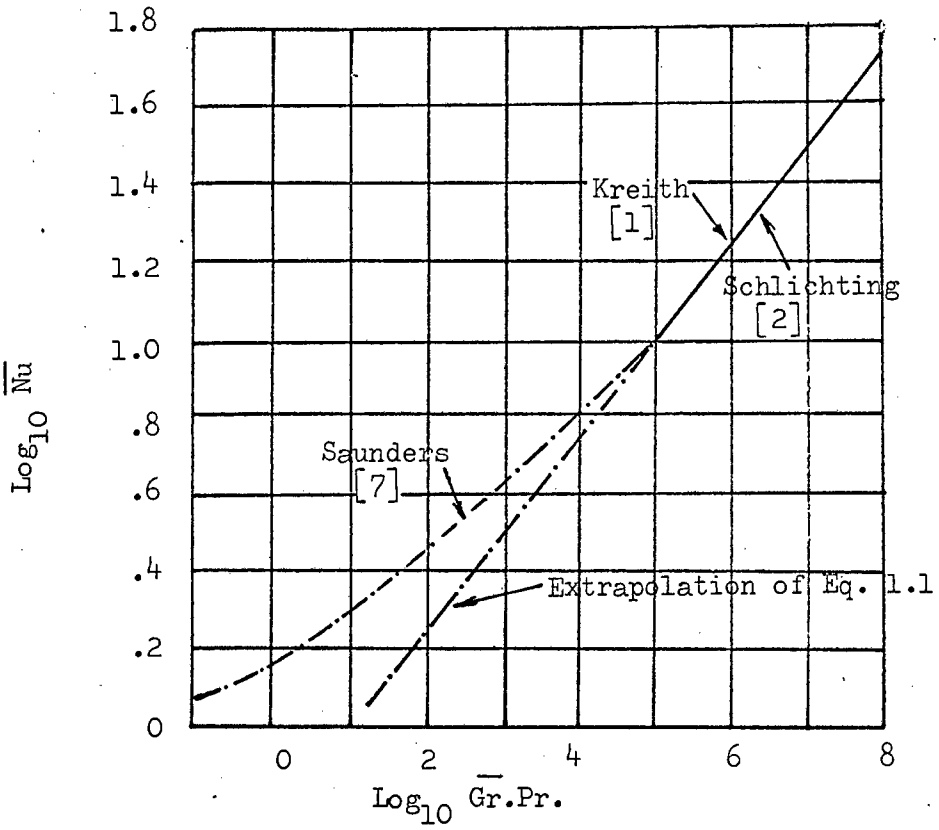

Fig. 1.6 Free Convection from Vertical Plates.

In 1960 Goldstein and Eckert [15] used a Mach-Zehnder interferometer to study the free convective boundary layer about a uniformly heated vertical plate. The experiments were performed when the plate was immersed in water. Their results substantiate the analysis presented by Sparrow and Gregg [10] and extend the range of Grashof numbers down to approximately 10^3 in very good agreement with the power-law relationship. (See Figure 1.7).

In 1966 A.K. Rebrov and N.V Mukhina [16] used the Schlieren technique to photograph the thermal boundary layer near the vertical heated plate for the pressure range of 760 mm Hg to 10 mm Hg. abs. In reporting their findings they stated that the lowest temperature gradients that could be measured decreased proportionally to pressure decrease and the boundary layer thickness found by this optical method was not a physical property of the process, that is the observed boundary layer thickness was less than the actual. Furthermore they reported that in contrast to optical

methods/ ....

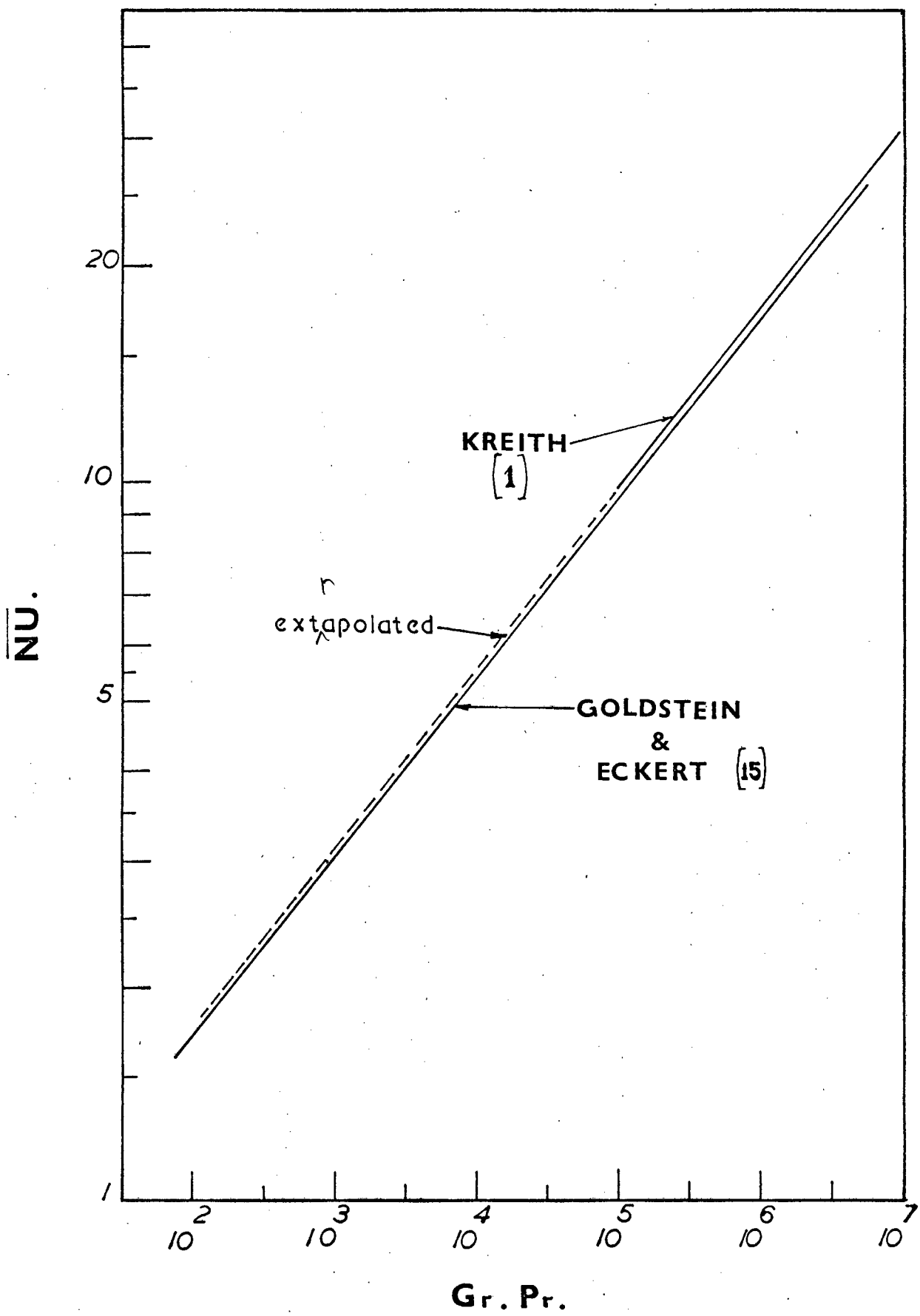
NU.
20
10
5
1
KREITH
[1]
extapolated
GOLDSTEIN
&
ECKERT [15]
10^2
10^3
10^4
10^5
10^6
10^7
Gr. Pr.

FIGURE 1-7

methods, investigation of the boundary layer by means of an assembly of thermocouples still yielded satisfactory results at low Grashof numbers, but they did not report any data. Finally the most recent experimental data were presented by R. Cheesewright [17] in 1968. Reporting on the turbulent region ($Gr.Pr. > 10^8$) in natural convection for a vertical plate, he presented experimental data for local heat transfer rates in the laminar boundary layer ($Gr.Pr. < 10^8$) which are in good agreement with the existing theory. (See Figure 1.8).

Perhaps the best description of the phenomenon of free convection from a vertical plate has come recently from K. Brodowicz [18] who attempted to explain the discrepancies between experimental results and theoretical predictions of the velocity and temperature profiles around a vertical plate. Using a Mach-Zehnder interferometer he obtained interferograms of the phenomenon which enabled him to consider the problem in much wider scope, and subdivide it into several zones.

1. The boundary layer, characterised by the temperature and velocity fields typical of viscous flow, which was further subdivided into:
   (a) the part of the boundary layer near the plate,
   (b) the part of the boundary layer near the leading edge,
   (c) the part of the boundary layer near the trailing edge of the plate.
2. The wake, an area above the trailing edge of the plate.
3. The area beyond the boundary layer zones and in which there is no flow and the temperature is uniform.

He showed that the lack of agreement observed between the accepted boundary layer solution and experimental data is due to

the conditions/ .....

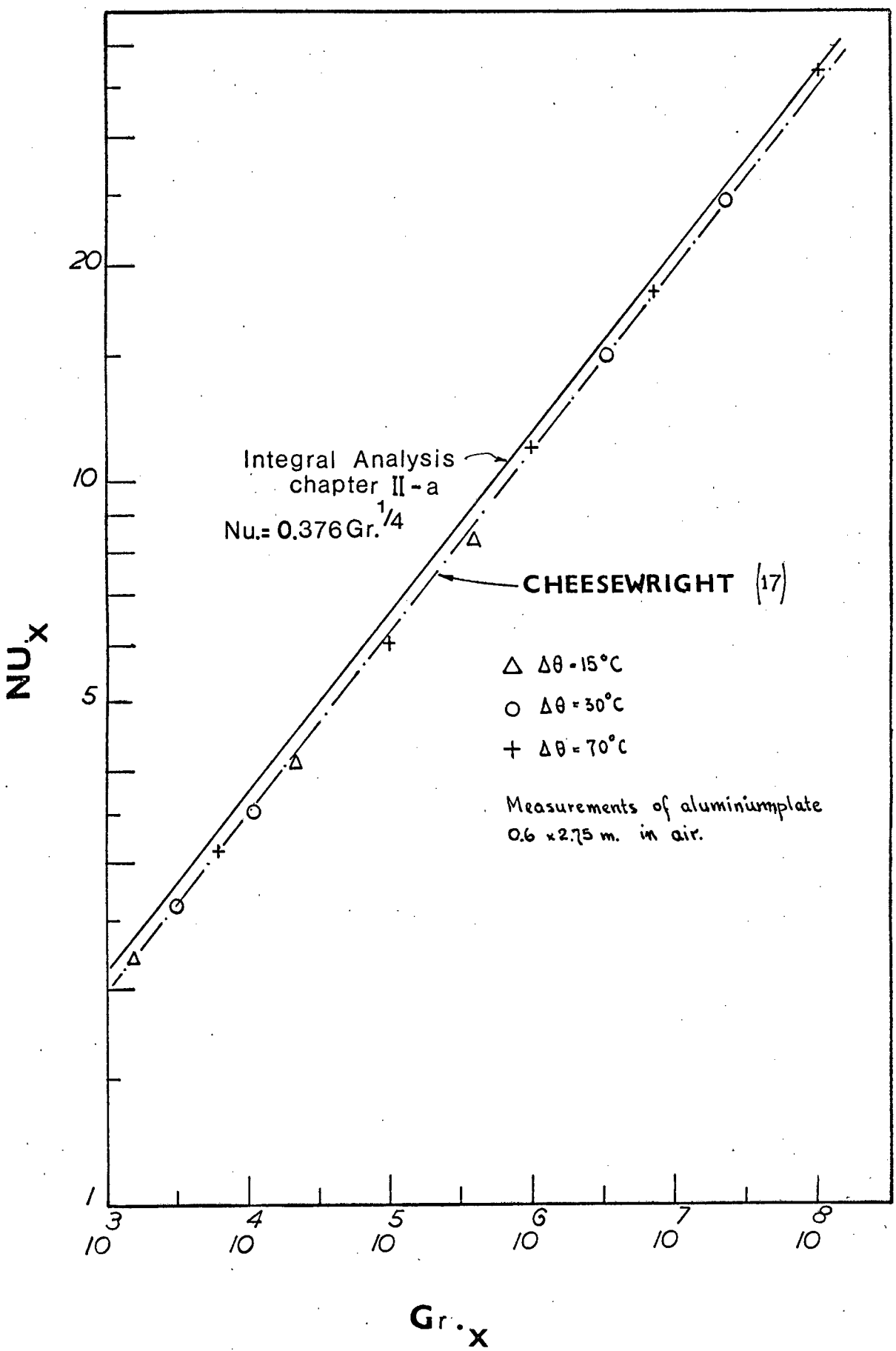
Integral Analysis
chapter II - a
Nu.= 0.376 Gr.^1/4
CHEESEWRIGHT (17)
Δ Δθ = 15°C
○ Δθ = 30°C
+ Δθ = 70°C
Measurements of aluminiumplate
0.6 x 2.75 m. in air.
Nu.x
Gr.x
20
10
5
1
10^3
10^4
10^5
10^6
10^7
10^8

FIGURE 1·8

the conditions under which experiments are run, such as control of the motion, if any, outside the boundary layer, construction of the plate to ensure uniform temperature, and the physical dimensions of the leading edge of the plate.

In summary of what has been presented so far in connection with the phenomenon of free convection from a vertical plate, some of the previous investigations dealt with specific problems and aspects of the process, such as velocity and temperature profile measurements, representative temperatures for the plate and boundary layer, effects of slip, the leading edge effects, etc; while other investigations presented experimental data obtained either by calorimetric or optical techniques. In some instances agreement, in others departure is noted from the classical boundary layer solution.

a - It is reasonable to assume that when the Grashof number is reduced, the convective currents become insignificant and can be neglected, thus allowing the energy to be dissipated by pure conduction alone; but the question remains of how low Grashof numbers can be reached and still have the phenomenon of free convection predicted adequately by equation 1.1. Therefore detailed experimental data in the low Grashof number range is needed in order to establish the region where the pure conduction effects become predominant, and establish the pure "conduction limit".

Saunders [7] data covers the low Grashof number range and has shown departure from the classical solution, (See Figure 1.6), as high as $Gr \simeq 5 \times 10^4$, but more recent data by Goldstein and Eckert [15] and Cheesewright [17] (See Figures 1.7, 1.8), although not reaching as low as Saunders' [7], have not shown any departure from the classical solution.

b - In addition to the pure "Conduction limit" aspect of the natural/.....

natural convection phenomenon there is speculation concerning the leading edge effects on the heat transfer rate. The data that produced the power-law relationship, eq. 1.1 lie approximately 8% higher than the theoretical solution given by Schmidt and Beckmann [9]. This is to be expected since the experimental data have been collected using vertical plates with a free leading edge, while Schmidt and Beckmann's [9] solution is based on a vertical flat plate with a boundary extending perpendicular to the leading edge. Without a free leading edge to induce a flow ahead of the plate the resistance to heat flow increases and consequently lower Nusselt numbers are predicted.

Furthermore, most experimentors take the liberty to transform local heat transfer values to average values by integrating over the entire length of the vertical plate. The author's feelings are, that the problem of the range of applicability of boundary layer concepts is perhaps significantly different for local data and for overall data near the leading edge, and proposes to investigate along these lines.

c - Schlichting [2] has indicated a relationship between the Grashof and Reynolds numbers existing when small velocities are involved, coupled with large temperature differences. This suggests the possibility of an analogy between forced convection on a flat plate and free convection from a vertical heated surface. In free convection the density changes give rise to a velocity in the boundary layer. It is surprising that dimensional considerations do not indicate any dependence on this "induced velocity", but the author feels that since there is a velocity distribution within a boundary layer, a relationship exists between the Reynolds number used in the laminar forced convection equation, and the Grashof number used in the laminar free convection.

d - / .....

d - There is no evidence of experimental data for a plate in free convection subject to an arbitrary variable wall temperature distribution. The question here is, what effect does a variable wall temperature have on the boundary layer of a vertical plate in free convection?

The author proposes to investigate along these lines.

e - It was mentioned in the preface that there are four general methods for the evaluation of convective heat transfer but all of them deal on a macroscopic scale. The author proposes to investigate the problem microscopically. In other words, since the fluid particles exhibit Brownian motion, using Langevin's equation an attempt will be made to evaluate a buoyancy diffusion coefficient and consequently evaluate the energy transported by the fluid's molecules. This will involve the solution of a stochastic differential equation which is not the same thing as solving ordinary differential equations, but rather specifying a probability distribution for the velocity and position of the molecules. Such an approach is rather new in the field of convective heat transfer.

The points raised above in a, b, c, d and e provided the incentive for this investigation which led to what is described in the following chapters.

CHAPTER II

THEORETICAL BACKGROUND

a. Boundary Layer Considerations.

An analytical approach follows utilizing the Von Karman method [19] . The author does not claim originality of applying this method since it is one of the accepted methods of investigating convective heat transfer problems, but wishes to point out that, in the case of free convection from a vertical plate, the thermal and hydrodynamic boundary layer thicknesses, which in the past for reasons of simplicity were assumed to be equal, have been proven in the following analysis to be equal. [20] .

Assume a heated vertical surface surrounded by a fluid which experiences an increase in its temperature as a result of heat transfer from the heated surface, and begins to flow in an upward direction. In this case the boundary layer is initiated with zero thickness at the lower point of the vertical surface and builds up with increasing thickness in the upward direction.

The distance along the length of the plate will be denoted as x and perpendicular to it as y. Within the boundary layer the temperature T decreases from the value at the plate T_w, to the value of the fluid outside the layer T_∞. The distance where this temperature gradient takes place will be defined as the thermal boundary layer, δ_t. The assumption here is that the plate is at uniform temperature throughout its surface. The velocity along the x direction, U, is zero at the plate's surface and also zero outside the hydrodynamic boundary layer. The above description leads to the following representation.

Fig 2.1 .....

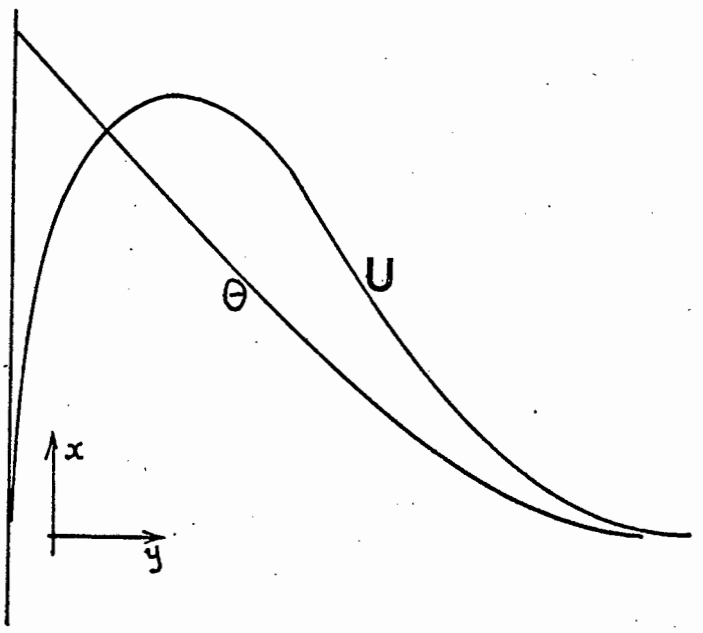

Fig. 2.1 Temperature and velocity profiles in free-convection flow from a vertical heated wall.

For the calculations of heat transfer it is necessary to know the characteristics of the boundary layer. Using the von Karman [19] method, and assuming constant properties, the momentum equation in the x direction is developed.

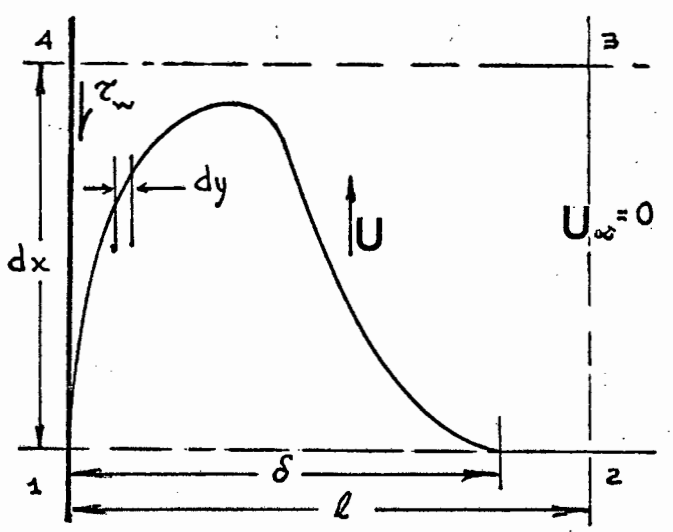

Fig 2.2 Calculation of the flow boundary layer.

The x/ .....

The x momentum is the mass flow rate times the velocity, and through plane 1 - 2 the total momentum is given by

$$\rho \int_o^{\ell} U^2 \, dy$$

The change in momentum in the x direction is

$$\rho \frac{d}{dx} \left(\int_o^{\ell} U^2 \, dy \right) dx = \rho dx \frac{d}{dx} \int_o^{\ell} U^2 \, dy \qquad (a)$$

which is the difference between the planes 1 - 2 and 3 - 4 and since the flow cannot enter through 1 - 4 it must have entered through surfaces 2 - 3. The velocity component through this plane is U_∞, (see Figure 2.2) and the x momentum

$$\rho U_\infty \, dx \frac{d}{dx} \int_o^{\ell} U dy = 0 \quad \text{since } U_\infty = 0.$$

The external forces acting on the control volume in the x direction are the shear stress at the wall

$$dx \, \mu \left. \frac{dU}{dy} \right|_{y = 0} \qquad (b)$$

and the pressure p and $p + \frac{dp}{dx} dx$ on the planes 1 - 2 and 3 - 4 respectively.

In addition to these forces a buoyancy force exists, which arises due to the temperature difference within the fluid. This force is $g\beta\rho \, (T - T_\infty)$ and it acts on a volume element dx by ℓ , so that the total force for the element is

$$dx \, g\beta\rho \int_o^{\ell} (T - T_\infty) \, dy \qquad (c)$$

Considering the small velocities that arise from free convection the pressure can be assumed constant. Summing expressions a, b and c, the momentum equation is obtained

$$\frac{d}{dx} \int_o^{\ell} U^2 \, dy = g\beta \int_o^{\ell} (T - T_\infty) dy - \frac{\mu}{\rho} \left. \frac{dU}{dy} \right|_{y = 0} \qquad (2.1)$$

Using the/ .....

Using the same control volume (Figure 2.2) the energy equation can be derived. Here the length ℓ is assumed to be greater than the thermal boundary layer thickness δ_t.

Through plane 1 - 2 the energy transported per unit time is

$$\rho C_p \int_o^{\ell} UT \, dy.$$

Through plane 3 - 4 this energy changes by an amount

$$\rho C_p \, dx \, \frac{d}{dx} \int_o^{\ell} UT \, dy$$

Through plane 2 - 3 energy is transported by the amount of

$$\rho C_p \, U_\infty \, dx \, \frac{d}{dx} \int_o^{\ell} T \, dy$$

and through plane 4 - 1 energy is transported by conduction alone since U = 0.

$$dQ = - k dx \, \frac{dT}{dy} \Big|_{y = 0}.$$

Summation of all the energy terms yields the energy integral equation

$$\frac{d}{dx} \int_o^{\ell} (T - T_\infty) \, U dy = - \alpha \, \frac{dT}{dy} \Big|_{y = 0}. \qquad (2.2)$$

If $(T - T_\infty)$ is represented by θ equation 2.2 becomes

$$\frac{d}{dx} \int_o^{\ell} \theta U dy = - \alpha \, \frac{d\theta}{dy} \Big|_{y = 0}. \qquad (2.2a)$$

The temperature profile can be approximated by a second degree equation (see figures 1.1 and 2.1)

$$\theta = a + by + cy^2$$

The boundary conditions that satisfy the problem are:

at $y = 0$ $\qquad \theta = \theta_w = (T_w - T_\infty)$

at $y = \delta_t$ $\qquad \theta = 0 \;, \; \frac{\partial \theta}{\partial y} \Big|_{y = \delta_t} = 0.$

at y = 0/ .....

at $y = 0$

$$\theta = \theta_w = a.$$

$$\left.\frac{d\theta}{dy}\right|_{y = \delta_t} = b + 2c\delta_t \quad \therefore\ b = -2c\delta_t.$$

$$\theta = 0 = \theta_w - 2c\delta_t^2 + c\delta_t^2 \quad \therefore\ c = \frac{\theta_w}{\delta_t^2}.$$

therefore

$$\theta = \theta_w - 2\theta_w \frac{Y}{\delta_t} + \theta_w \left(\frac{Y}{\delta_t}\right)^2$$

OR

$$\theta = \theta_w \left(1 - \frac{Y}{\delta_t}\right)^2 \tag{2.3}$$

The velocity profile shown in Figures 1.2 and 2.1 is represented by the following equation

$$U = U_1 \frac{Y}{\delta} \left(1 - \frac{Y}{\delta}\right)^2 \tag{2.4}$$

where U_1 is an arbitrary function with dimensions of velocity, and the boundary conditions,

at $y = 0$ $\quad U = 0$

$y = \delta$ $\quad U = 0,$ $\quad \left.\frac{\partial U}{\partial y}\right|_{y = \delta} = 0$

are satisfied.

Introducing the velocity profile into the velocity integral of equation 2.1

$$\int_o^{\ell} U^2\, dy = \int_o^{\ell} U_1^2 \left(\frac{Y}{\delta} - \frac{2y^2}{\delta^2} + \frac{Y^3}{\delta^3}\right)^2 dy$$

$$\therefore \int_o^{\ell=\delta} U^2\, dy = \frac{1}{105} U_1^2\, \delta.$$

Introducing the temperature profile into the temperature integral of equation(2.1) $\int_o^{\ell} \theta /$ .....

$$\int_o^{\ell} \theta dy = \int_o^{\ell=\delta_t} \theta_w (1 - \frac{y}{\delta_t})^2 dy = \frac{1}{3}\theta_w \delta_t .$$

In the integral of the energy equation 2.2a two possibilities exist

$$\int_o^{\ell=\delta} \quad \text{or} \quad \int_o^{\ell=\delta_t}$$

If δ_t is assumed less than δ, $\theta = 0$ outside the thermal boundary layer thickness so the integration must be done for θ up to δ_t.

If δ_t is assumed greater than δ, $U = 0$ outside the hydrodynamic boundary layer thickness so the integration of θ must be done up to δ.

In the first case the integral becomes

$$\int_o^{\delta_t} \theta_w (1 - \frac{y}{\delta_t})^2 - U_1 (\frac{y}{\delta}) (1 - \frac{y}{\delta})^2 dy$$

$$= \theta_w U_1 \frac{\delta_t^2}{\delta} \left[\frac{1}{12} - \frac{1}{15}\frac{\delta_t}{\delta} + \frac{1}{60}\frac{\delta_t^2}{\delta^2}\right]$$

In the second case the integral becomes

$$\int_o^{\delta} \theta_w (1 - \frac{y}{\delta_t})^2 \cdot U_1 (\frac{y}{\delta})(1 - \frac{y}{\delta})^2 \, dy$$

$$= \theta_w U_1 \delta \left[\frac{1}{12} - \frac{1}{15}\frac{\delta}{\delta_t} + \frac{1}{60}\frac{\delta^2}{\delta_t^2}\right]$$

Equation (2.1)

$$\frac{d}{dx}\int_o^{\ell} U^2 dy = g\beta \int_o^{\ell} \theta dy - \nu \left.\frac{dU}{dy}\right|_{y=o}$$

becomes

$$\frac{1}{105}\frac{d}{dx} U_1^2 \delta = \frac{1}{3} g\beta\theta_w \delta_t - \nu \left.\frac{dU}{dy}\right|_{y=o} \qquad (2.5)$$

Equation (2.2a)/ .....

Equation (2.2a)

$$\frac{d}{dx}\int_o^{\ell}\theta U dy = -\alpha\left.\frac{d\theta}{dy}\right|_{y=o}$$

becomes in the first case

$$\frac{d}{dx}\theta_w U_1 \frac{\delta_t^2}{60\delta}\left[5-4\frac{\delta_t}{\delta}+\frac{\delta_t^2}{\delta^2}\right] = 2\alpha\frac{\theta_w}{\delta_t}$$

and in the second case

$$\frac{d}{dx}\theta_w U_1 \frac{\delta}{60}\left[5-4\frac{\delta}{\delta_t}+\frac{\delta}{\delta_t^2}\right] = 2\alpha\frac{\theta_w}{\delta_t}$$

which indicates that

$$\frac{\delta_t^2}{60\delta}\left[5-4\frac{\delta_t}{\delta}+\frac{\delta_t^2}{\delta^2}\right] = \frac{\delta}{60}\left[5-4\frac{\delta}{\delta_t}+\frac{\delta^2}{\delta_t^2}\right]$$

letting $\frac{\delta_t}{\delta} \neq \lambda$

$$\lambda^2\left[5-4\lambda+\lambda^2\right] = \left[5-\frac{4}{\lambda}+\frac{1}{\lambda^2}\right]$$

Graphical solution (see figure 2.3) of the above expressions yields the value of $\lambda = 1$ where the two expressions intercept each other

$$\therefore \delta = \delta_t.$$

Since $\delta = \delta_t$ for both cases the energy equation (2.2a) can be expressed as

$$\frac{\theta_w}{30}\frac{d}{dx}(U_1\delta) = 2\alpha\frac{\theta_w}{\delta} \qquad (2.6)$$

and the momentum equation (2.5) can be expressed as

$$\frac{1}{105}\frac{d}{dx}(U_1^2\delta) = \frac{1}{3}g\beta\theta_w\delta - \nu\frac{U_1}{\delta} \qquad (2.7)$$

In order to solve equations (2.6) and (2.7) exponential functions for U_1 and δ are assumed

$$U_1 = Ax^m, \quad \delta = Bx^n$$

Introducing these/ .....

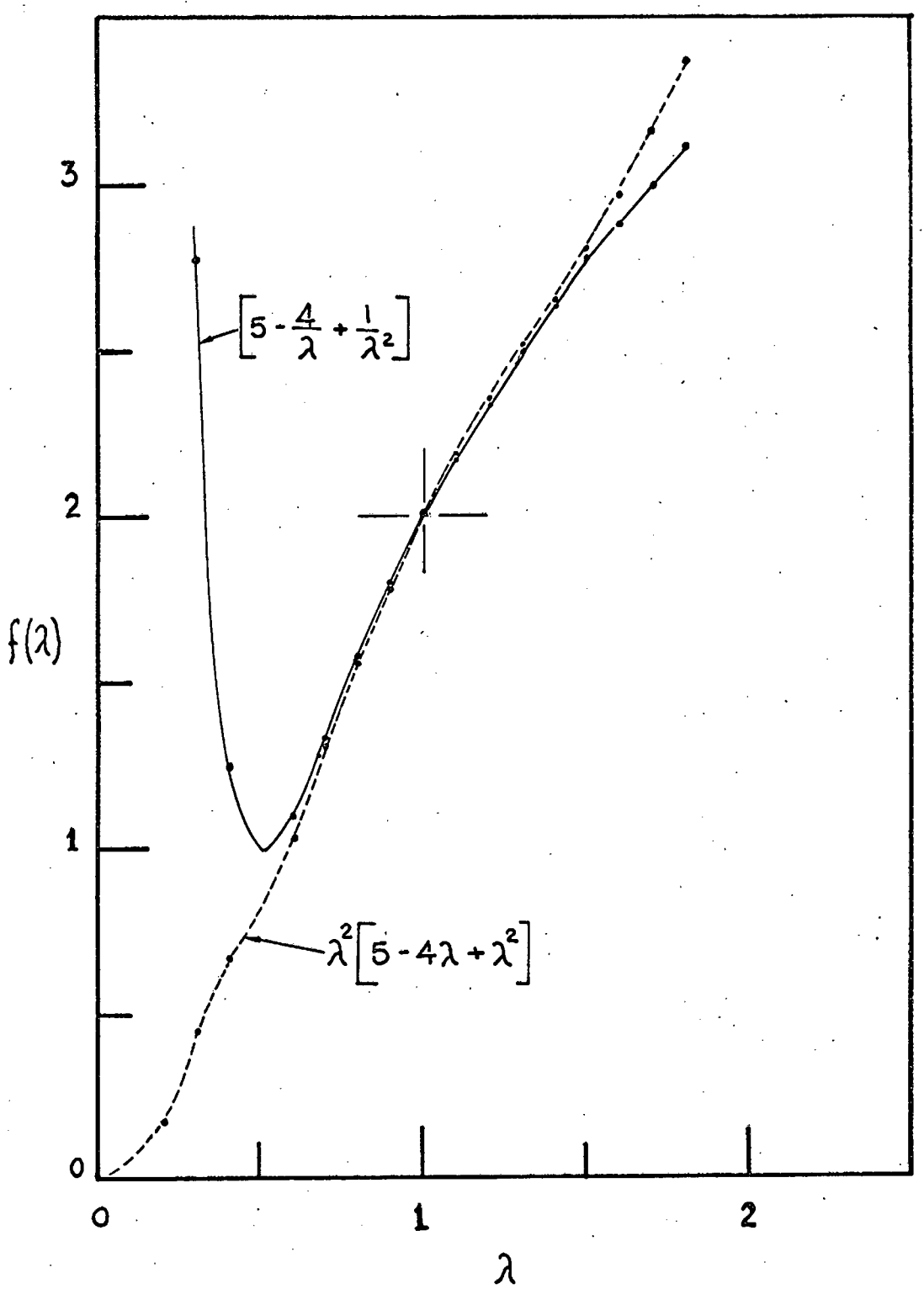
3
2
1
0
f(λ)
$\left[5-\frac{4}{\lambda}+\frac{1}{\lambda^2}\right]$
$\lambda^2\left[5-4\lambda+\lambda^2\right]$
0
1
2
λ

FIGURE 2-3

Introducing these functions into equations (2.6) and (2.7)

$$\frac{1}{105}\frac{d}{dx}(A^2 Bx^{2m+n}) = \frac{1}{3} g\beta\theta_w Bx^n - \frac{\nu A x^{m-n}}{B}$$

$$\frac{1}{30}\theta_w(ABx^{m+n}) = \frac{2\alpha\theta_w x^{-n}}{B}$$

performing the differentiation

$$\frac{2m+n}{105}(A^2 Bx^{2m+n-1}) = \frac{1}{3} g\beta\theta_w Bx^n - \frac{\nu A x^{m-n}}{B}$$

$$\frac{m+n}{30}(ABx^{m+n-1}) = \frac{2\alpha\ x^{-n}}{B}$$

The equations must be valid for any value of x, therefore the exponents must have the same value for every term.

$2m+n-1 = n = m-n$

$m+n-1 = -n \quad \therefore\ m = \frac{1}{2},\ n = \frac{1}{4}.$

Substituting these values into equations (2.6) and (2.7)

$$\frac{A^2 B}{84} = \frac{1}{3} g\beta\theta_w B - \frac{\nu A}{B} \qquad (2.7a)$$

$$\frac{AB}{40} = \frac{2\alpha}{B} . \qquad (2.6a)$$

Solving for the constant A from the above expressions

$$A = \frac{80\alpha\ (\frac{g\beta\theta_w}{\nu^2})^{\frac{1}{2}}}{(\frac{228.6}{Pr^2} + \frac{240}{Pr})^{\frac{1}{2}}}$$

Solving for the constant B from the above expressions

$$B = (\frac{g\beta\theta_w}{\nu^2})^{-\frac{1}{4}}\ (\frac{228.6}{Pr^2} + \frac{240}{Pr})^{\frac{1}{4}}$$

and the boundary layer thickness becomes from $\delta = Bx^n$

$$\delta = (\frac{g\beta\theta_w}{\nu^2})^{-\frac{1}{4}}\ (\frac{228.6}{Pr^2} + \frac{240}{Pr})^{\frac{1}{4}}\ x^{\frac{1}{4}} \qquad (2.8)$$

dividing δ by/ .....

dividing δ by x to make it a dimensionless quantity

$$\frac{\delta}{x} = \left(\frac{g\beta\theta_w x^3}{\nu^2}\right)^{-\frac{1}{4}} \left(\frac{228.6}{Pr^2} + \frac{240}{Pr}\right)^{\frac{1}{4}} \qquad (2.8a)$$

The first term of the above expression is recognised as the local Grashof number. For air the Prandtl number is nearly constant at 0.71 so equation (2.8a) reduces to

$$\frac{\delta}{x} = 5.31\ (Gr_x)^{-\frac{1}{4}} \qquad (2.9)$$

which indicates that the ratio of the boundary layer thickness to the plate's height approaches an infinite value as the Grashof number approaches zero (see figure 2.4). This is in accordance with Pohlhausen [8] as seen in chapter I.

On the other hand the heat flow from the surface is represented by $Q = -k \left.\frac{d\theta}{dy}\right|_{y=o}$

and from equation(2.3)

$$Q = 2k \frac{\theta_w}{\delta}$$

also from the defining equation of convection

$$Q = h_c \theta_w$$

$$h_c = \frac{2k}{\delta} \qquad (2.10)$$

and in dimensionless form

$$\frac{h_c x}{k} = Nu_x = \frac{2x}{\delta} \qquad (2.11)$$

Introducing the expression for $\frac{\delta}{x}$ (eq. 2.9) for air yields

$$Nu_x = 0.376(Gr_x)^{\frac{1}{4}} \qquad (2.12)$$

Inspection of equation (2.12) indicates that the phenomenon of free convection is a function of the dimensionless groups Nu (Nusselt) and Gr(Grashof), if the Prandtl number is assumed

constant./ .....

constant. Dimensional analysis also indicates the same (see appendix A).

According to expression(2.12)the local heat transfer coefficient h_c decreases with increasing x or

$$h_c \propto x^{-\frac{1}{4}}$$

The average heat transfer coefficient for a surface of height L is obtained by integrating expression (2.12) between the limits of zero and L and dividing by L.

$$\bar{h}_c = \frac{\int_0^L 0.376 \frac{k}{x} (Gr_x)^{\frac{1}{4}} dx}{L}$$

$$\bar{h}_c = 0.376 \frac{k}{L} \cdot \frac{4}{3} (Gr_L)^{\frac{1}{4}}$$

$$\bar{h}_c = 0.501 \frac{k}{L} (Gr_L)^{\frac{1}{4}} \qquad (2.13)$$

and in dimensionless form

$$\overline{Nu} = 0.501 (Gr_L)^{\frac{1}{4}} \qquad (2.14)$$

Comparison of equation (2.12) and (2.14) indicates that the average free convective heat transfer coefficient along a surface from origin to height x is equal to $\frac{4}{3}$ the local value at x.

$$\bar{h}_c = \frac{4}{3} h_c \qquad (2.15)$$

or alternatively the average value of the heat transfer coefficient for any x is $\frac{4}{3}$ the local value at x.

b. Analogy Between/ .....

b. Analogy Between Forced and Free Convection from a Vertical Flat Plate

It has been shown by Schlichting [2] that when rendering dimensionless the Navier-Stokes equations for plane flow, the Grashof number is approximately equal to the square of the Reynolds number, if the buoyancy forces are of the same order of magnitude as the inertia and viscous forces. This condition occurs only with very small velocities and considerable temperature differences, i.e. it is true for the phenomenon of free convection from a vertical plate, and indicates a possible analogy between forced and free convection.

It is surprising that investigators have not looked more into this analogy between Grashof and Reynolds numbers either analytically or experimentally.

Analysis.

Using the velocity distribution of the form

$$U = U_1 \frac{y}{\delta}\left(1 - \frac{y}{\delta}\right)^2 \qquad (2.4)$$

for the flow created by convective currents from a heated vertical plate, it can be shown that the maximum velocity in the profile exhibited occurs at $y = \frac{\delta}{3}$ and it is given by

$$U_{max} = 0.421\alpha \left(\frac{g\beta\theta_w}{\nu^2}\right)^{\frac{1}{2}} x^{\frac{1}{2}} \qquad (2.16)$$

and the local Nusselt number from a plate in free convection is given by

$$Nu_x = 0.376\ (Gr.)^{\frac{1}{4}} \qquad (2.12)$$

which is in very good agreement with the expression derived by [9]

$$Nu_x = 0.360\ (Gr.)^{\frac{1}{4}} \qquad (1.2)$$

Holman [21] gives the equation for laminar forced convection

past a/ .....

past a plate, based on the solution of the boundary layer equations

$$Nu_x = 0.332\ Re_x^{1/2}\ Pr^{1/3} \qquad (2.17)$$

which reduces for air to

$$Nu_x = 0.296\ Re_x^{1/2} \qquad (2.18)$$

This is in agreement with dimensional considerations that indicate the following relationship for the same phenomenon

$$Nu_x = C\ Re_x^{n} \qquad (2.19)$$

At this point the assumption is made that for the region $y = 0$ to $y = \frac{\delta}{3}$ the buoyancy forces accelerate the fluid from rest (see figure 2.1), it is analogous to a forced flow having a free stream velocity equal to U_{max} given by equation (2.16).

Substituting the value of U_{max} into equation (2.19) we obtain

$$Nu_x = C\ \left(\frac{0.421}{Pr}\right)^{n} \left(\frac{g\beta\theta_w x^3}{\nu^2}\right)^{n/2} \qquad (2.20)$$

which can be written as:

$$Nu_x = C_1\ Gr_x^{m} \qquad (2.21)$$

where the transformation of the Reynolds number to the Grashof number is noted.

At this point experimental data is needed in order to solve for the constant C_1 and the exponent m.

/ .....

Making use of figure 1.2 which has been verified experimentally by Schmidt and Beckmann [9] we see that the maximum velocity in the boundary layer is given by

$$U_{max} = \frac{(0.285)\ 2\sqrt{gx}}{\sqrt{\frac{T_\infty}{T_w - T_\infty}}} \qquad (2.22)$$

The Reynolds number based on this velocity is

$$Re_{Umax} = \frac{(0.570)g^{1/2}\ x^{3/2}}{\nu\sqrt{\frac{T_\infty}{T_w - T_\infty}}} \qquad (2.23)$$

Squaring equation (2.23) and rearranging we obtain

$$Re^2_{Umax} = 0.325\ Gr_x \qquad (2.23)$$

Where the transformation of the Reynolds number to the Grashof number is again noted, and the condition of $Re^2 \approx Gr$ is satisfied.

Returning to equation (1.2) and substituting the value of Gr_x from equation (2.23) we obtain

$$Nu_x = 0.476\ Re^{1/2}_{Umax} \qquad (2.24)$$

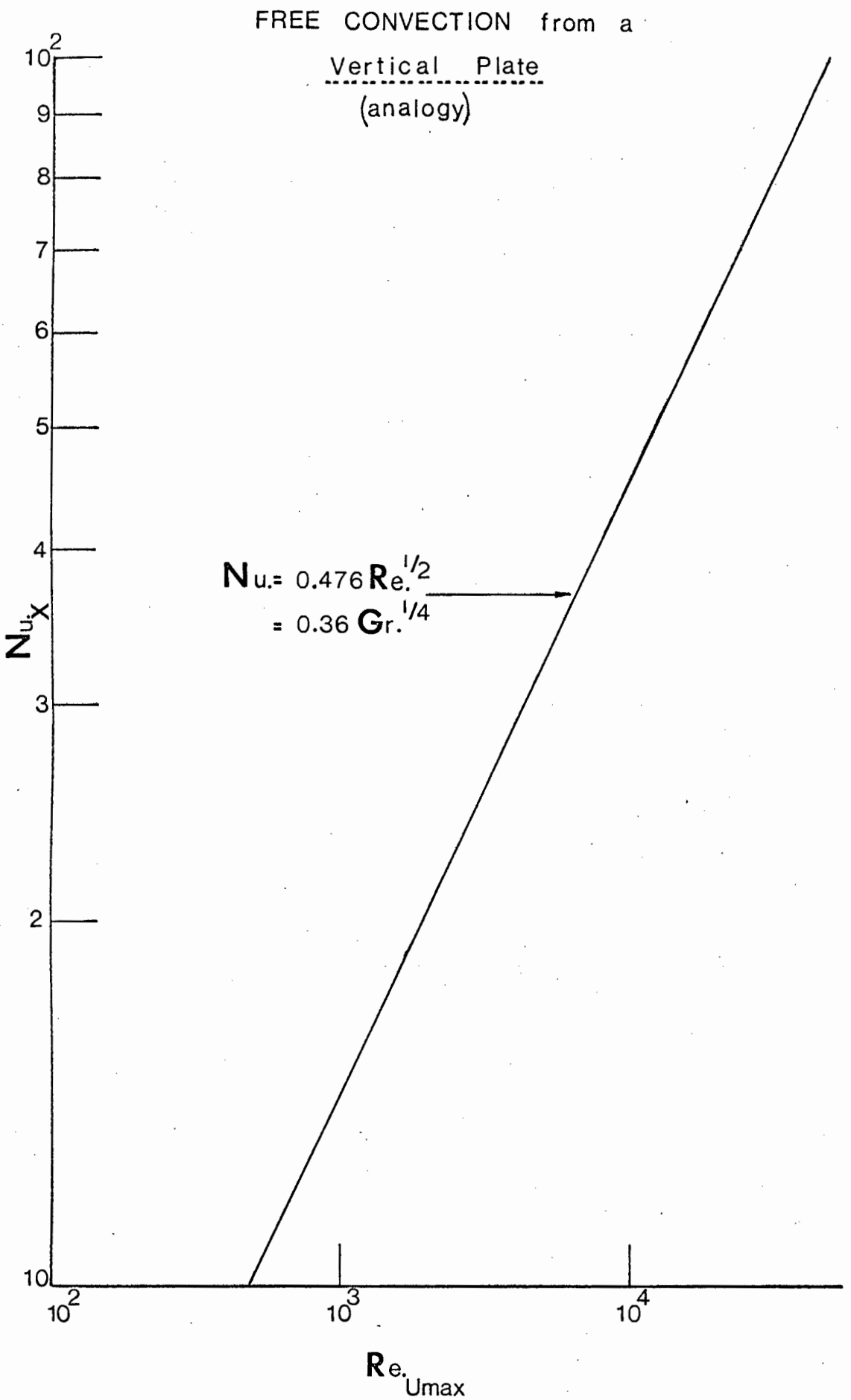
FREE CONVECTION from a
Vertical Plate
(analogy)
10^2
9
8
7
6
5
4
3
2
10
N_{u_x}
$N_{u.} = 0.476 R_{e.}^{1/2}$
$= 0.36 G_{r.}^{1/4}$
10^2
10^3
10^4
$R_{e._{Umax}}$

FIGURE 2·5

c. A Note on the Equation of Motion for Natural Convection from a Vertical Plate.

Schlichting [2] in dealing with the phenomenon of free convection introduces the buoyancy forces in the equation of motion of a viscous fluid and treats them as "impressed" forces. The buoyancy forces are caused by changes in volume which are associated with the temperature differences. It is shown that the relative change in volume of the hotter fluid is a function of the coefficient of expansion β, the temperature difference between the hot fluid particle and the colder surroundings $(T - T_\infty)$, and the vector of gravitational acceleration g.

He [2] presents the equation of motion for the x direction (along the direction of flow), in the form

$$\rho\left(U\frac{\partial U}{\partial x} + v\frac{\partial U}{\partial y} + w\frac{\partial U}{\partial z}\right) = -\frac{\partial P}{\partial x} + \rho g\beta(T - T_\infty) + \mu\left[\Delta^2 U + \frac{1}{3}\frac{\partial}{\partial x}\operatorname{div} w\right] \qquad (2.25)$$

and states that the pressure in each horizontal plane is equal to the gravitational pressure and is thus a constant. With $\frac{\partial P}{\partial x} = 0$ and further simplifications for two dimensional steady incompressible flow the equation of motion becomes

$$U\frac{\partial U}{\partial x} + v\frac{\partial U}{\partial y} = \nu\frac{\partial^2 U}{\partial y^2} + g\beta\,(T_w - T_\infty)\theta \qquad (2.26)$$

Where θ is the dimensionless local temperature

$$\theta = \frac{(T - T_\infty)}{(T_w - T_\infty)}$$

On the other/ .....

On the other hand Holman [21] presents the equation of motion for the same phenomenon in the form

$$\rho(U\frac{\partial U}{\partial x} + v\frac{\partial U}{\partial y}) = -\frac{\partial p}{\partial x} - \rho g + \mu\frac{\partial^2 U}{\partial y^2} \qquad (2.27)$$

where the term $-\rho g$ represents the force due to the weight of the particle, i.e. the body force. He [21] states that the change of pressure over a height dx is equal to the weight per unit area of the fluid element so $\frac{\partial p}{\partial x} = \rho_\infty g$ and not zero as stated by Schlichting [2].

Equation (2.27) is rewritten as

$$\rho(U\frac{\partial U}{\partial x} + v\frac{\partial U}{\partial y}) = (\rho_\infty - \rho)\, g + \mu\,\frac{\partial^2 U}{\partial y^2} \qquad (2.27a)$$

and making use of the definition of β

$$\beta = \frac{1}{V}(\frac{\partial V}{\partial T})_P = \frac{1}{V_\infty}\,(\frac{V - V_\infty}{T - T_\infty}) = \frac{\rho_\infty - \rho}{\rho(T-T_\infty)}$$

he obtains the same equation of motion as eq. (2.26)

Firstly, let us examine the term $-\frac{1}{\rho}\frac{\partial p}{\partial x}$; making use of the ideal gas law it may be expressed as

$$-\frac{1}{\rho}\frac{\partial P}{\partial x} = -\frac{1}{\rho}R(T\frac{\partial \rho}{\partial x} + \rho\frac{\partial T}{\partial x}) = -\frac{R}{\rho}T\frac{\partial \rho}{\partial T}\frac{\partial T}{\partial x} + R\frac{\partial T}{\partial x}$$

since by definition $-\frac{1}{\rho}\frac{\partial \rho}{\partial T} = \beta$

$$-\frac{1}{\rho}\frac{\partial P}{\partial x} = R\frac{\partial T}{\partial x}(T\beta - 1)$$

but $\beta = \frac{1}{T}$ for an ideal gas

$$\therefore -\frac{1}{\rho}\frac{\partial P}{\partial x} = R\frac{\partial T}{\partial x}(0) = 0.$$

since $\frac{1}{\rho} \neq 0$ we conclude that $\frac{\partial P}{\partial x} = 0$

as it was assumed in section a (page 26).

Secondly,/ .....

Secondly, let us examine the body force. Since the only cause of motion is the difference in density between the boundary layer and the bulk fluid, it is more appropriate to write the nett body force which must be considered as "impressed",

$$X = (\rho_\infty - \rho)g.$$

and the equation of motion for two dimensional incompressible steady state flow and no pressure gradient is written

$$\rho(U\frac{\partial U}{\partial x} + v\frac{\partial U}{\partial y}) = (\rho_\infty - \rho)g + \mu\frac{\partial^2 U}{\partial y^2}$$

Dividing by ρ and making use of $P = \rho RT$, and the difinition of β we obtain the identical equation as (2.26)

$$U\frac{\partial U}{\partial x} + v\frac{\partial U}{\partial y} = g\,\beta_\infty(T - T_\infty) + \frac{\mu}{\rho}\,\frac{\partial^2 U}{\partial y^2} \qquad (2.28)$$

the solution of which is already known.

Since, the velocities involved are very small, most investigators have assumed the density to remain constant. This assumption is certainly substantiated partially by our proof that $\frac{\partial p}{\partial x} = 0$ and if the plate is assumed to be isothermal we can safely neglect any variation of density along x since $\frac{\partial T}{\partial x} = 0$; however, if large temperature gradients exist on the plate, (along x) the density varies inversely proportionally to temperature and should affect the viscous term of equation (2.28) as well as the body force. In such a case, it is more appropriate to write the equation of motion in the following form

$$U\frac{\partial U}{\partial x} + v\frac{\partial U}{\partial y} = g\beta_\infty\,(T_w(x) - T_\infty)\theta + \frac{\mu}{P_\infty}\,RT_w(x)\,\frac{\partial^2 U}{\partial y^2} \qquad (2.29)$$

where $T_w(x)$ is some arbitrary wall temperature distribution, the solution of which, coupled with the continuity and energy equations becomes a formidable task, since a new similarity variable must be found.

d. The Effects of Variable Wall Temperature on the Boundary Layer of a Vertical Plate.

The latter part of the previous section served as an introduction to the following, because in many real cases the surface from which heat is being transferred is not isothermal. In this respect, for the pnenomenon of free convection from a vertical plate, very few analytical works have been presented. Sparrow and Gregg [10], in an early paper, presented results for a uniform wall temperature and in a latter paper [22], they have given results for the following two families of surface temperatures

$$(T_w - T_\infty) = Nx^n \qquad (2.30)$$

$$(T_w - T_\infty) = Me^{mx} \qquad (2.31)$$

which appear to be the only ones that render to similarity solutions. By defining η the similarity variable and using equation (2.30)

$$\eta = C_1 y x^{\frac{(n-1)}{4}}$$

where $C_1 = (g\beta N/4\nu^2)^{\frac{1}{4}}$

they solved for the velocity and temperature profiles and heat transfer rates.

Similarity solutions are what we term "exact", however, when dealing with the boundary layer equations that are deduced from the Navier-Stokes equations, it is impossible to carry out a similarity transformation for any arbitrary temperature distribution, but rather for special cases such as equations (2.30) and (2.31).

The author wishes to point out that the solution based on equation (2.30) is questionable because it has a singularity point. When x is zero it requires that the wall temperature (T_w) be equal to the bulk fluid temperature (T_∞) which can hardly be the case! Furthermore, if the exponent of equation (2.31) is unity, the

similarity/ .....

similarity variable η becomes independent of x!!

It is proposed here that a less "exact" method of solution be used where an arbitrary wall temperature distribution can be applied. Again here the term "less exact" applied to the integral method is misleading. One has only to look at the excellent agreement, with experimental data and similarity solitions for free and forced convection, which were obtained using these methods. Furthermore, the integral methods give far more information concerning the boundary layer thickness while the similarity solutions, being series solutions that converge very slowly, fail to define quantitatively the boundary layer.

It was shown in section (a) that the boundary layer equations using integral methods assume the form

$$\frac{1}{30}\ \frac{d}{dx}\ (\theta_w\ U_1 \delta) = \frac{2\alpha\theta_w}{\delta} \qquad (2.6)$$

$$\frac{1}{105}\ \frac{d}{dx}(U_1^2 \delta) = \frac{1}{3}\ g\rho\theta_w \delta - \frac{\nu U_1}{\delta} \qquad (2.7)$$

Following the same procedure and introducing the following form for the wall temperature variation

$$T_w(x) = T_{w_{x=0}} + C(\frac{x}{L})^p \qquad (2.32)$$

where C and p are positive constants, equations (2.6) and (2.7) become

$$\frac{1}{30}\ \frac{d}{dx}\ (\theta_{w_{x=0}} U_1 \delta + U_1 \delta\ C(\frac{x}{L})^p) = \frac{2\alpha\ (\theta_{w_{x=0}} + C(\frac{x}{L})^p)}{\delta} \qquad (2.33)$$

$$\frac{1}{105}\ \frac{d}{dx}\ (U_1^2\ \delta) = \frac{1}{3}\ g\beta\delta\ (\theta_{w_{x=0}} + C(\frac{x}{L})^p) - \nu\frac{U_1}{\delta} \qquad (2.34)$$

performing the differentiation we obtain the following

expressions/ .....

expressions for the exponents of x

$$m + n - 1 = p + m + n - 1 = p - n = -n$$

$$2m + n - 1 = n = p + n = m - n$$

In order to have a solution the exponents must have the same value for every sum and we obtain

$$m = \tfrac{1}{2}, \quad n = \tfrac{1}{4}, \quad p = 0 \text{ !}$$

This is very interesting because it indicates that the boundary layer thickness is still proportional to $x^{\frac{1}{4}}$, regardless of the wall temperature variation.

Continuing with the solution, equations (2.33) and (2.34) become

$$\frac{A^2 B}{84} = \frac{1}{3} g\beta B(\theta_{w_{x=0}} + C) - \frac{\nu A}{B} \qquad (2.35)$$

$$\frac{AB}{40} = \frac{2\alpha}{B} \qquad (2.36)$$

which are identical with equations (2.6a) and (2.7a), except for the term in the brackets, which now assumes the "local" temperature difference between the wall and the bulk fluid.

$$\theta_{w_{Local}} = (\theta_{w_{x=0}} + C) \qquad (2.37)$$

Solving for the constants A and B we obtain an expression for the boundary layer thickness

$$\delta = \frac{5.31\ x}{(Gr)^{\frac{1}{4}}_{Local}} \qquad (2.38)$$

which is identical to equation (2.9) except for the ΔT involved in the Grashof number. This analysis has shown that the boundary layer thickness is not affected by the wall variation and that we should expect the temperature profiles to be similar to the ones obtained for a constant wall plate. This is in variance with the results presented by Sparrow and Gregg [22] and therefore experimental data is needed to verify the validity of the present solution.

e. / .....

e. BUOYANCY DIFFUSION COEFFICIENT.

Nomenclature Used in this Section.

A(t)	Brownian motion fluctuations
a	radius of a molecule
β	dynamic friction coefficient
B	buoyancy coefficient
D	diffusion coefficient
$\frac{du}{dt}$	acceleration of a molecule
η	absolute viscosity of the fluid
k	Boltzman's constant
m	mass of a molecule
r	position of a molecule
t	time
T	Temperature
u	velocity of a molecule
W(r)	positional probability distribution
W(u)	velocity probability distribution
W(R,S)	bivariate probability distribution

INTRODUCTION

Generally the validity of the Navier-Stokes equations can hardly be doubted because known solutions agree so well with experiment. However, the enormous mathematical difficulties when solving these equations, have prevented us from obtaining a single solution in which the convective terms interact in a general way with the friction terms.

Therefore the following method is a departure from the conventional methods used in dealing with boundary layer problems.

It is/ .....

It is proposed that the motion of the fluid can be described microscopically as a motion of large numbers of molecules in random flight, (Brownian motion), within a specified region which the macroscopic approach terms "the boundary layer".

We will begin by using Langevin's equation which describes the motion of a particle in the absence of an external force.

$$\frac{du}{dt} = -\beta u + A(t) \qquad (2.39)$$

where βu represents the dynamic friction generated and governed by Stoke's law. ($\beta = 6\pi a\eta/m$). $A(t)$ is the fluctuating part which is characteristic of the Brownian motion. The buoyancy forces play a major role, when present, to the motion of a fluid near a surface, thus we replace β in equation (2.39) by $\alpha = B - \beta$, where B is the buoyancy effect, and equation (2.39) becomes

$$\frac{du}{dt} = -\alpha u + A(t) \qquad (2.40)$$

The above equation is not an ordinary differential equation because it involves the term $A(t)$ but rather a stochastic one. In order to solve it we must specify probability distributions for the velocity and position of the particle.

Solution

Following Chandrasekhar's [23] solution of equation (2.39) we obtain the following three probability distributions:

the displacement probability distribution of the particle

$$W(r,t) = (m\alpha^2/2\pi kT\,(2\alpha t - 3 + 4e^{-2\alpha t} - e^{-2\alpha t}))^{3/2} \cdots$$
$$\cdots \exp - (m\alpha^2 (r\alpha^{-1}(1 - e^{-\alpha t}))^2/2\pi kT\,(2\alpha t - 3 - 4e^{-\alpha t} - e^{-2\alpha t})) \qquad (2.41)$$

the velocity probability distribution of the particle,

$$W(u,t) = (m/2\pi kT\,(1 - e^{-2\alpha t}))^{3/2} \exp - (mu^2/2kT\,(1 - e^{-2\alpha t})) \qquad (2.42)$$

and the/ .....

and the bivariate probability distribution of the particle

$$W(R,S) = \left(\frac{FG - H^2}{8\pi^3}\right)^{-3/2} \exp - (GR^2 - 2HRS + FS^2)/(2FG - 2H^2) \tag{2.43}$$

where $R = r$,

$S = u$,

$F = q\alpha^{-2}(2\alpha t - 3 - 4e^{-\alpha t} - e^{-2\alpha t})$,

$G = q\alpha^{-1}(1 - e^{-2\alpha t})$,

$H = q\alpha^{-2}(1 - e^{-2\alpha t})$,

$q = kT\alpha/m$.

One of the principal assumptions concerning A(t) is that it varies extremely rapidly compared to any other quantities, therefore in order for the position and the velocity of the particle to change appreciably, long time approximations must be given; i.e. for $t \to \infty$ equations (2.41), (2.42) and (2.43) reduce to:

$$W(r,t) = (4\pi Dt)^{-3/2} \exp - (r^2/4Dt) \tag{2.44}$$

where $D = kT/m\alpha$ and is defined as the diffusion coefficient

$$W(u,t) = (m/2\pi kT)^{3/2} \exp - (mu^2/2kT) \tag{2.45}$$

$$W(R,S) = 1/(8\pi^3 (2q^2 \alpha^{-3} t - q^2 \alpha^{-4})^{3/2}) \ldots\ldots$$

$$\ldots\ldots \exp - (q\alpha^{-1} r^2 - 2q\alpha^{-2} ru + 2q\alpha^{-2} tu^2)/(4q^2 \alpha^{-3} t - 2q^2 \alpha^{-4}) \tag{2.46}$$

Since we are interested in the average value of displacements we differentiate equation (2.44) with respect to time, holding r constant, and set it equal to zero thus obtaining

$$r^2 = 6Dt \tag{2.47}$$

which is Einstein's result.

From equation (2.45), which is the Maxwellian velocity distribution we obtain the most probable velocity of the particles

$$u^2_{m.p} = 2kT/m \tag{2.48}$$

For the bivariate/ .....

For the bivariate velocity and displacement distribution the exponent of equation (2.46) must be equal to unity; i.e.

$$q\alpha^{-1}r^2 - 2q\alpha^{-2}\,ru + 2q\alpha^{-2}\,tu^2 = 4q^2\,\alpha^{-3}\,t - 2q^2\,\alpha^{-4}$$

and solving for α from the above we obtain

$$\alpha = u/r = \sqrt{2kT/m}\ .\ (1/r) \qquad (2.49)$$

Having solved for α a number of useful expressions are obtained:

$$t = 1/3\alpha,\ r = u/\alpha,\quad D = r\,\frac{(2kT/m)^{\frac{1}{2}}}{2}$$

From our definition of α we may solve for B the buoyancy effect,

$$B = \frac{(2kT/m)^{\frac{1}{2}}}{r} + \frac{6\pi a\eta}{m} \qquad (2.50)$$

and subsequently obtained expressions for the buoyancy acceleration

$$Bu = 2kT/mr + 6\pi a\eta/m\ .\ (2kT/m)^{\frac{1}{2}} \qquad (2.51)$$

and the Buoyancy force

$$F_b = 2kT/r + 6\pi a\eta\ (2kT/m)^{\frac{1}{2}} \qquad (2.52)$$

Finally we are in a position to define the buoyancy diffusion coefficient

$$D_b = (kT/m)/(\ (2kT/m)^{\frac{1}{2}}\ /\ r) + 6\pi a\eta/m) \qquad (2.53)$$

CHAPTER III

Experimental Apparatus, Instrumentation and Procedure In Obtaining Average Heat Transfer Rates at low Grashof Numbers.

1. Vacuum Chamber.

It was necessary to construct a chamber where conditions of pressures lower than atmospheric could be produced. Such a chamber was constructed (See pictorial in Figure 3.1) by welding two 8-in × 18-in × $\frac{1}{4}$-in to two 10-in × 18-in × $\frac{1}{4}$-in steel plates. The two ends were sealed with 8-in × 10-in × 3/8-in steel plates. Suitable windows were machined on the two faces of the chamber as well as an opening at the top of the chamber. The latter was sealed with $4\frac{1}{2}$-in × 8-in × 3/5-in steel plate, where connections were made for the vacuum pump, the manometer and the McLeod gauge. The windows were sealed with $\frac{1}{4}$-in thick glass plates. All surfaces were machined and grooved to receive 1/8-in rubber sealing rings.

An additional port was constructed on the vacuum chamber to receive the power and thermocouple leads. Sealing of this port was made with a specially machined gland and 1-in O.D. O-ring.

The chamber was tested under vacuum and pressure, and all leaks were sealed. Prolonged periods under vacuum assured that no leaks were present. Vacuum as low as 0.05 mm.Hg. were obtained and maintained for periods as long as sixty hours without any detectable leakage.

Since another requirement of the chamber was that it should simulate a "black body" environment for the radiating heated vertical plate, its inside surface was painted with a dull black paint with practically no reflection. All

connections/ ...

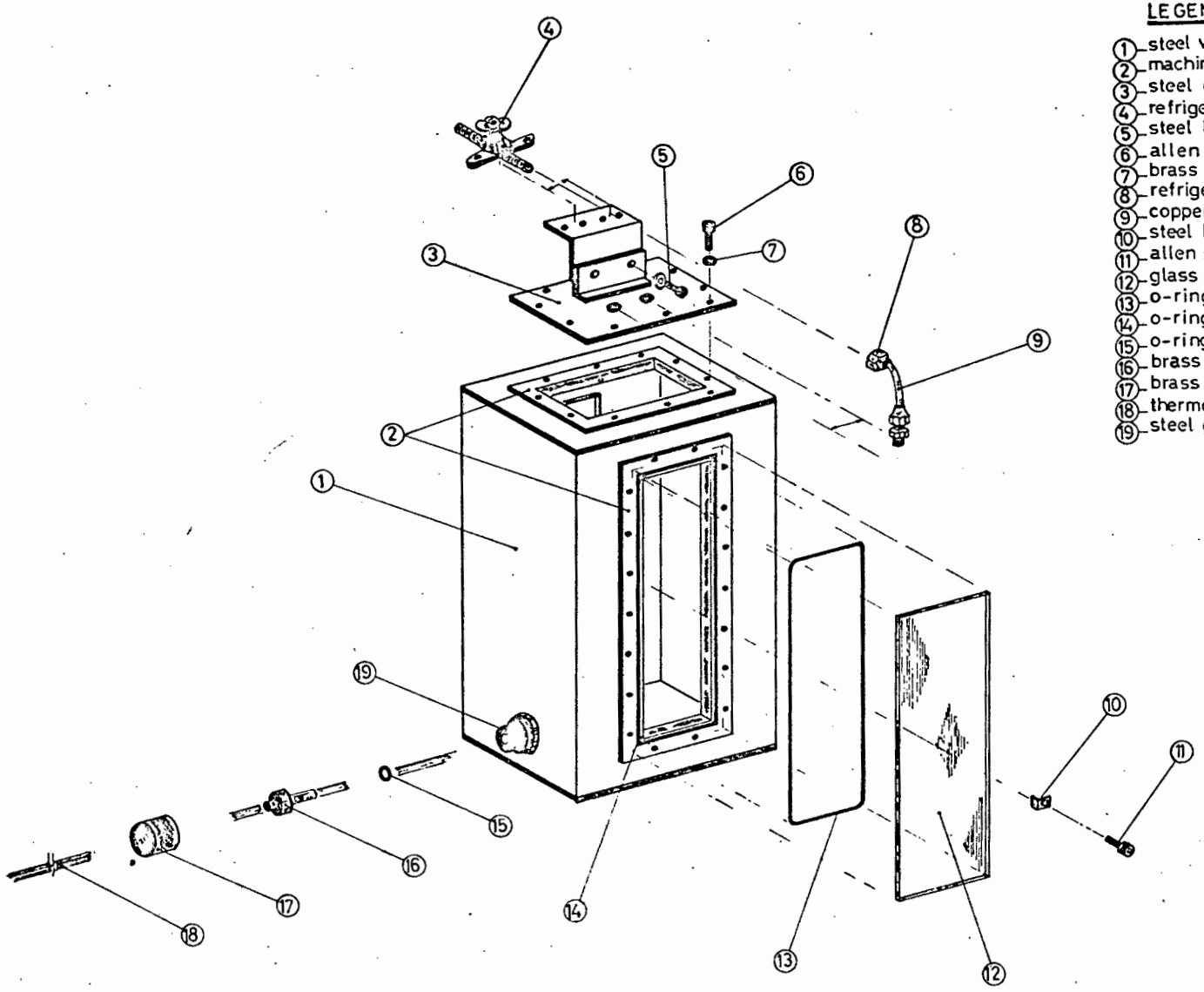

LEGEND

1. steel vacuum chamber
2. machined angle iron
3. steel cover
4. refrigeration valves
5. steel bolts
6. allen screws
7. brass washers
8. refrigeration fittings
9. copper tubing
10. steel brackets
11. allen screws
12. glass plates
13. o-rings
14. o-ring grooves
15. o-ring
16. brass gland (male)
17. brass nut
18. thermocouple and power leads
19. steel gland (female)

VACUUM CHAMBER

not to scale

FIGURE 3·1

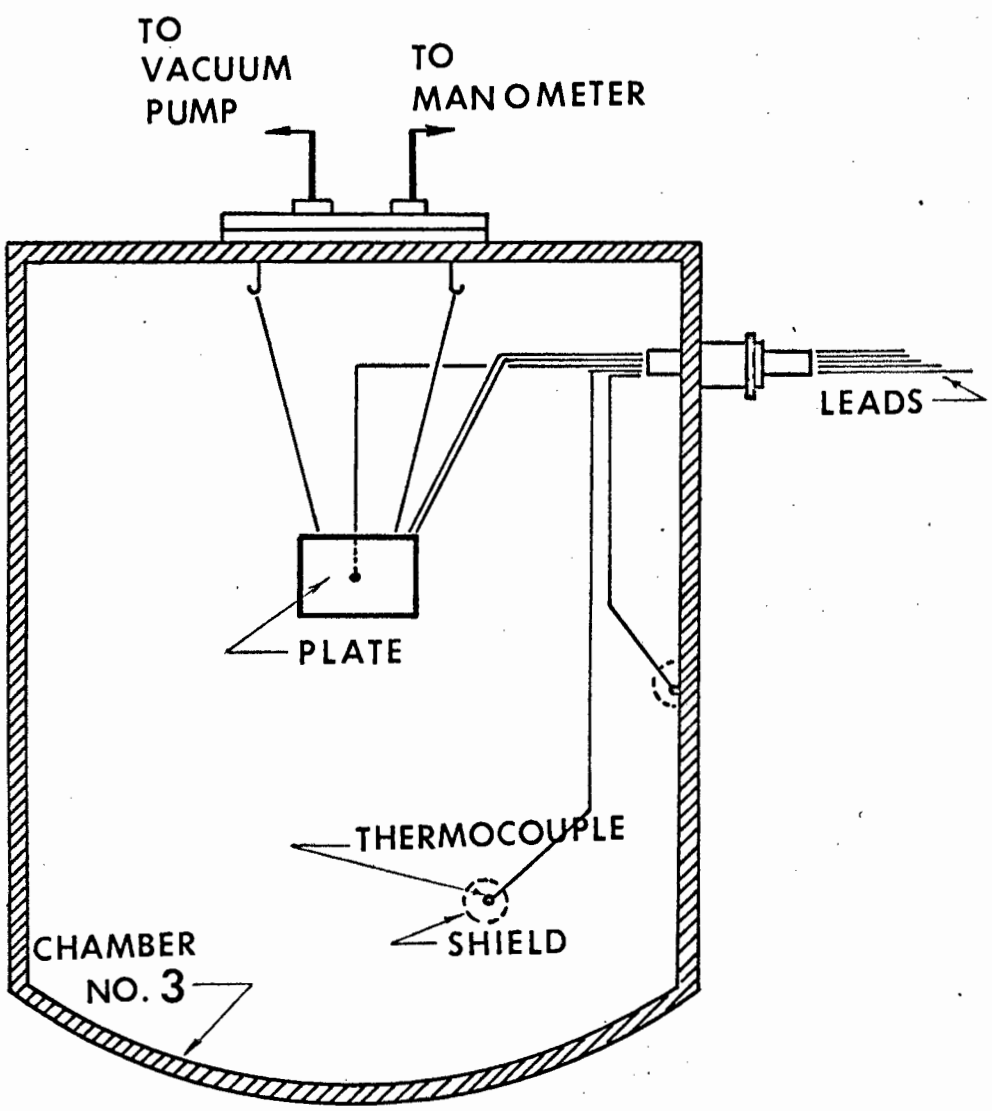
TO
VACUUM
PUMP
TO
MANOMETER
LEADS
PLATE
THERMOCOUPLE
SHIELD
CHAMBER
NO. 3

FIGURE 3·2

connections from the chamber to the control valves, pump, and gauges were made using standard refrigeration fittings which were adapted to receive O-rings.

At first the chamber stood vertically (on its long axis) and the vertical plate was placed in the middle allowing a space of approximately 5 inches between the plate and the walls of the chamber.

Later it was found necessary to modify the set-up and the chamber was modified slightly and placed horizontally. This new arrangement provided effectively a new chamber. Still later on in the evaluation of data it was found necessary to increase the dimensions of the chamber, along the leading and trailing edge of the vertical plate. A cylindrical vessel, 18-in O.D. and 22-in high, was used after it was adapted to receive the various connections used on the previous chamber.(See pictorial 3.2). So in all, three distinct vacuum chambers were employed in this investigation.

Chamber No. 1 as shown in pictorial 3.1.
Chamber No. 2 as shown in pictorial 3.1, rotated 90^{o}.
Chamber No. 3 as shown in pictorial 3.2.

2. Vertical Plate.

In order to simulate a vertical heated surface it was necessary to construct plates that would approximate conditions of constant wall temperature.

The size of the first plate was 12-in × 4-in. Since the plate was to be as evenly heated as possible, a heating element was designed and constructed as follows:

Ni-chrome resistance type strip, 0.0075 × 1/8-in, 1.73 ohms/yd., was used closely wound on a sedania board.

Two/ .....

Two 1/8-in thick 12-in × 4-in copper plates were prepared to sandwich the heating element. The plates were electrically insulated from the heating element with thin mica sheets. Since it was desired to have the average temperature of the plate, five heavy (0.038-in) constantan wires were fused inside small holes that went to the surface of the plate, and grooves with porcelain insulation were provided for the exit of these wires. (See pictorial 3.3).

Thus five constantan wires were used as one leg of the thermocouples and the plate itself as the other leg, making up five suitable copper-constantan thermocouples. A copper wire fused at the edge of the plate was common to all thermocouples. Calibration of these thermocouples proved very satisfactory since the readings that were obtained were almost identical to the tabulated values of copper-constantan tables. Leeds and Northrup [24]. (See figure 3.4.)

As a check measure the other plate was grooved only at the center and the two corresponding thermocouples gave identical readings during the tests that were performed. The two copper plates were fastened on the heating element with brass screws. Dental gypsum was used to make suitable fillets at the leading edges of the copper plates. During the investigation it was necessary to construct additional plates. Two more plates were constructed having the following dimensions: height 6.44 -in, 3-in and width 4.31 -in, 2-in respectively.

As the investigation progressed, the experience gained allowed certain simplifications to be made in the construction of the new plates. For example, in plate No. 2 it was not necessary to place a thermocouple midway in one of the

copper/ .....

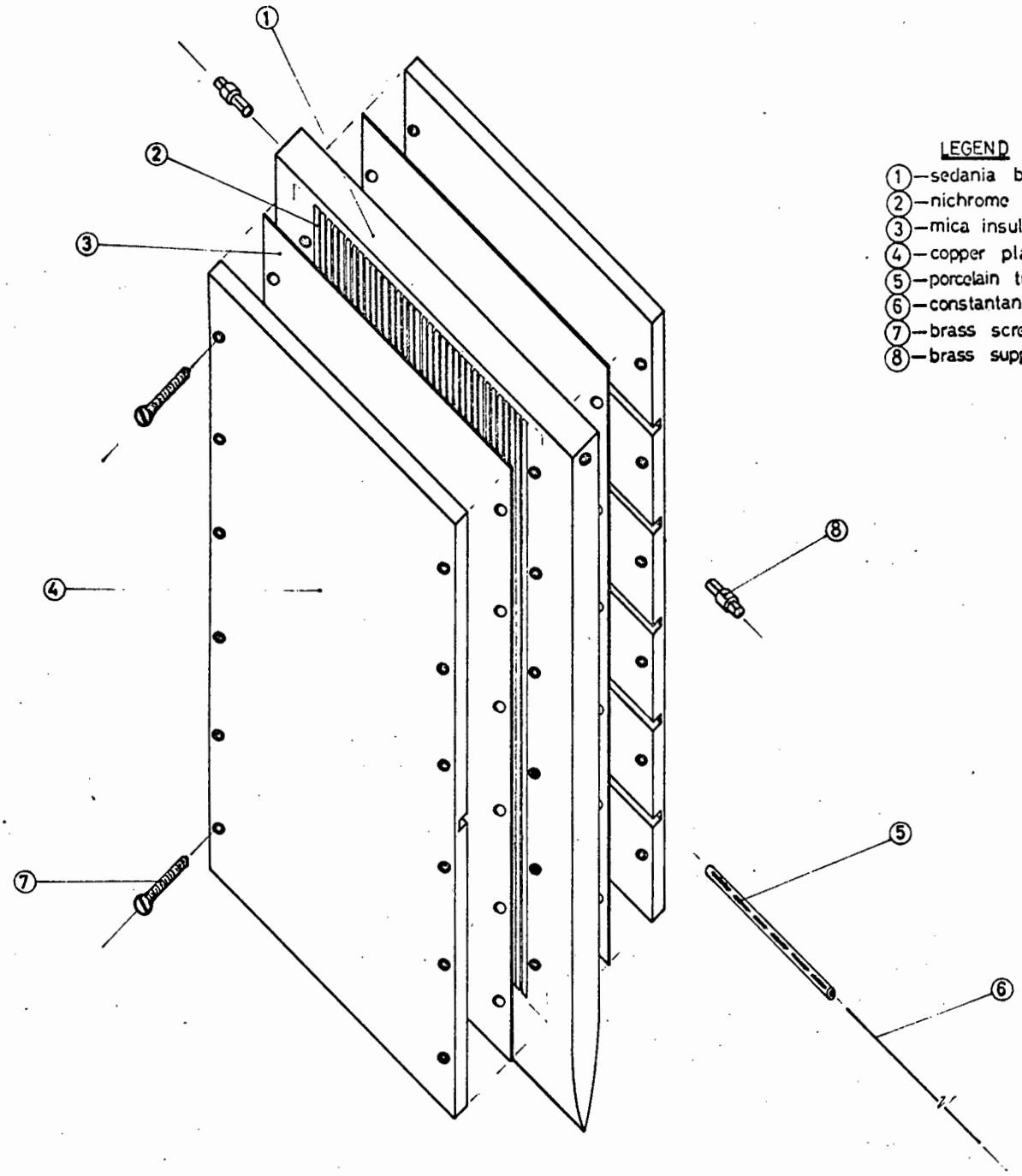

PLATE CONSTRUCTION

FIGURE 3·3

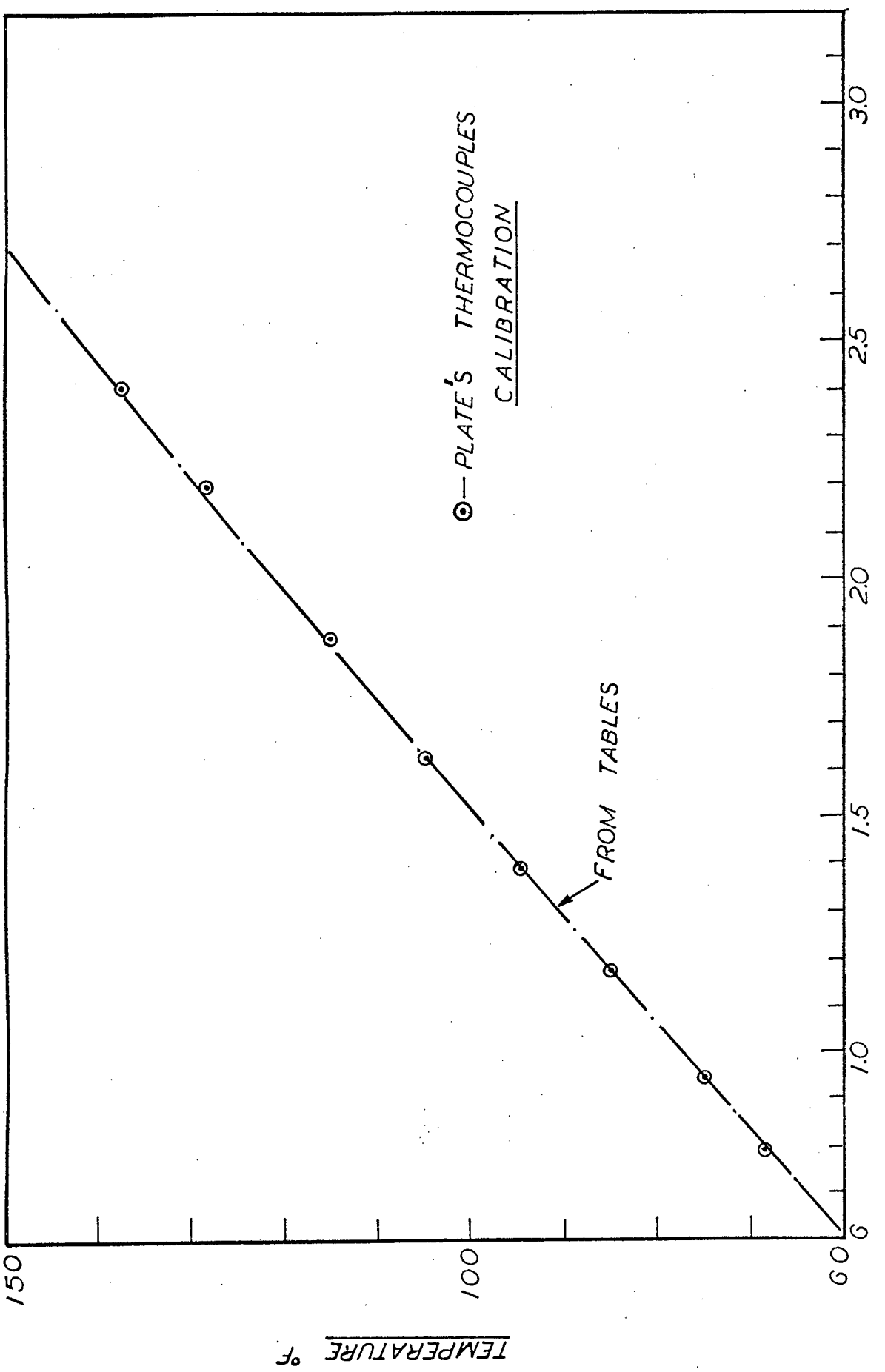
PLATE'S THERMOCOUPLES
CALIBRATION
FROM TABLES
TEMPERATURE °F
150
100
60
6
1.0
1.5
2.0
2.5
3.0
MILLIVOLTS

FIGURE 3.4

copper plates as done for plate No. 1. This new plate carried only five thermocouples in one of the copper plates. Later, when this plate was used turned 90° (plate No. 3) the position of the five thermocouples allowed measurements along the horizontal center line of the plate which showed negligible gradients, (less than 0.5°F). The smallest of all plates (No. 4) was constructed with further simplifications. This plate carried only one thermocouple in the center of one of the copper plates. Experience showed that when calculating average Nusselt numbers, the average temperature of the plate was very near the one indicated by the center line thermocouple. This is in agreement with Sparrow and Gregg [10] as presented in Chapter I, who have demonstrated that using the temperature half way along the height approximates a uniform temperature plate. The same plate was used turned 90° also from its original position (No. 5), its former width becoming the height.

In summary, the following plates were used in this investigation:

Plate.	Height.	Width.
No. 1	12-in	4-in
No. 2	6.44-in	4.31-in
No. 3	4.31-in	6.44-in
No. 4	3-in	2-in
No. 5	2-in	3-in

Instrumentation/ .....

Instrumentation

Power.

The power input to the heating element was regulated by means of a variable transformer (0-260 volts Yokoyama) which fed from a constant voltage transformer was used to remedy the fluctuation of voltage of the mains. The current and voltage input to the heating element was read with two Philips Universal Measuring Instruments coupled to the power leads. A Cambridge multirange wattmeter was used in conjunction with the Philips meters to determine that the power factor of the heating element was very near unity.

Pressure.

The vacuum in the chamber was obtained by using a single stage Vac-Uubrand pump RE-3 with a capacity of 3.5 m^3/hr and a pressure limit of 0.03 mmHg. For the recording of the pressure in the chamber a McLeod gauge was used (10-0.01 mm.Hg) and for the range of 10-760 mm Hg. a mercury manometer was employed. The McLeod gauge read absolute pressure, but when the mercury manometer was used a mercury barometer was employed for atmospheric corrections.

Temperature.

For the temperature measurements of the system, thermocouples were used.

The plate thermocouples have been discussed previously in the construction of the vertical plate. Additional copper constantan thermocouples were used for the fluid temperature as well as the temperature of the walls of the chamber.

A portable Cambridge laboratory potentiometer was used coupled to the thermocouple's multi-switch. This way any individual thermocouple could be selected. A Kipp and Zonen

recorder/ .....

recorder was also coupled to the multiswitch indicating when steady state conditions were established.

Compensating Thermopile.

During the experiments it was found necessary to obtain the emissivity of the plate's surface by other means than those used earlier (see experimental procedure). For this reason a compensating thermopile, in conjunction with the Kipp and Zonen recorder, the potentiometer and the variable transformer, were used to determine the emissivity of the flat plate.

Schlieren Apparatus.

When the construction of the chamber No. 1 took place the need for windows was forseen, that would enable visual observation of the system.

A Schlieren Apparatus was rigged and photographs of the boundary layer on the vertical plate were taken. The apparatus consisted of a mercury vapour lamp as a light source, a condensing lens which focussed the light onto a knife edge, two six inch field Schlieren lenses to produce a parallel light beam and another knife edge. The image was photographed with a polaroid camera using positive-negative polaroid film. (See figure 3-5 for the Schlieren system).

Thermocouple Probe.

During the experimental stages it was necessary to probe the boundary layer of the heated vertical plate. This was done by constructing an array of thermocouples which were shielded from the radiation emitted from the plate by aluminium foil shields, and placed on a support at distances $\frac{1}{4}$, 1.0, $1\frac{3}{4}$, $2\frac{1}{2}$, $3\frac{1}{4}$, and 4.0 inches from the heated surface, running horizontally and at the same level near the top of the plate No. 1.

Procedure/ .....

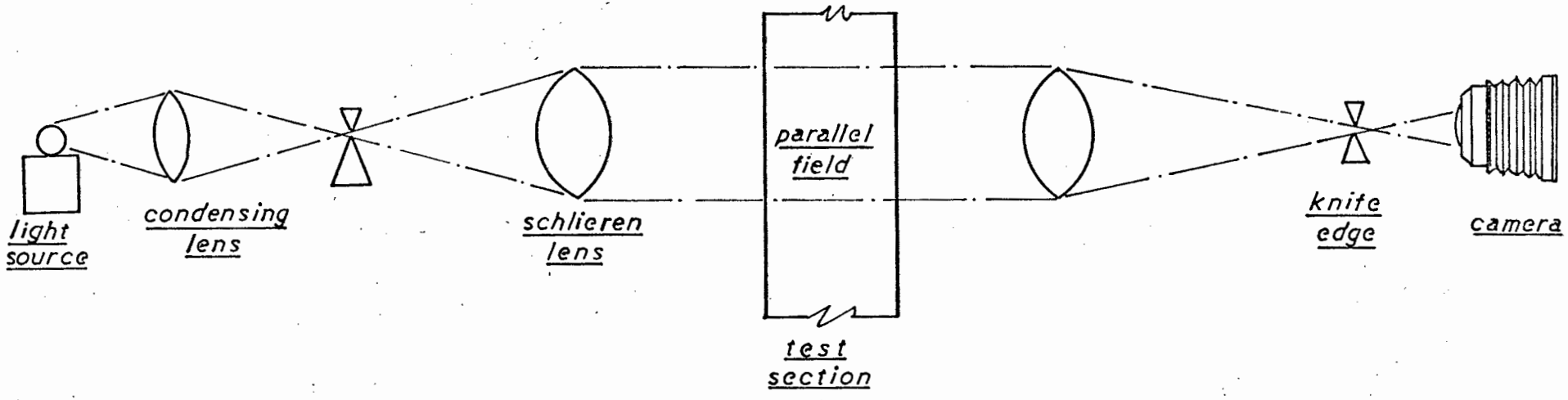

SCHEMATIC DIAGRAM OF
SCHLIEREN APPARATUS

FIGURE - 3.5

Procedure

The calorimetric technique was chosen to collect the experimental data, based on the following;

The total heat input to the plate could be controlled and measured by the instruments already discussed, and calculated from

$$Q_{in} = (I.V)(3.413) \quad \text{Btu/hr.} \tag{3.1}$$

In steady state conditions

$$Q_{in} = Q_{out} = uA\,(T_w - T_\infty) \tag{3.2}$$

where u is the overall heat transfer coefficient and defined by

$$u = h_r + h_c \tag{3.3}$$

which combines the heat flow by convection and radiation between a surface and a fluid. Since provisions were made for recording T_w and T_∞, u was calculated from equation 3.2.

Under the assumption that the apparatus was constructed simulating a grey body (vertical plate) at T_1 radiating to a black body (vacuum chamber) at T_2, the rate of heat transfer by radiation is given by the defining equation

$$Q_r = \sigma\varepsilon_1 A_1 (T_1^4 - T_2^4) \tag{3.4}$$

where ε_1 is the emissivity of the grey surface A_1.

From the defining equation of the radiant heat transfer coefficient,

$$h_r = \frac{Q_r}{A_1 (T_w - T_\infty)} \tag{3.5}$$

$$h_r = \frac{\sigma\varepsilon_1 (T_w^4 - T_c^4)}{(T_w - T_\infty)} \tag{3.6}$$

Provisions were made to record the temperatures appearing in equation 3.6 and establishing the emissivity of the surface, h_r was calculated from equation 3.3; once u and h_r were known h_c

was calculated/ .....

was calculated.

Heat losses due to conduction were negligible since the vertical plates were suspended in the chamber by thin wires. The radiation losses from the edges of the plates (due to their thickness) were neglected.

The integral analysis of chapter II yielded equation 2.14

$$\overline{Nu} = 0.501(Gr_L)^{\frac{1}{4}}$$

and the dimensional analysis (see appendix A) yielded

$$\overline{Nu} = C_1(Gr_L)^e$$

where the Prandtl number in both cases is assumed to be a constant.

In case the Prandtl number is a variable the following expression is applicable

$$\overline{Nu} = C_2(Gr.Pr)^e$$

or

$$\frac{h_c L}{k} = C_2 \left(\frac{\rho^2 \beta g(T_w - T_\infty)L^3}{\mu^2} \cdot \frac{C_p u}{k}\right)^e \qquad (3.7)$$

The density of the fluid was determined from the pressure and temperature of the fluid inside the vacuum chamber, using the ideal gas law $\frac{P}{\rho} = RT$.

All properties were evaluated at the T_r as given by equation (1.5) with the exception of β which was evaluated at T_∞. (See appendix A). Thus the data were used to evaluate the dimensionless groups in equation (3.7) and the results are presented in log.log. plots of $\overline{Nu}$ vs (Gr Pr). See appendix C for sample calculations.

Before the actual tests were performed, it was necessary to determine the plates' emissivity. In order to do this it was decided to take the chamber down to the highest vacuum obtainable (approx. 0.05 mm.Hg) and make an energy balance assuming that the

convection/ .....

convection losses from the plate were so small that they could be neglected. Thus from

$$Q_{in} = Q_r = \sigma\varepsilon_1 A(T_w^4 - T_c^4)$$

the emissivity was determined.

Later on during the investigation, it was found necessary to determine the emissivity by other means than those described above, and a compensating thermopile was used. (See appendix B for emissivity determination).

The data for convection from the plate at atmospheric pressures were obtained as follows.

The power input was regulated by means of the variable transformer. When steady state conditions were established, the power input was recorded as well as the temperature of the plate, the temperature of the air inside the chamber, and the temperature of the chamber's walls. The data for sub-atmospheric conditions were obtained by evacuating the chamber to approximately 1.0 mmHg and when steady state conditions were established the pressure in the chamber, the various temperatures, and the power input were recorded.

Subsequently, keeping the power input constant, air was allowed into the chamber raising the pressure to a new level and a new set of data was recorded. This procedure was carried out until the pressure inside the vacuum chamber reached atmospheric level.

To investigate any effects of the Prandtl number of the fluid, in addition to tests performed in air, helium and argon were used.

An attempt was made to photograph the thermal boundary layer about the plate using the Schlieren technique, and the photographs, together with the results obtained using all the chambers and all the plates, appear in Chapter IV.

CHAPTER IV

Results of the Investigation for Average Heat Transfer Rates at Low Grashof Numbers

Firstly tests were performed at atmospheric conditions using plate No. 1 and chamber No. 1. It is seen from figure 4-1, that the data obtained are in very good agreement with the accepted relationships for the range of $10^5 < Gr\ Pr < 10^9$. This indicated that the apparatus and technique chosen were adequate.

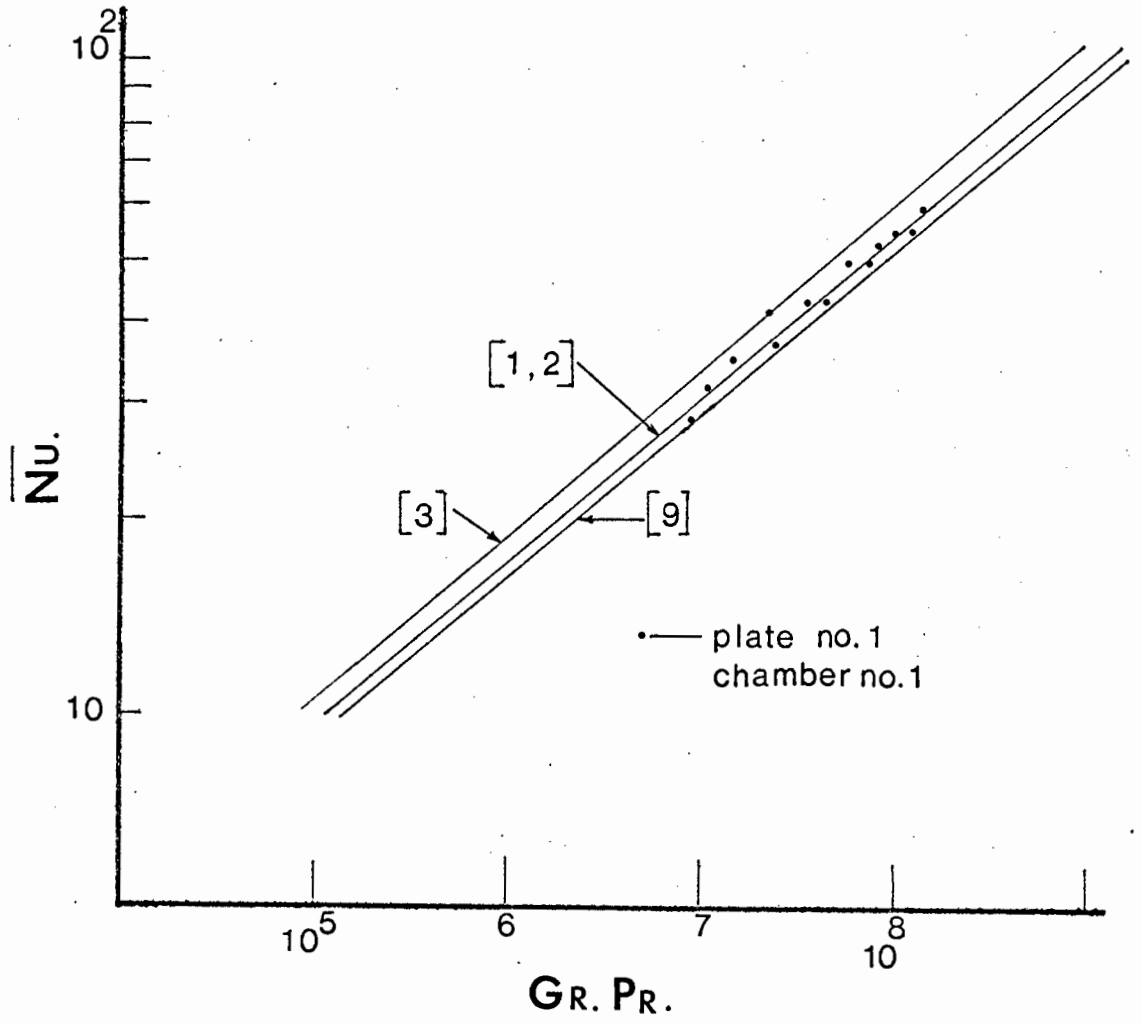

Figure 4-1.

The variation of pressure in the vacuum chamber yielded the data appearing in figure 4-2. It can be seen that down to where the arrow appears the data followed the accepted relationships with very good agreement, however below this point there was a

marked/ .....

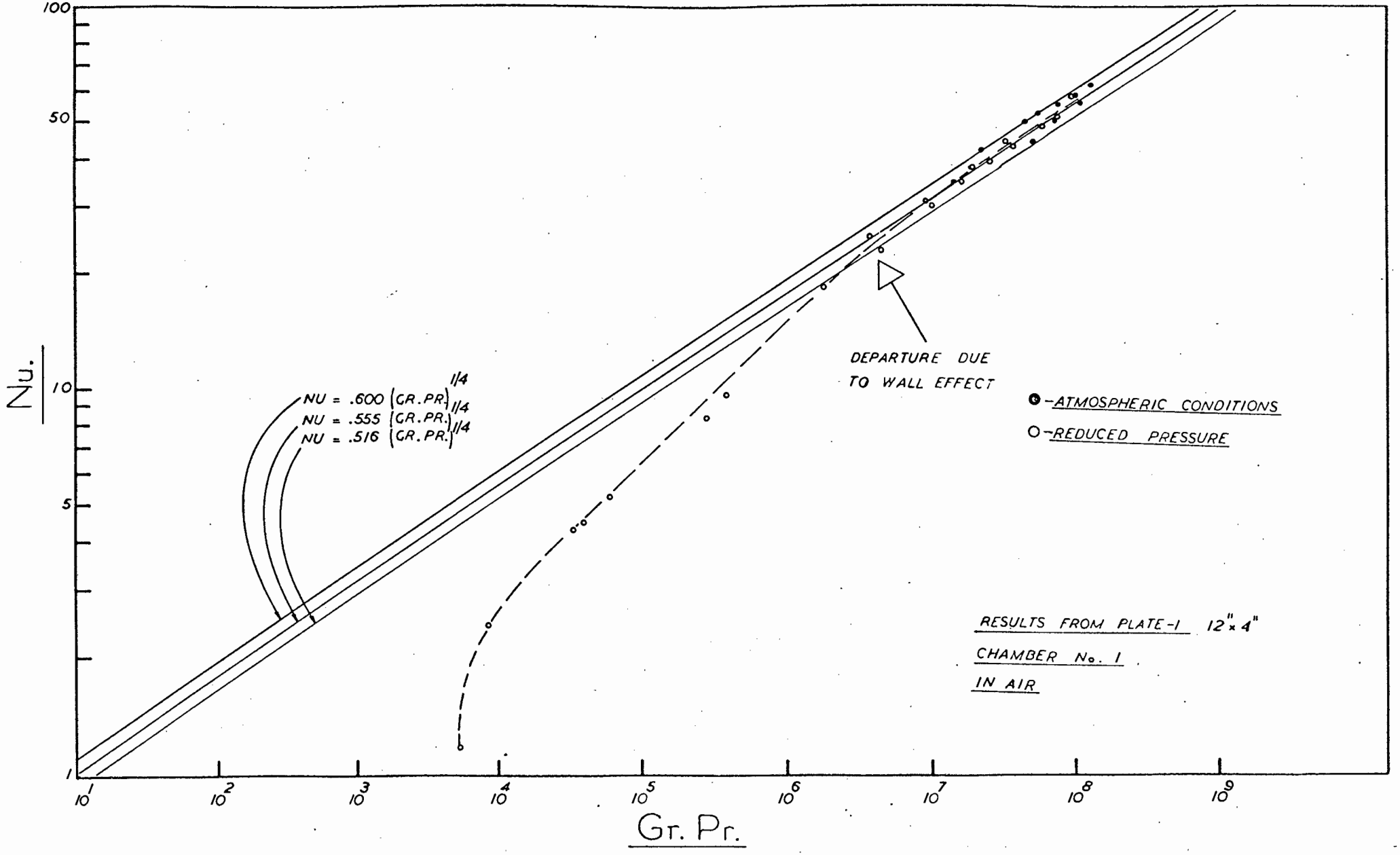
100
50
10
5
1
Nu.
NU = .600 (GR.PR.)^1/4
NU = .555 (GR.PR.)^1/4
NU = .516 (GR.PR.)^1/4
DEPARTURE DUE TO WALL EFFECT
●-ATMOSPHERIC CONDITIONS
○-REDUCED PRESSURE
RESULTS FROM PLATE-1 12" × 4"
CHAMBER No. 1
IN AIR
10^1
10^2
10^3
10^4
10^5
10^6
10^7
10^8
10^9
Gr. Pr.

FIGURE -42

marked departure. At first it was thought that this departure, which occurred at approximately 150 mm Hg. abs pressure, was due to convection having become insignificant, that is, boundary layer flow was no longer present. In order to observe the boundary layer the Schlieren apparatus was used and photographs were obtained. The photographs showed that the thermal boundary layer just became visible at approximately 150 mm. Hg. abs. pressure in the chamber. This coincided with the point where the data began to agree with the power law relationship; however what the Schlieren photographs showed was not conclusive, because the sensitivity of the Schlieren apparatus is questionable.

The density gradient in the air normal to the surface of the heated plate causes the rays of light to deflect outwards. This deflection is largest at points where the density gradient is steep, that is very near the surface. It was possible that the density gradient would not be picked up if it were very small, as it is conceivably below 150 mm. Hg. abs. pressure. So any further attempts to photograph the boundary layer were abandoned.

The Schlieren photographs however, showed the growth of the boundary layer ahead of the leading edge of the plate.

Under the assumption that something was happening to the boundary layer near the region indicated previously, and since Schlieren photography was not conclusive, it was decided to probe the temperature field extending from the vertical plate.

Eight curves of the temperature distribution for the range of pressures in the chamber of 1.75 mm Hg to 620 mm Hg abs. were obtained (see figure 4-3). The qualitative results show that there exists a thermal boundary layer below the 150 mm Hg abs. pressure "limit".

Curves E/ .....

4. This photograph was taken at approximately 320 mm.Hg. absolute pressure in the vacuum chamber. The boundary layer has intensified and the growth towards the leading edge has increased considerably.

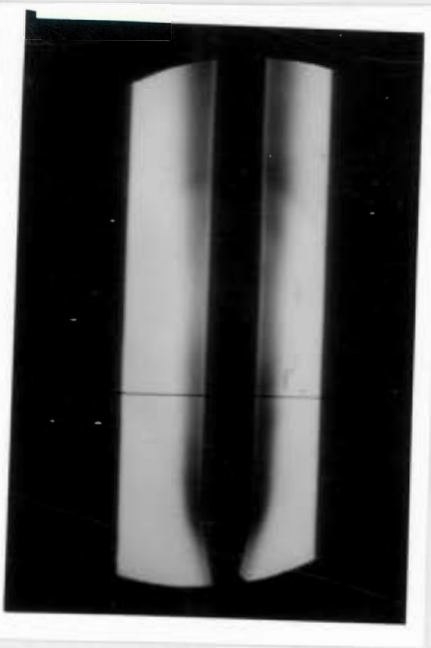

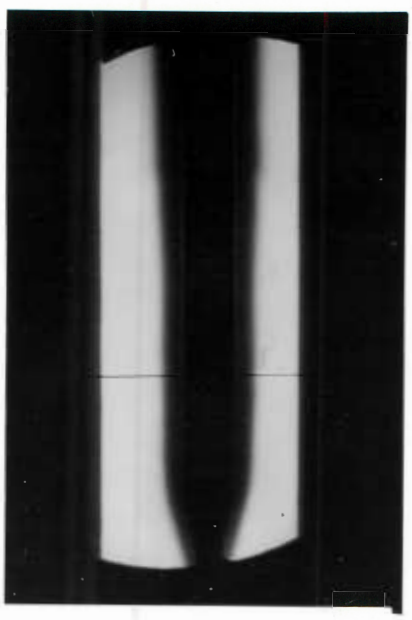

5. The pressure in the chamber is at 510 mm. Hg. abs. The plate's outline is barely visible. The leading edge is covered by the boundary layer.

6. At atmospheric pressure the boundary layer has become so intense that it obscures the outline of the plate. Apparently its thickness has not changed since it first was observed.

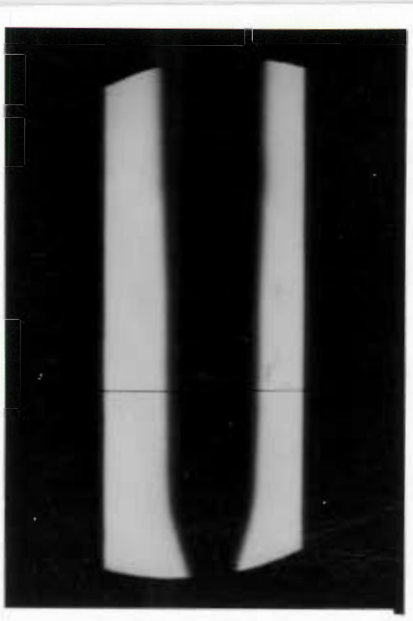

1. The vertical plate photographed at approximately 1.5 mm.Hg. absolute pressure in the vacuum chamber. The black line across the picture is a piece of wire used to focus the camera. There is no visible boundary layer.

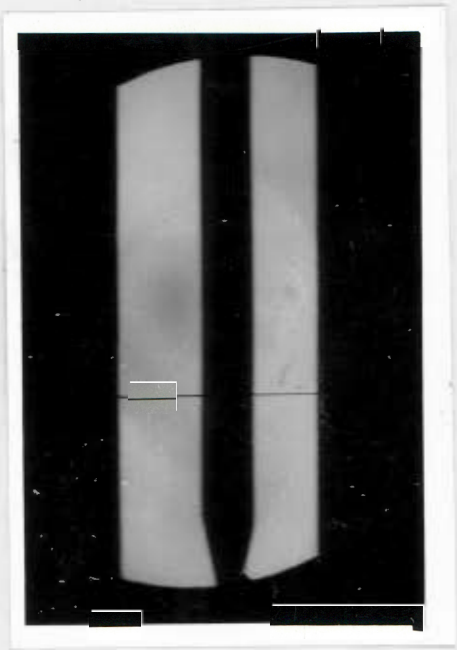

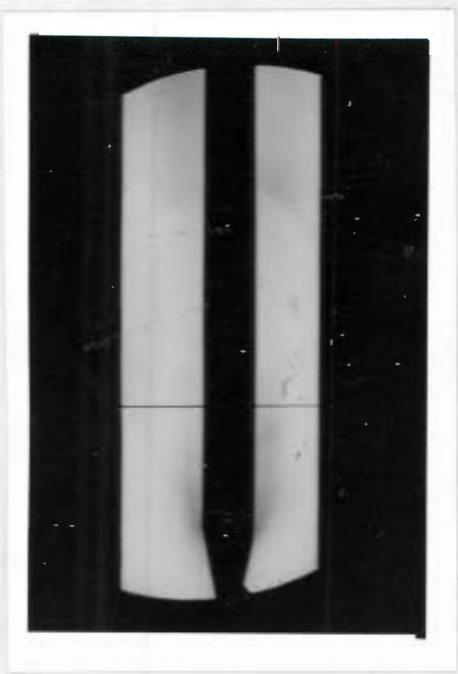

2. Photograph taken when the pressure in the vacuum chamber was approximately 150 mm.Hg. The boundary layer just becomes visible at the lower edge of the plate.

3. Photograph taken at approximately 226 mm.Hg. pressure in the vacuum chamber. The boundary layer has become more visible over the entire length of the plate. A growth towards the leading edge may be observed.

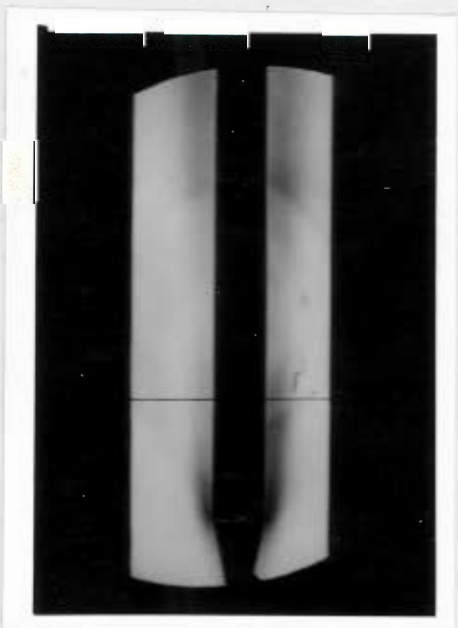

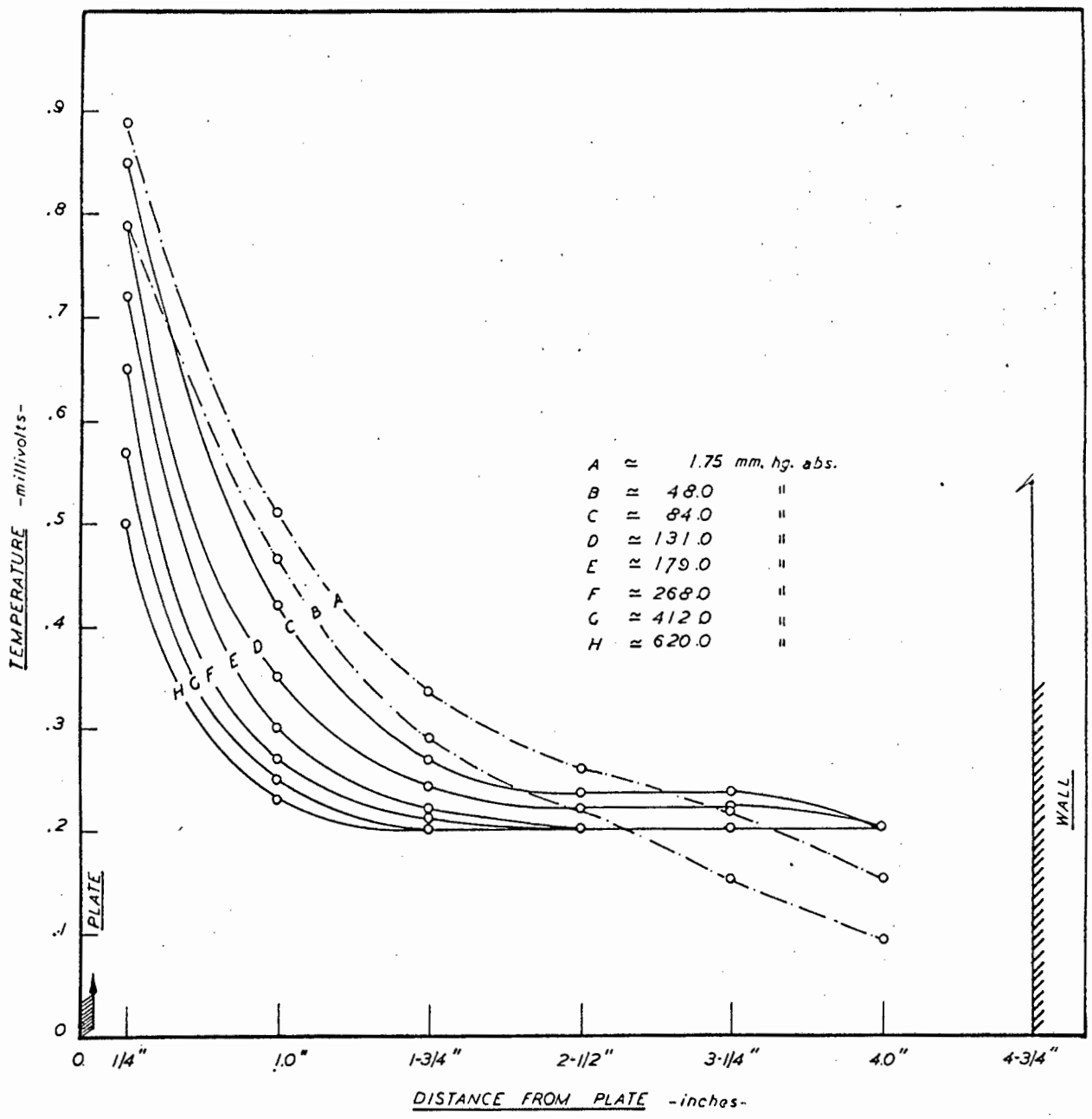

FIGURE-4.3

Probing the thermal boundary layer at different pressures.

(Plate No. 1 in Chamber No. 1)

Curves E,F, G and H showed that the temperature had levelled out, that is, the bulk fluid temperature was reached and for all practical purposes $\frac{dT}{dy} = 0$ at $y = \delta_t$.

Curves C and D showed that the bulk fluid temperature was approached and only the last thermocouple positions showed a discrepancy. Curves A and B did not behave at all as expected for the last three thermocouple positions.

The overall behaviour of the curves A, B, C and D suggested that there was indeed a boundary layer but it was being influenced by the downdraught of the air on the chamber's side.

It was shown in Chapter II that the boundary layer increases rapidly at low Grashof numbers and calculations showed that indeed the space allowed between the plate and the chamber was inadequate, therefore interference resulted.

Further evidence that it was due to the inadequacy of the enclosure for a given plate size that the results departed from the accepted relationships, was obtained when tests were performed using plates no. 2 and 4 with chamber no. 1.

It is seen from figures 4.4 and 4.5 that agreement with the accepted relationships was extended to the low Grashof number range.

Some tests were performed using plate no. 3 and chamber no. 2 investigating edge effects on the plates. The thermocouples of plate no. 3 were placed in an horizontal plane throughout the width of the plate (at the mid point) enabling detection of temperature gradients widthwise. If the thermocouples registered such gradients it would indicate three dimensional effects on the boundary layer, however the tests showed negligible temperature gradients. The results using argon as the surrounding fluid

appear/ .....

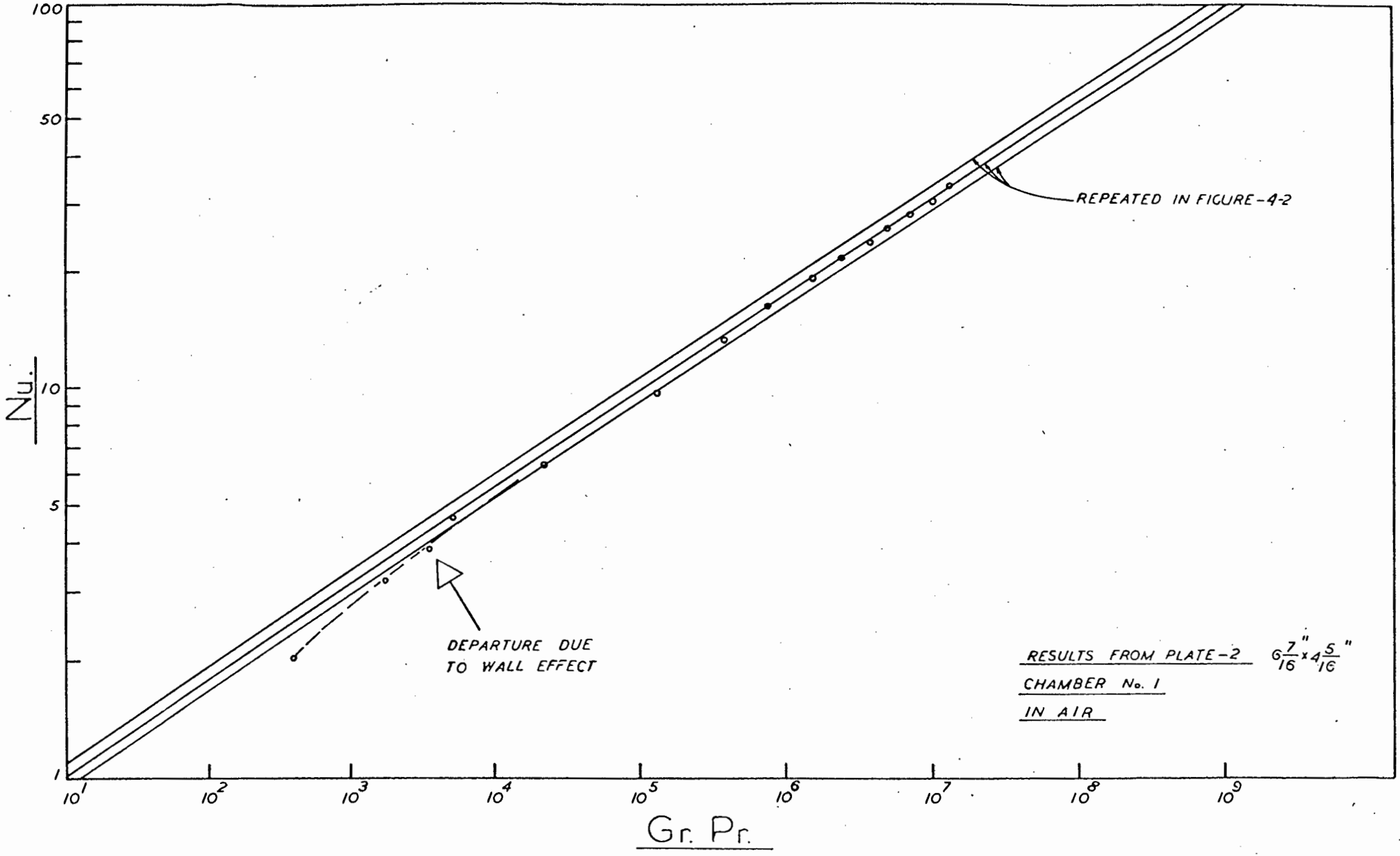
100
50
10
5
1
Nu.
10^1
10^2
10^3
10^4
10^5
10^6
10^7
10^8
10^9
Gr. Pr.
REPEATED IN FIGURE-4-2
DEPARTURE DUE TO WALL EFFECT
RESULTS FROM PLATE-2 $6\frac{7}{16}" \times 4\frac{5}{16}"$
CHAMBER No. 1
IN AIR

FIGURE-4.4

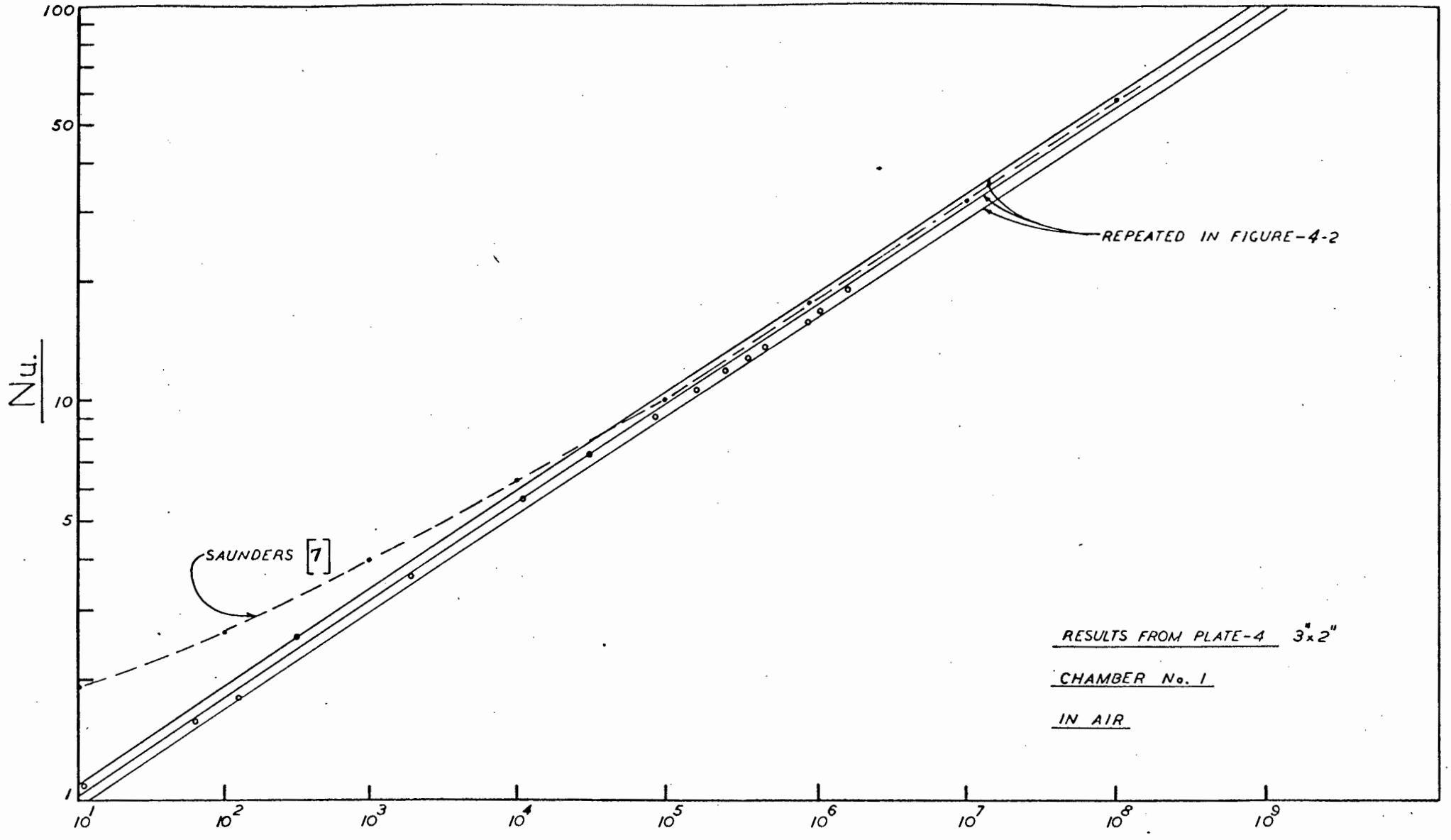
100
50
10
5
1
Nu.
SAUNDERS [7]
REPEATED IN FIGURE-4-2
RESULTS FROM PLATE-4 3"x2"
CHAMBER No. 1
IN AIR
10^1
10^2
10^3
10^4
10^5
10^6
10^7
10^8
10^9
Gr. Pr.

FIGURE-4-5

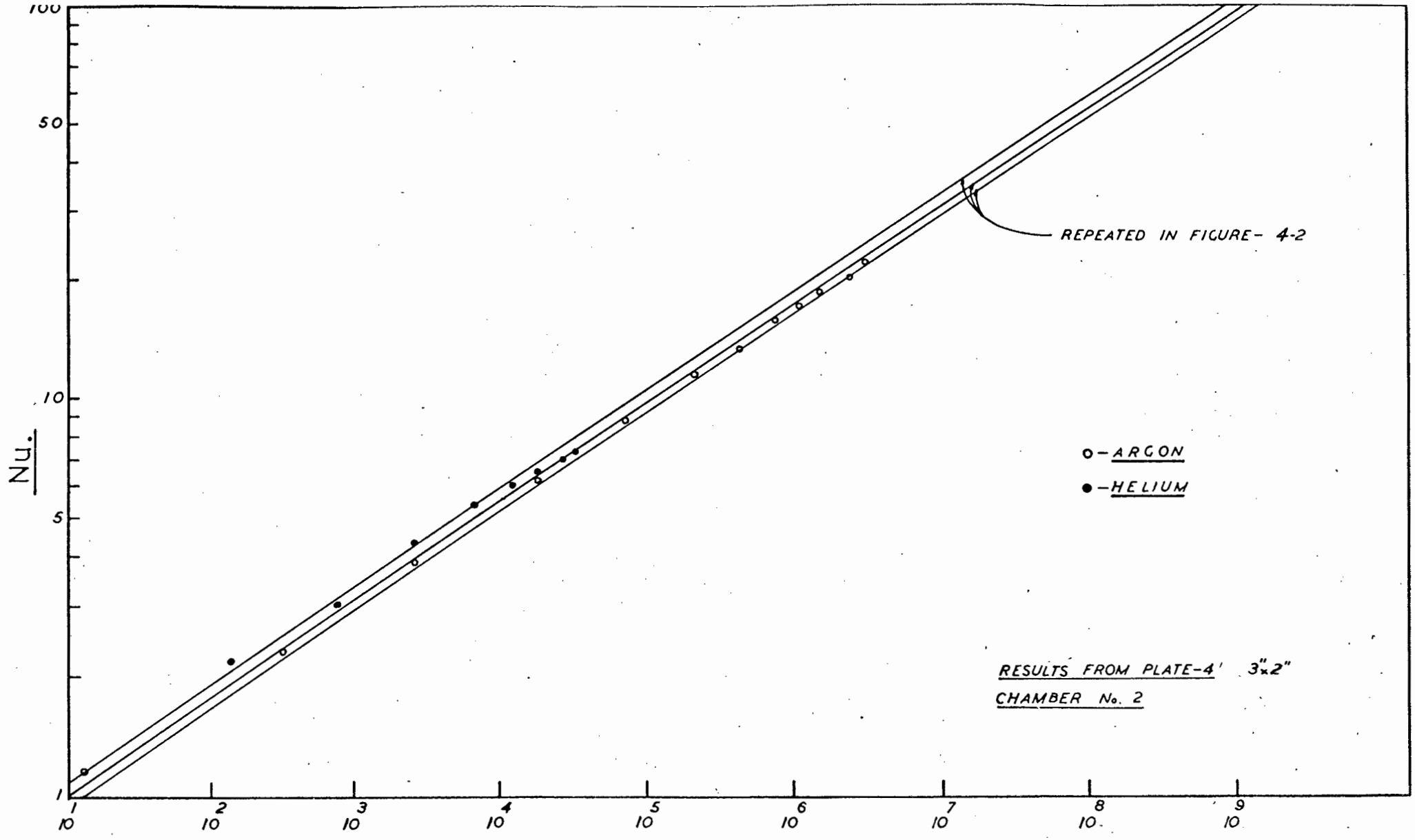
100
50
10
5
1
Nu.
REPEATED IN FIGURE- 4-2
o - ARGON
● - HELIUM
RESULTS FROM PLATE-4' 3"x2"
CHAMBER No. 2
10^1
10^2
10^3
10^4
10^5
10^6
10^7
10^8
10^9
Gr. Pr.

FIGURE-4-6

appear in figure 4-6. Here it is seen that the data followed very well the same relationship as found for air. Although the Prandtl number of argon is slightly lower than that for air, that did not affect the free convection characteristics.

Also in figure 4-6 are presented the results for helium which has a Prandtl number slightly lower than argon, but a much higher thermal conductivity. It was found that working with helium it took considerably longer to reach steady state conditions. Due to helium's higher thermal conductivity, even with higher power input than that used for argon, only half the range of Grashof numbers was covered. Again helium did not behave differently at low pressures.

Possibility of erroneous bulk fluid temperature: Since the boundary layer grew to such proportions care should be taken to ensure that the thermocouples measuring the bulk fluid temperature were not in the boundary layer region, but no such possibility exists since the thermocouples were placed at a level below and away from the leading edge of the heated plate.

The possibility of errors in the emissivity of the plates:

In figure 4-5, if a particular point from the results was taken, say when $\overline{Nu}$ = 1.57 and an error of 7% was applied on the value of the emissivity used, the results are notable. The new Nusselt number calculated is 2.46 which represents a 56.7% error over the previous value and places the result on the curve given by Saunders [7]. At the other end of the curve, where the results yielded a Nusselt number of 19.0 the same error of 7% in the value of the emissivity yielded a new Nusselt number of 19.9 which represents a 5.7% error over the previous value. The variation of percentage in error in the Nusselt numbers is due to the relative values of the free-convective heat transfer coefficient and radiation coefficient at the respective ends of the curve. It appears that the determination of the free convective heat transfer coefficient from the defining equation

$$u = h_r + h_c$$

becomes very critical at low pressures, due to the fact that at low pressures the radiation coefficient is larger by more than a factor of ten, than the free convective coefficient. Typical values are presented in the table below

Table 4.1 / ..... .

TABLE 4.1

(Using plate no. 4 chamber no. 1).

Press. mm Hg abs.	h_c	h_r
1.4	0.077	0.796
3.5	0.107	0.794
20.0	0.230	0.758
372.0	0.825	0.676
750.0	1.115	0.653

In determining the emissivity of the plates it was assumed that below 0.5 mm Hg abs. pressure, the heat transfer by convection was negligible. Therefore from the energy balance the heat input to the plate should equal the heat lost by radiation from it. Wiebelt [25] states that calorimetric methods for determining the emissivity are specially accepted as very accurate. So it becomes imperative to show that the calorimetric method used in this investigation yielded satisfactory values for the emissivity of the copper plates.

From the energy balance

$$Q_{net} = uA(T_1 - T_2) = h_r A(T_1 - T_2) + h_c A(T_1 - T_2) \qquad (4.3)$$

since

$$h_r = \frac{\sigma\varepsilon\,(T_w^4 - T_c^4)}{(T_1 - T_2)}$$

and solving for h_c in equation 1.1

$$h_c = 0.555\,\left(\frac{\rho^2 \beta g (T_1 - T_2) C_p k^3}{L\mu}\right)^{\frac{1}{4}}$$

equation 4.3 can be re-written

$$u(T_1 - T_2) = \sigma\varepsilon(T_1^4 - T_2^4) + 0.555\,\rho^{\frac{1}{2}}\left(\frac{\beta g C_p k^3}{L\mu}\right)^{\frac{1}{4}}(T_1 - T_2)^{5/4} \qquad (4.3a)$$

let $\sigma\varepsilon$/ .....

let $\sigma\varepsilon = k_1$ (constant).

and $0.555 \left(\frac{\beta g C_p k^3}{L \mu}\right)^{\frac{1}{4}} = k_2$ (constant).

$$u(T_1 - T_2) = k_1(T_1^4 - T_2^4) + k_2\rho^{\frac{1}{2}}(T_1 - T_2)^{5/4} \qquad (4.3b)$$

for simplicity assume that the temperature remains constant and equation 7.5b becomes

$$u(k_T) = k_r + k_c \rho^{\frac{1}{2}} \qquad (4.3c)$$

where $k_T = (T_1 - T_2)$

$k_r = k_1(T_1^4 - T_2^4)$

$k_c = k_2(T_1 - T_2)^{5/4}$

From the assumption that the temperatures are constant it is seen in equation (4.3c) that the convection heat transfer increases by the square root of the fluid's density.

The radiation heat transfer remains constant, which is expected since it is a function of temperature alone.

From table 1 in appendix B, when the pressure in the chamber was 0.45 mm Hg abs. evaluation of the terms in equation 4.3c) yielded that the convection contribution in the total heat transfer rate was 0.76%. Since there exists a direct proportionality between radiation heat transfer and emissivity, it is seen that the calorimetric method yielded a value for the emissivity of the copper plate within one per cent.

However the weak point in the above analysis rests on the fact that the relationship

$$\overline{Nu} = 0.555 (Gr\ Pr)^{\frac{1}{4}}$$

is assumed to hold true down to these low pressures. If the relationship is different, then obviously it can no longer be stated that the accuracy of determining the emissivity was within

one/ .....

one per cent.

As far as using values for the emissivity of the copper plate from the ones available in tables is concerned, it was found to be very impractical.

The values in the tables range from 0.04 (highly polished) to 0.87 (black oxidized), depending on the condition of the copper. However, the descriptions of the conditions are very vague and it becomes a matter of individual opinion of how well polished, tarnished or oxidized the surface may be. So it appears that the results cannot be ascertained unless the value for the emissivity of the plates is irrefutable. For this reason further tests were performed.

The surface of the vertical plate no. 4 was covered with acetylene soot for which the emissivity is known to be 0.99 [26], and chamber no. 2 was used. A higher power input was used but the surface temperatures of the plate were lower, as would be expected because the plate was able to radiate more. The results of these tests appear in figure (4-7) with particular emphasis on the lower region of Grashof numbers where deviations might be expected, but the agreement with the power law relationship is still noted.

The above-mentioned results are still a little uncertain due to the fact that there could still be some interference in the leading and trailing-edge of the flat plate, since the dimensions of the chamber were very small in that direction, plus the fact that a very high radiation coefficient was calculated due to the high emissivity of the plate.

Additional tests were performed using a radically different chamber (chamber no 3) and plate no. 5. In this set-up the chamber provided ample clearance for the leading and trailing

edges/ .....

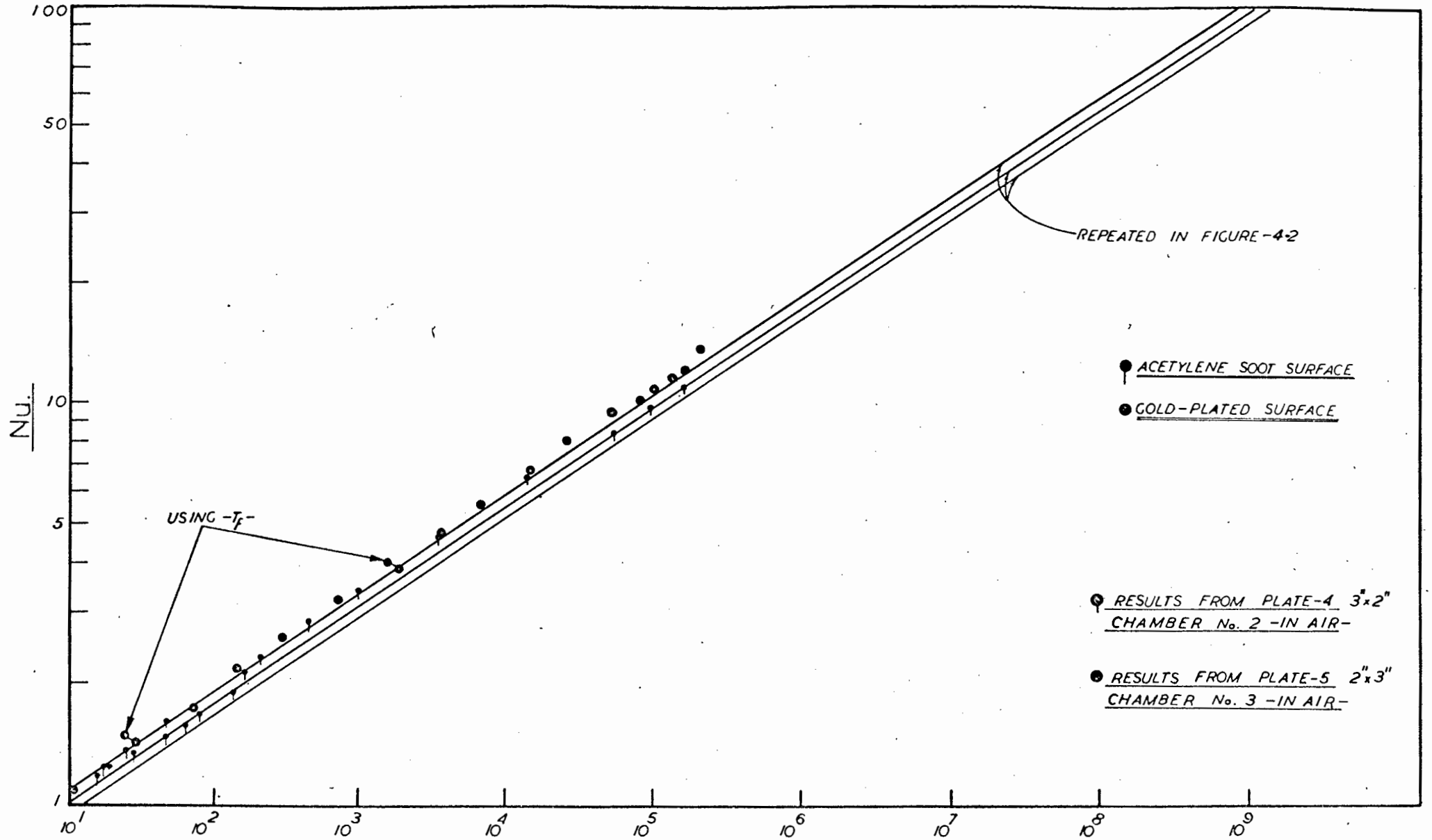
100
50
10
5
1
Nu.
10^1
10^2
10^3
10^4
10^5
10^6
10^7
10^8
10^9
Gr. Pr.
REPEATED IN FIGURE-4·2
USING $-T_f-$
ACETYLENE SOOT SURFACE
GOLD-PLATED SURFACE
RESULTS FROM PLATE-4 3"x2"
CHAMBER No. 2 -IN AIR-
RESULTS FROM PLATE-5 2"x3"
CHAMBER No. 3 -IN AIR-

FIGURE -4·7

edges of the plate. The plate's surfaces were gold-plated and measurements with a compensating thermopile yielded an emissivity of 0.071 (see appendix B). Here it should be pointed out that the emissivity of the gold plated surface was nearer the other extreme as compared to the acetylene soot, and therefore low (h_r) radiation coefficient should be obtained. Typical values are presented in the table below.

TABLE 4.2

(plate no. 5)

Pressure mm Hg abs.	h_c	h_r
3.0	0.112	0.123
8.0	0.172	0.112
48.0	0.364	0.096
482.0	0.992	0.083
755.0	1.259	0.082

The results appear in figure 4-7 and again agreement is noted with the power law relationship.

It should be noted that no correction has been made for the edge areas of the plates, as far as radiation is concerned. The author feels that this can be justified by the fact that the same areas were not included in the convective term of the energy balance either. It must be borne in mind that this investigation was performed simulating a semi-infinite plate in an infinite medium. Furthermore if such correction for radiation was made, it would have been to the advantage of this investigation as compared to Saunders' [7], since it would tend to increase the value of the energy transport by radiation and consequently yield lower values for the convective term. i.e. lower Nusselt numbers.(See example in sample calculations pg.144)

It was/ .....

CHAPTER V

Experimental Apparatus, Instrumentation, Procedure and Results of the investigation for local heat rates near the leading edge of a vertical plate.

Chapters III and IV dealt with the apparatus instrumentation, etc., involved in the investigation of average heat transfer rates from a vertical plate in free convection at low Grashof numbers. Invaluable experience was gained, which enabled the author to continue with this investigation, which deals with local heat rates near the leading edge.

For obvious reasons visual observation of the phenomenon was desired, therefore the author chose to investigate this problem by constructing and using an Interferometer.

THE MACH-ZEHNDER INTERFEROMETER

Introduction

Optical measurements in the fields of heat transfer, Gas Dynamics and Aerodynamics have a principle advantage that they permit one to investigate and arrange in such a way as to show in one picture, the entire temperature or density field around the body under study.

As an additional advantage, it is not necessary to interpose any devices such as pitot tubes, hot wire anemometers, etc., into the investigating field, which would disturb it and lead to errors in the measurements.

The limitation of an optical system is that the effect over the whole path length is integrated, thus making it especially suited for two-dimensional problems.

/ .....

In the last few years, the Mach-Zehnder interferometer has been used to a greater extent in studies of heat transfer. Basically in this instrument a parallel light beam is sent through the test section which is thereafter united with a second light beam coming from the same source but routed around the test section. In this way if certain conditions are satisfied, an interference picture can be obtained on a screen. Usually it is shown as a succession of dark and bright lines. When the refraction coefficient of any object within the light beam is changed the lines are displaced on the screen. In gases, the refraction coefficient is known to be a linear function of the density, therefore, from the displacement of the lines, the density can be determined.

Design of the Instrument.

The most difficult problem in the fabrication of the instrument is the glass plates. Their surfaces must be optically flat within fractions of a wavelength of light. The difficulty in fabrication, and therefore the cost, of such plates increases greatly with their size.

After careful study of the demands required by the problem to be investigated, the plates were chosen with a diameter of approximately four inches.

The glass plates were located in a frame sufficient in size to suit the object to be investigated, in a position which allowed extremely accurate adjustments. Vibrations or deformation of the frame were diminished by rigid construction and shock absorbent pads (see photograph of the complete instrument: page (85).)

Main Interferometer Frame.

The frame was constructed from $\frac{1}{2}$-in aluminium bars 6-in wide

with/ .....

with $\frac{1}{4}$-in aluminium sheet for the sides bolted at short intervals for rigidity. The frame was suspended on short legs resting on anti-vibrational mountings. The sizes of the apertures were determined by the size of object to be studied (5-in diameter holes).

Integral Components

Monochromatic light from a mercury lamp (1) is united by a condenser (2), passes through a green filter (3) onto an iris (4) and through the lens (5) where it is established as a parallel beam. The beam is split by a half mirror (plate 1) into two parallel beams. One of the beams is fully reflected by (plate 2) and passes through the half mirror (plate 4) where it is united with the other beam, which is reflected from the full mirror (plate 3). The combined beam falls onto a screen (6) and the image is photographed by the camera (7).

Optical Plate Suspension and Adjustments.

Although it was found that once the interferometer was adjusted it remained so, and any further slight adjustment required only movements of plates 3 and 4, initially, when all plates were mounted, various degrees of freedom were provided.

For plates numbers (1) and (4) the following degrees of freedom are possible:

Vertical movement (up and down).

Lateral movement (perpendicular to the long axis [horizontal] of the frame).

Rotation of the plates (around the vertical axis of the frame).

Tilt of the plates (with respect to their support).

For plates numbers (2) and (3) the following degrees of freedom are possible:

Translation/ .....

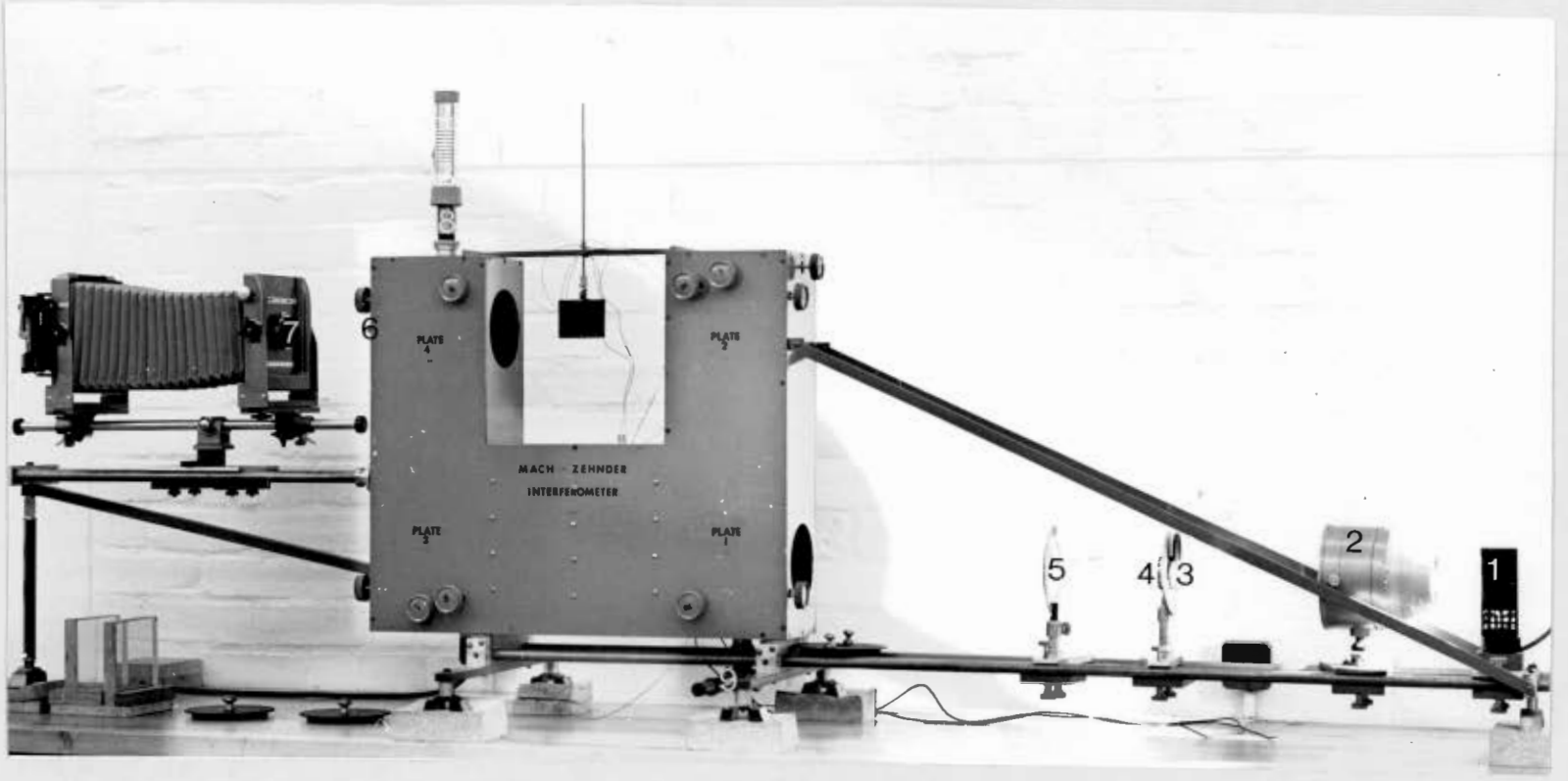

THE MACH-ZEHNDER INTERFEROMETER CONSTRUCTED AND USED BY THE AUTHOR

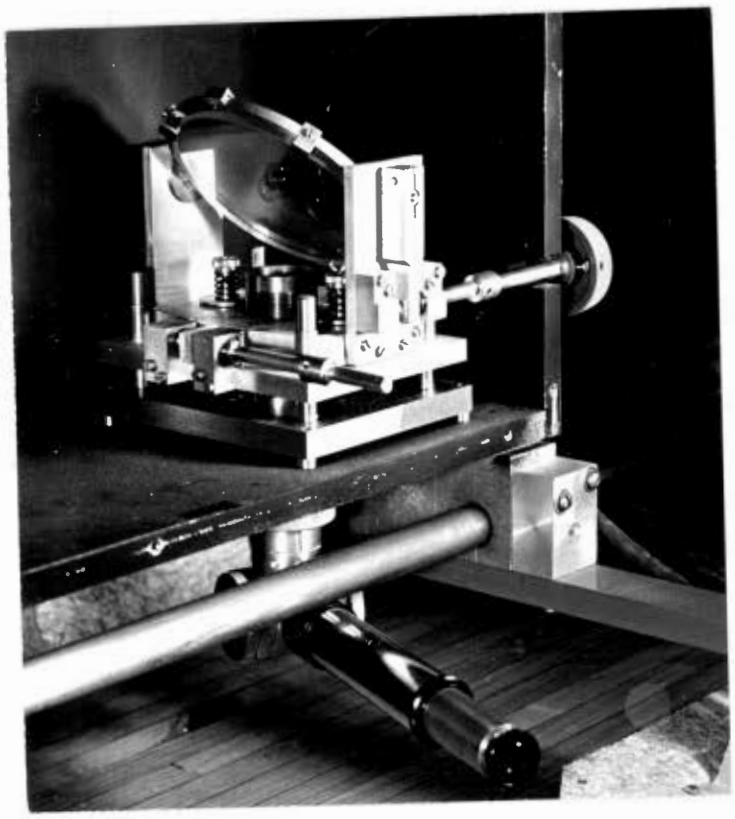

Suspension and controls of plate no. 1
(half mirror)

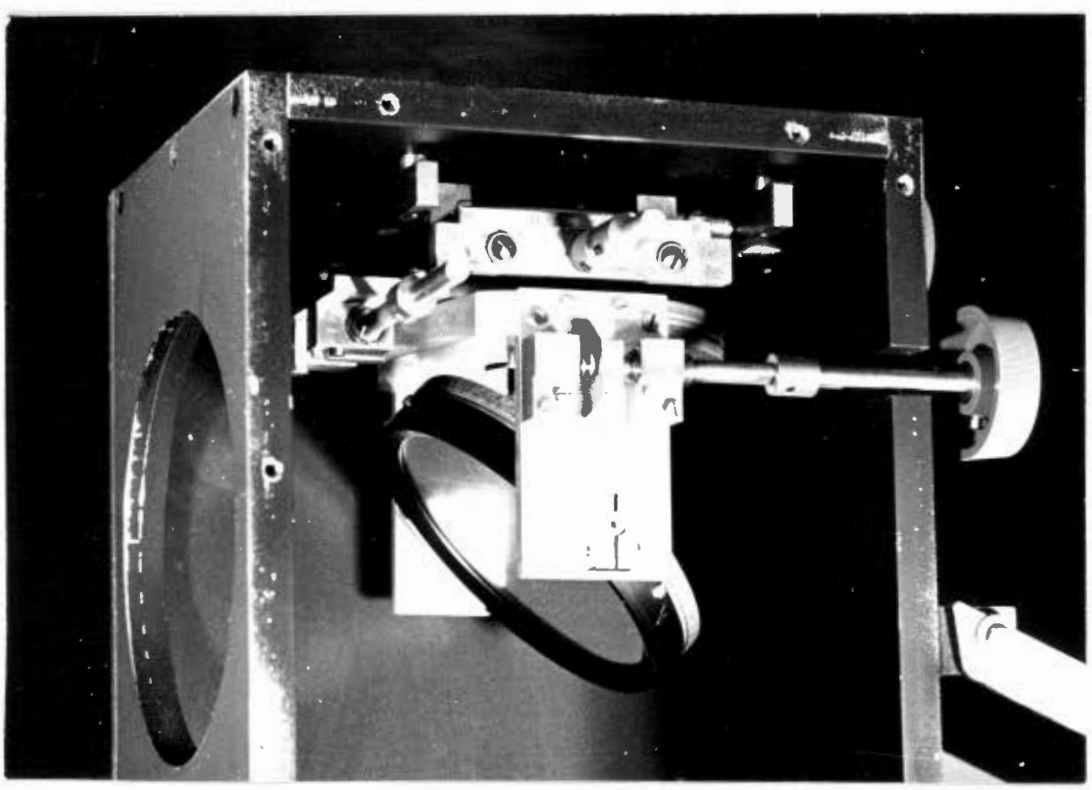

Suspension and controls of plate no. 2
(full mirror)

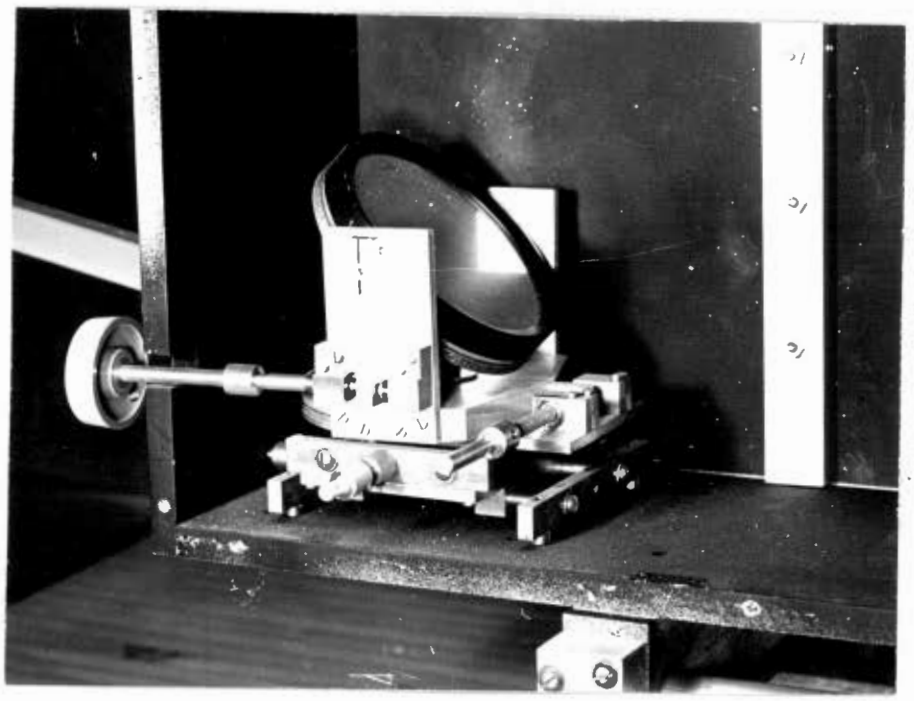

Suspension and controls od plate no. 3
(full mirror)

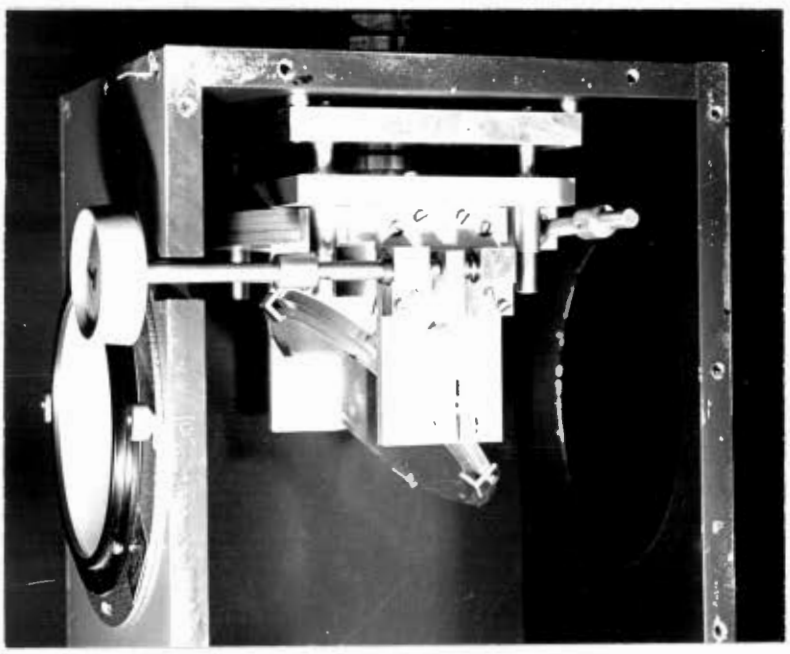

Suspension and controls of plate no. 4
(half mirror)

Translation (along the horizontal axis of the frame).

Lateral movement as in (1) and (4).

Rotation as in (1) and (4).

Tilt as in (1) and (4).

Furthermore, plates (1) and (4) were mounted in such a way as to enable a cross image (8) projected from behind plate (4) to be viewed under plate (1), through a telescope (9). When the cross image was projected it appeared double when viewed from (9) if the interferometer was out of adjustment. By manipulating the controls of plates (3) and (4) the double images coincided, indicating that all mirrors were now parallel to each other and the interferometer adjusted, with fringes appearing in the field. This adjustment was time-consuming and required extreme patience, but once effected, it remained so because of the rigidity of the frame. (See photographs of mountings and controls for the plates).

Tests.

The instrument was tested for ease of adjustment, for its capacity to maintain its adjustment, for illumination, for resolving power for the interference lines and for straightness of the lines, and was found to be satisfactory in all these respects.

The theory of interference fringes and the derivation of equations used in evaluating the interferograms are presented in most of the references in the literature. For our purpose a brief summary of the relations used will suffice.

The type of interference pattern used for a particular study may be varied by proper adjustment of the optical system.

The undisturbed field of interference fringes may be adjusted to any desired fringe spacing or direction. The width of the fringe may be increased until one fringe covers the entire field

of/ .....

of view. This is referred to as the adjustment for infinite fringe width. Temperature distributions are determined from the interferograms by measuring the fringe displacements. The fringe displacement at a point in an interferogram is the change in optical path length in wavelengths of light through that part of the field, due to the disturbance in the test section. If the interferometer has been adjusted for infinite fringe width, the fringes appearing in the field are lines of constant phase change or isodensity lines.

In the case of a vertical plate with the fringes oriented perpendicular to the surface, each fringe is, in effect, a plot of the temperature distribution in the air adjacent to the plate. The plate surface temperature is indicated by the displacement of the fringe where it intersects the plate surface, and the slope of the fringe at the plate surfaces is related directly to the rate of heat loss from the surface by convection. Since the fluid velocity at the surface is zero, the heat from the surface is transmitted to the first layer of fluid by conduction so that the heat flow may be described by the conduction equation:

$$Q = -k \left.\frac{dT}{dy}\right|_{y=0} \qquad (5.1)$$

The value of the thermal conductivity of the fluid is taken at the surface temperature. The value of the temperature gradient at the surface may be obtained from the evaluation of the interferogram. Temperatures are evaluated using the following equation which relates the fluid temperature change ΔT, length of the model parallel to the light beam L, wavelength of light λ, refractive index for air n, the undisturbed fluid temperature T_∞, and the fringe shift ΔN:

$$\Delta T = \frac{T_\infty \, \Delta N}{\frac{L}{\lambda}(n-1)-\Delta N} \qquad (5.2)$$

The Vertical/ .....

The Vertical Plate.

In order to obtain local Nusselt numbers near the leading edge, a new plate was constructed having the following dimensions: Height 2,5-in, width 4.0-in and thickness 0,197-in. The plate was equipped with six copper-constantan thermocouples spaced 0,393-in apart starting from the leading edge. These thermocouples were provided simply in order to verify the temperature of the plate when evaluated using equation (5.2).

Instrumentation.

The following instruments were used in this investigation:

(a) Power input to the plate was regulated by means of a variable transformer.

(b) A portable Cambridge laboratory potentiometer was used to monitor the plate thermocouples.

(c) A mercury barometer and wet bulb thermometer were used to obtain ambient conditions for the determination of the refractive index of air.

(d) A travelling microscope was used to evaluate the interferogram.

Procedure.

The interferometer was adjusted for wedge fringes field and when steady state conditions were established for the plate, a photographic record was taken using 4" × 5" positive negative polaroid film. The plate thermocouples were recorded, as well as ambient pressure and wet and dry bulb temperatures.

From the ambient conditions and the use of tables [27] the refractive index of air was evaluated. From the inteferogram (see samples) the plate temperature was evaluated using equation (5.2). In each case the temperature evaluated was identical to the one

indicated/ .....

The leading edge photographed with the interferometer adjusted for infinite fringe field.

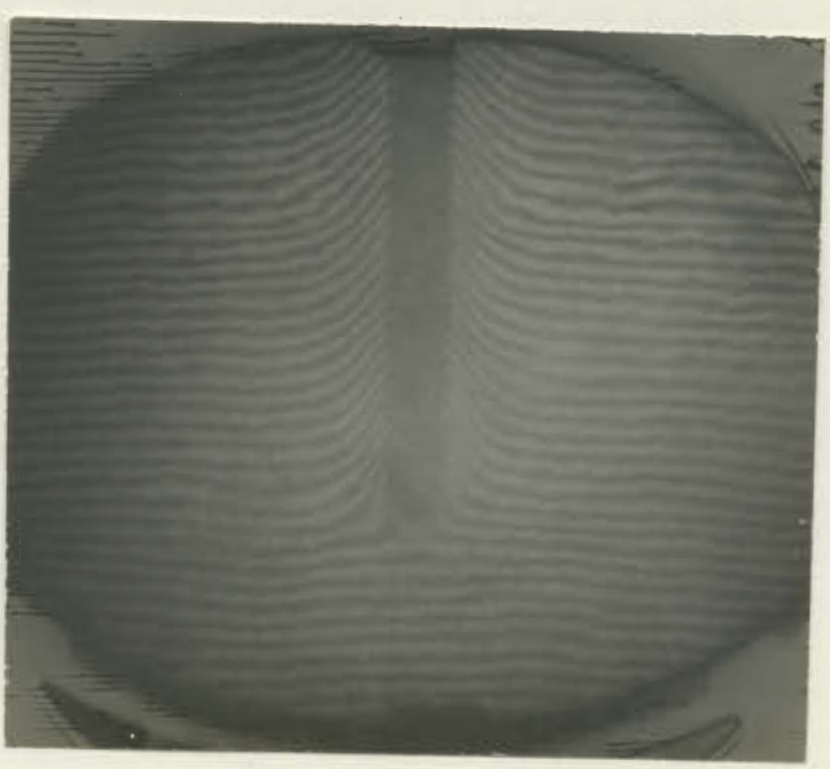

The leading edge photographed with the interferometer adjusted for wedge fringe field.

indicated by the corresponding thermocouple on the plate.

The heat flow from the surface was calculated using the conduction equation (5.1). The values of the temperature gradients at the surface were obtained from the interferogram using the travelling microscope, for any desired distance from the leading edge, and the thermal conductivity of the air was evaluated at the plate's surface temperature.

The heat loss from a surface by convection is usually calculated from the relation

$$q = h_c (T_w - T_\infty) \qquad (5.3)$$

and from the above the local free convective coefficients were evaluated, and subsequently the local Nusselt numbers.

The local Grashof numbers were evaluated at the film temperature as defined previously. The results of this investigation appear in figure (5.1) showing excellent agreement with equation (2.12) derived in Chapter II by integral methods, and equation (1.2) derived by Schmidt and Beckmann [9], away from the leading edge. i.e. at high Grashof numbers. However, below $Gr \approx 5 \times 10^3$ it is shown conclusively that the leading edge effects influence considerably the local heat rates.

An interesting fact comes to light when examining the points of departure from the power law relationship.

The departure occurs at the same distance from the leading edge (≈ 0.5in) but due to different temperature differences it occurs at different Grashof numbers. In other words as the overall temperature difference $(T_w - T_\infty)$ decreases, for the same distance from the leading edge, the Grashof numbers become smaller and the agreement with the power law relationship is extended!

This /.....

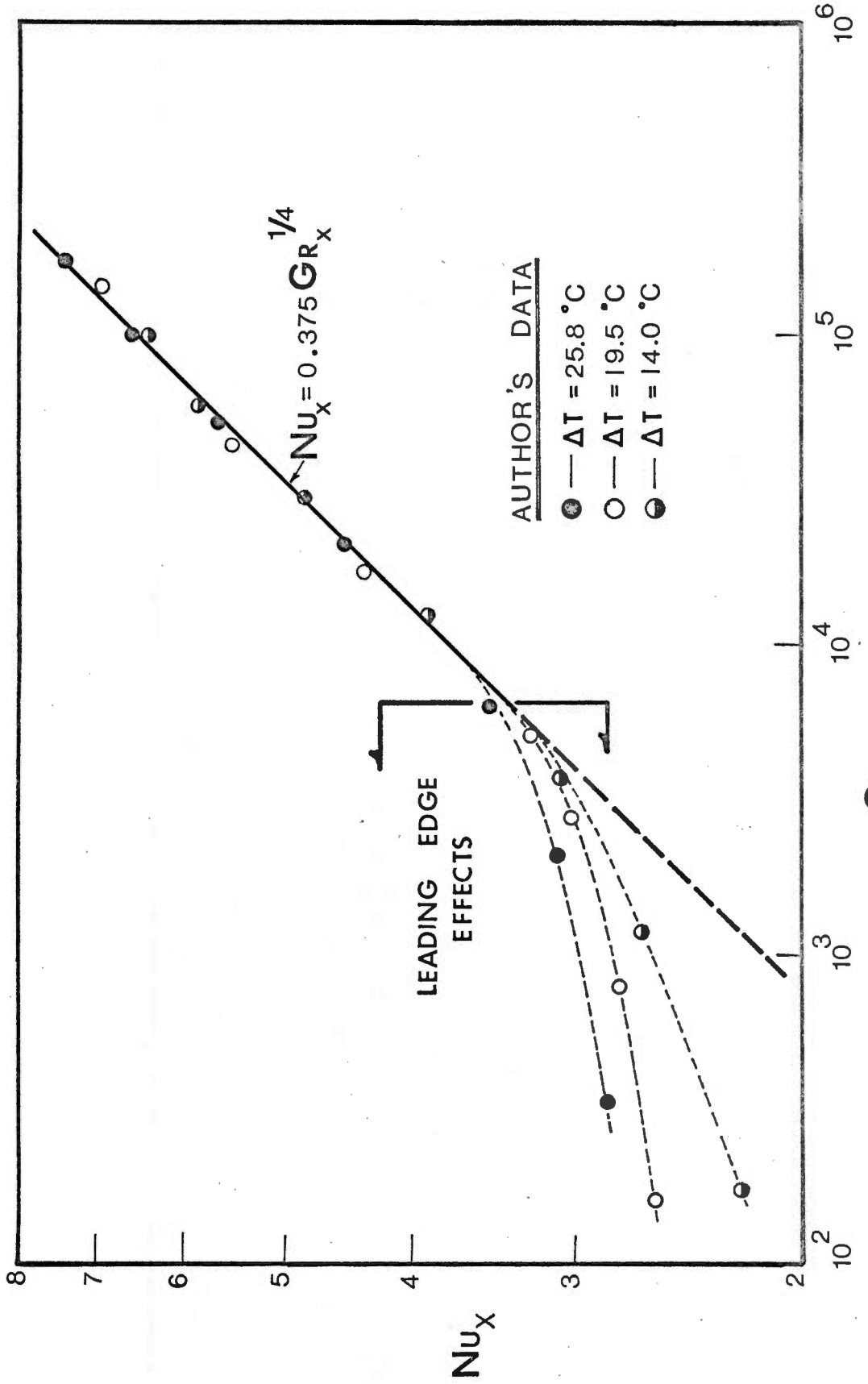
$Nu_x = 0.375 Gr_x^{1/4}$
AUTHOR'S DATA
● — ΔT = 25.8 °C
○ — ΔT = 19.5 °C
◐ — ΔT = 14.0 °C
LEADING EDGE EFFECTS
Nu_x
Gr_x
8
7
6
5
4
3
2
10^2
10^3
10^4
10^5
10^6

FIGURE 5·1

This phenomenon is partly explained by Scherberg [28] who demonstrated that the influence of the leading edge is on the vertical positions of the boundary layer and not on the thermal or velocity form.

Inspection of equation (2.11)

$$Nu_x = \frac{2x}{\delta}$$

also substantiates the above. For a constant x if the Grashof number is increased due to temperature difference, the effect is to decrease the boundary layer thickness δ, decreasing the resistance to heat flow and subsequently predicting higher Nusselt numbers.

Sources of Error.

The use of the interferometer in this investigation proved to be greatly advantageous.

Since there is no calorimetric method involved in gathering data the problem is greatly simplified. There is no need to account for radiation losses from the plate which involves a rather cumbersome procedure for the determination of the plate's emissivity as seen in Chapter IV. The method of suspension of the plate did not pose any problem either, because there was no need to account for any conduction losses. The slope of the fringes near the surface is directly related to the heat loss by convection.

The fringes may be distorted by disturbances placed in the path of the light, such as windows, however, in our case, there was no need to place windows on either end of the light path, therefore there is no possibility of disturbances along the path of ray to be integrated and included in the fringe shifts.

The relative positions and widths of dark and bright fringes may be distorted by poor processing of the negatives, but using positive-negative polaroid film the negatives were obtained on the

spot/ .....

spot, therefore no error could be introduced in this manner. Vibrations of the interferometer may cause oscillation in the fringe pattern but those were eliminated by suitable anti-vibration mountings. An ultimate limit is imposed by the accuracy with which fringes can be measured.

The author used a travelling microscope to evaluate the fringe shift and temperature gradients. Proof that this was done accurately is given by the fact that the surface temperatures evaluated from the inteferograms were identical to the ones measured with the thermocouples embedded in the plate.

CHAPTER VI

Experimental Apparatus, Instrumentation, Procedure and Results of the investigation for the effects of Variable Wall Temperature on the Boundary Layer.

In order to verify the results of the analysis presented in Chapter II section d, the following equipment was used:

Vertical Plate.

The plate was constructed in a similar manner to the previous plates, with one exception. Whereas previously the heating element was made with the strips running along the height of the plate (figure 3.3) for this plate the strips ran along the width. This was done in order to enable control of power input at different heights of the plate. The winding was divided into ten sections, each having the resistance of 20.5 ohms and coupled in parallel to each section, was an external resistance of the pot kind, with a range of zero to 250 ohms. The heating element was sandwiched by two 1/16-in thick steel plates which were chromed. The plate was equipped with six iron-constantan thermocouples. The first one was embedded 11/16-in from the leading edge of the plate, and each subsequent one at 2.0-in intervals. The overall dimensions of the plate were

length 12-in, width $6\frac{1}{4}$-in, thickness $\frac{1}{4}$-in.

Environment Control Chamber

For measurements of temperature profiles from the plate it was necessary to use a chamber, so that ambient conditions could be maintained constant and free from any disturbances.

The chamber employed had a test section of 9 × 9-in × 24-in where the plate was suspended. A suitable bell-mouth with wire mesh straighteners was attached to the inlet of the test

section/ .....

section.

One of the sides of the test section was removable for easy access to the plate, and equipped with railing and a suitable slot in the middle, where the traversing mechanism could operate.

Traversing Apparatus.

The hot-wire probe used in obtaining the temperature profiles, was mounted in a traversing mechanism constructed for the purpose (see figure 6.1). The traversing mechanism was capable of movement to the accuracy of 1/100 of a millimeter.

Hot-wire Probe.

The sensor of this probe made by DISA is 0.4 mm long, 1 mm dia. platinum wire, spot-welded to the tapered ends of the stainless steel prongs. The prongs are embedded in a 2 mm dia. ceramic stem body. The probe operates as a resistance thermometer for measuring the temperature of gases. The probe resistance is approximately 50 omhs at 20°C. The temperature coefficient of resistance is approximately 0.35% per °C. The probe's sensitivity to flow is kept very small by using low current, 1.0 mA or less. At a velocity of 60 m/sec the error in the temperature signal due to the velocity, corresponds to about 1.0°C. This makes this particular probe very suitable for temperature measurements in free convective phenomena, since the velocities involved are considerably smaller then 60 m/sec.

The sensor was mounted on a right angle support to ensure that while probing, the sensor's prongs were exposed to the same temperature field as the wire across them, thus minimizing any errors due to conduction from the wire to the prongs. (See figure 6.1a)

Additional Equipment.

A DISA anemometer unit as shown in figure 6.2 was employed for recording the probe sensor's signal. A constant voltage

transformer/ .....

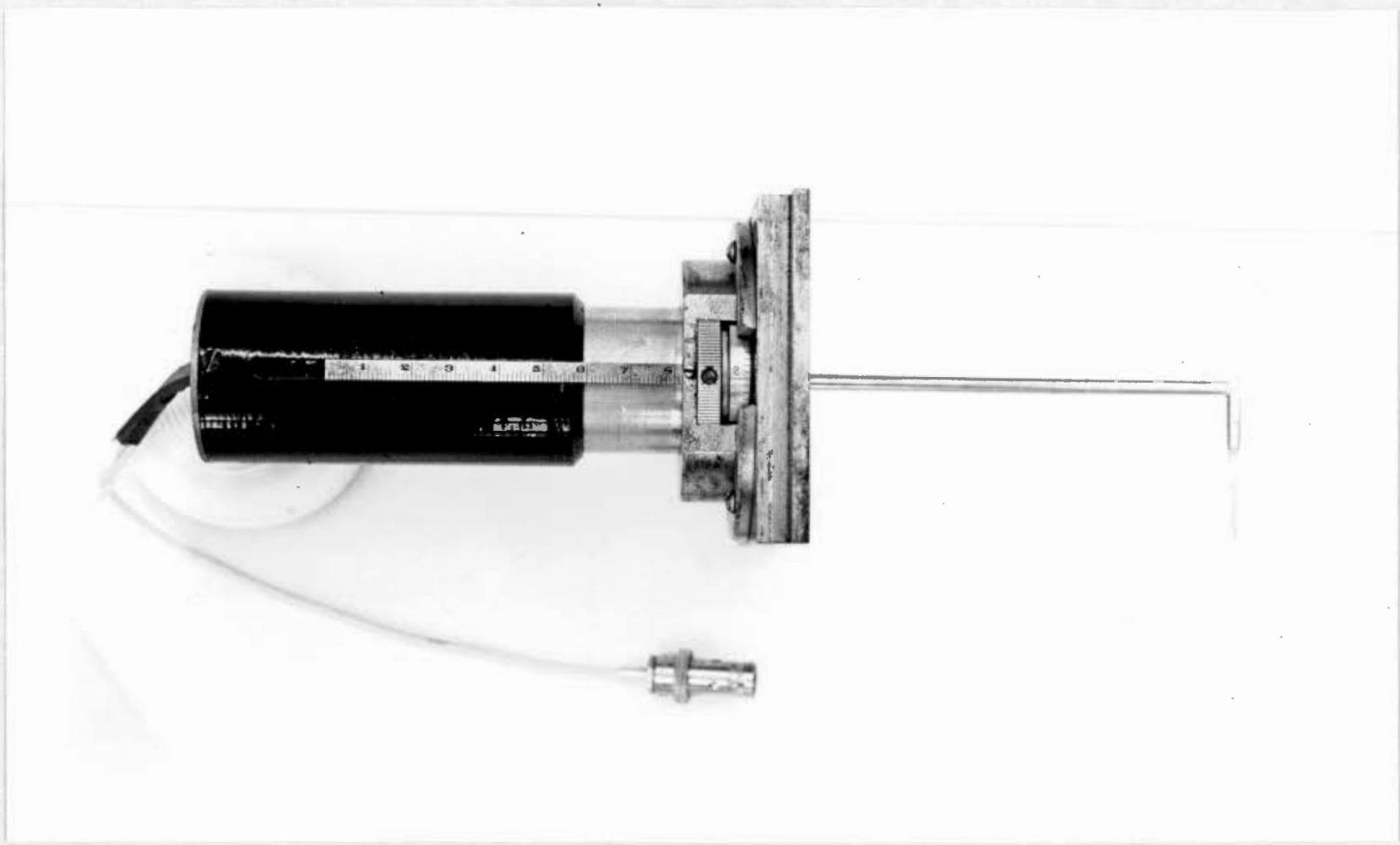

Fig. 6-1a Travessing mechanism and probe used in obtaining temperature profiles

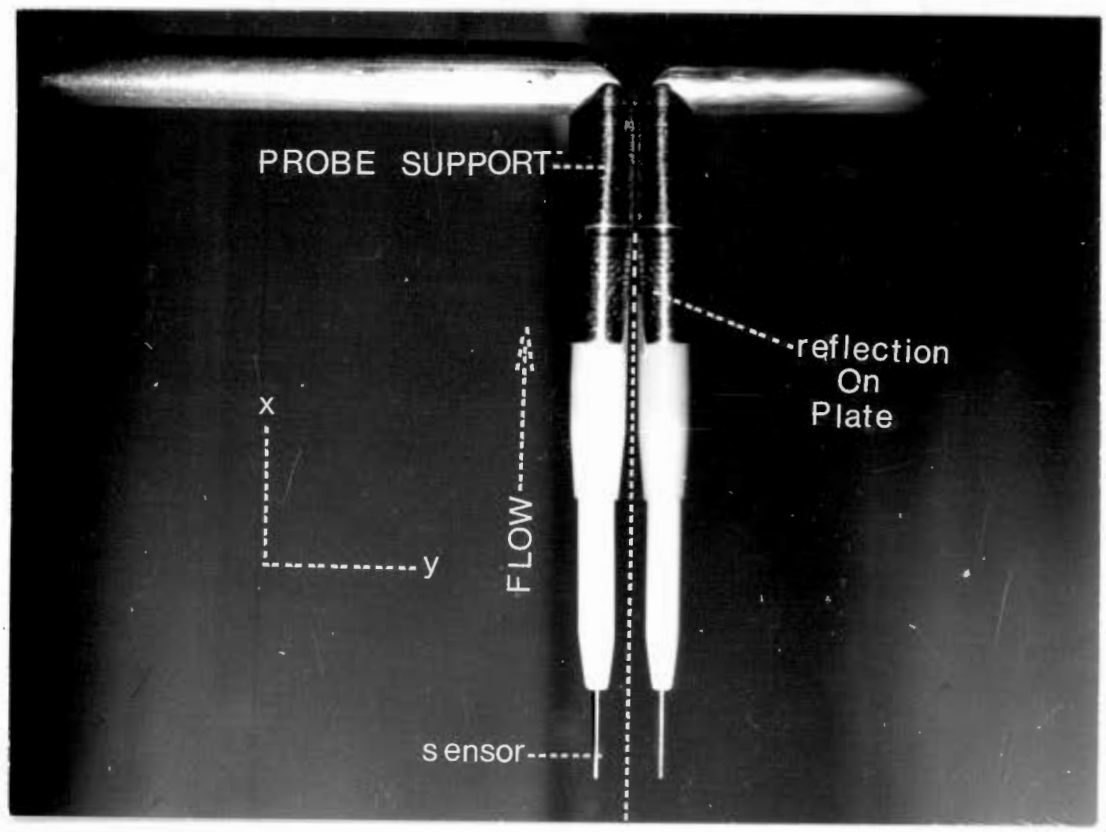

Fig. 6-1b Hot wire probe photographed in position for first reading. (Touching the plate)

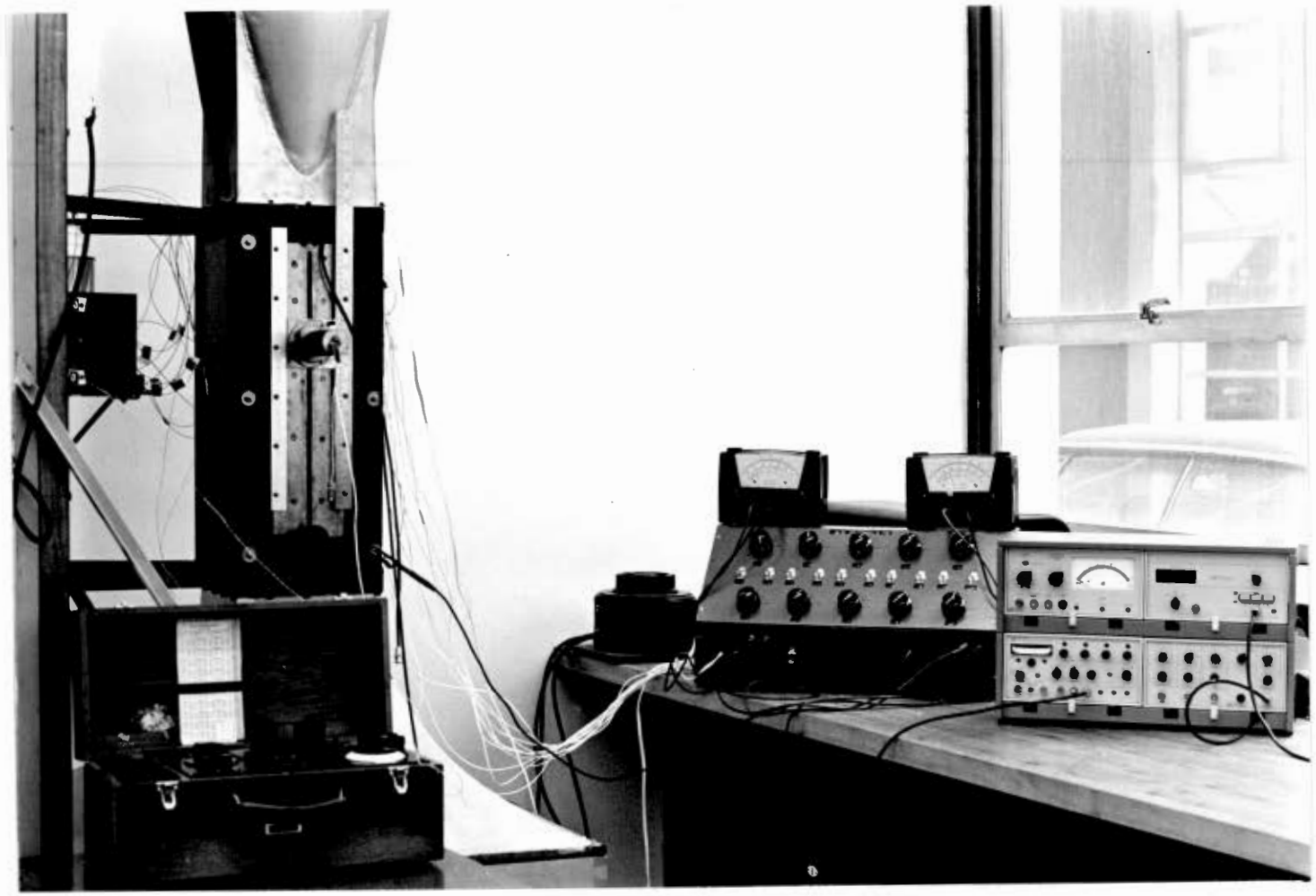

Fig. 6-2 General view of the apparatus for probing the thermal boundary layer

transformer supplied the power for the vertical plate. The power was regulated by a variac. An assembly of 10 variable resistances (0 to 250 Ohms) coupled in parallel with the plate's windings was used to further control the power input for each section of the heating element. A potentiometer was used to monitor the plate's thermocouples. The probe was earthed to the plate's supports through an Ohmeter which indicated when the probe touched the plate.

Procedure and Results.

The following is the procedure adopted for obtaining the temperature profiles.

Firstly, the probe was calibrated in order to determine its temperature coefficient of resistance. This was done by placing the probe in an oven where the temperature of the air was determined by thermocouples and glass thermometers. The data collected for different temperatures were applied in the following expression

$$R = R_o(1 + \alpha\Delta T) \qquad (6.1)$$

where R is the resistance of the probe at any temperature T above the reference temperature, R_o is the resistance of the probe at the reference temperature; Thus α the temperature coefficient of resistance was determined. (See figure 6.3 for probe calibration).

The procedure adopted for collecting data on the temperature profiles was verified by duplicating existing data from an isothermal wall. The plate's power input was so regulated that the thermocouples embedded on the plate showed identical values along the height of the plate and the probe was traversed at 2.69-in, 4.69-in and 6.69-in from the leading edge. i.e. at the position of thermocouples Nos. 2, 3 and 4.

Due to the thickness of the probe's support, the sensor was 2.1-mm away from the plate for the first reading (see figure 6.1b).

This was/ .....

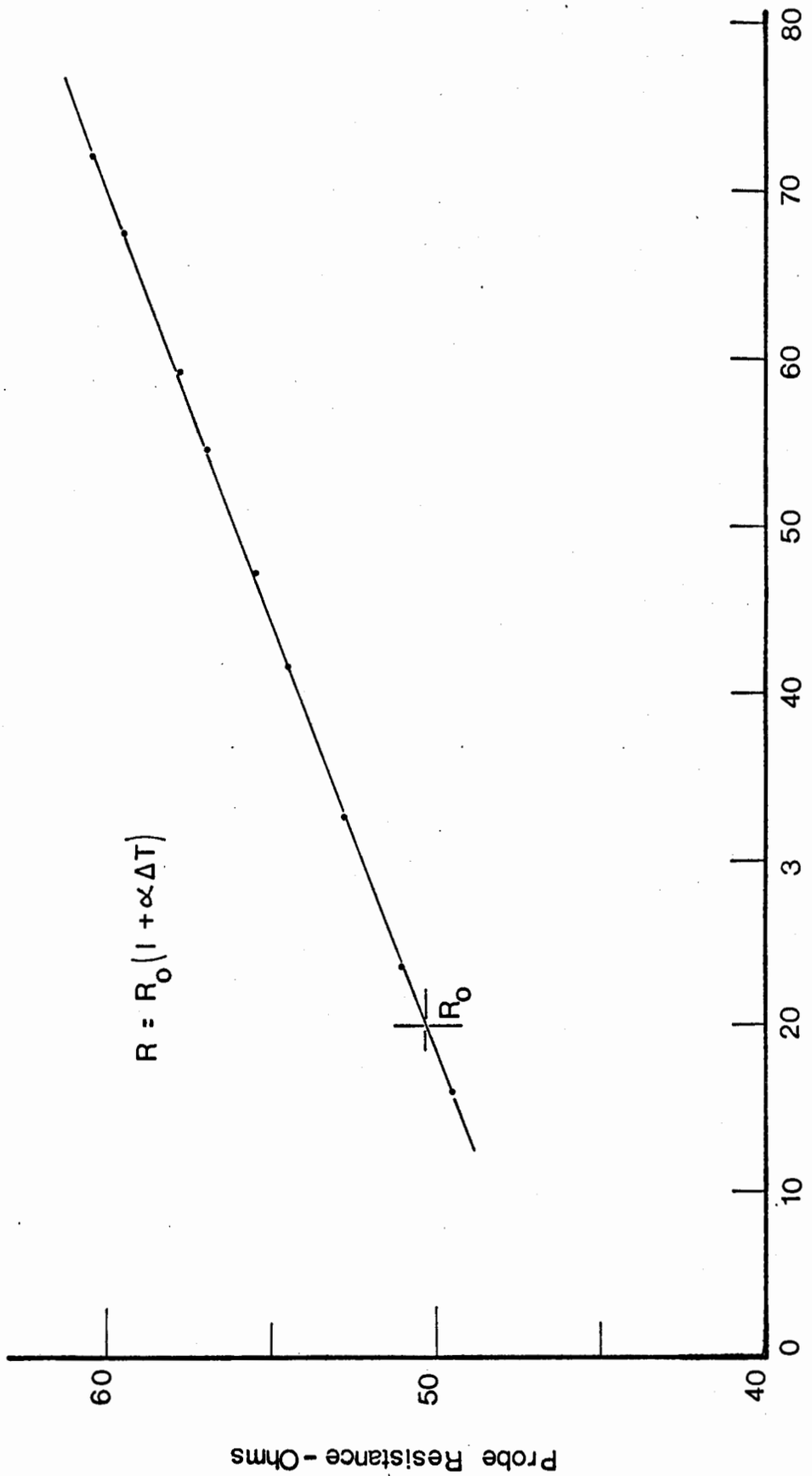
Probe Resistance - Ohms
60
50
40
0
10
20
30
40
50
60
70
80
Temperature - °C
$R = R_o(1 + \alpha \Delta T)$
R_o

FIGURE 6·3

This was established by using a height guage on the probe and also verified with a travelling microscope. Further verification of this initial distance was observed when evaluating the data. By extrapolating the resistance readings near the plate (see figure 6.4) the resistance extrapolated at 2.1-mm gave an identical temperature to that indicated by the thermocouple in the plate.

The traversing was done and data were collected in the following manner. The initial reading was taken just as the probe's support made contact with the plate, which as we have already seen, positioned the sensor 2.1-mm away from the plate's surface. During the following millimeter, readings were taken every 1/10 of a mm. For the next millimeter, every 2/10 of a mm and afterwards for every 1/2-mm. Traversing was stopped when practically no more change of resistance was indicated by the instrument which meant that the probe was in the undisturbed fluid.

From the data, the dimensionless parameters

$$\frac{\theta}{\theta_w} = \frac{T - T_\infty}{T_w - T_\infty} \quad , \quad \eta = \frac{y}{x} \left(\frac{Gr_x}{4}\right)^{\frac{1}{4}}$$

(see figure 1.1 which is the solution for an isothermal wall), were evaluated and the results appear in figure 6.5. The excellent agreement with the theory observed, indicated that the procedure adopted was quite adequate, so we proceeded to obtain data for a variable wall temperature distribution.

The power input to the plate was, after considerable adjustments, set to give a linear wall temperature distribution. By continuously monitoring the plate's thermocouples, it was established that from the second to the sixth thermocouple, which were spaced two inches apart, a constant difference of 3.36°F existed between them. An additional thermocouple on the leading edge of the plate indicated

a temperature/ .....

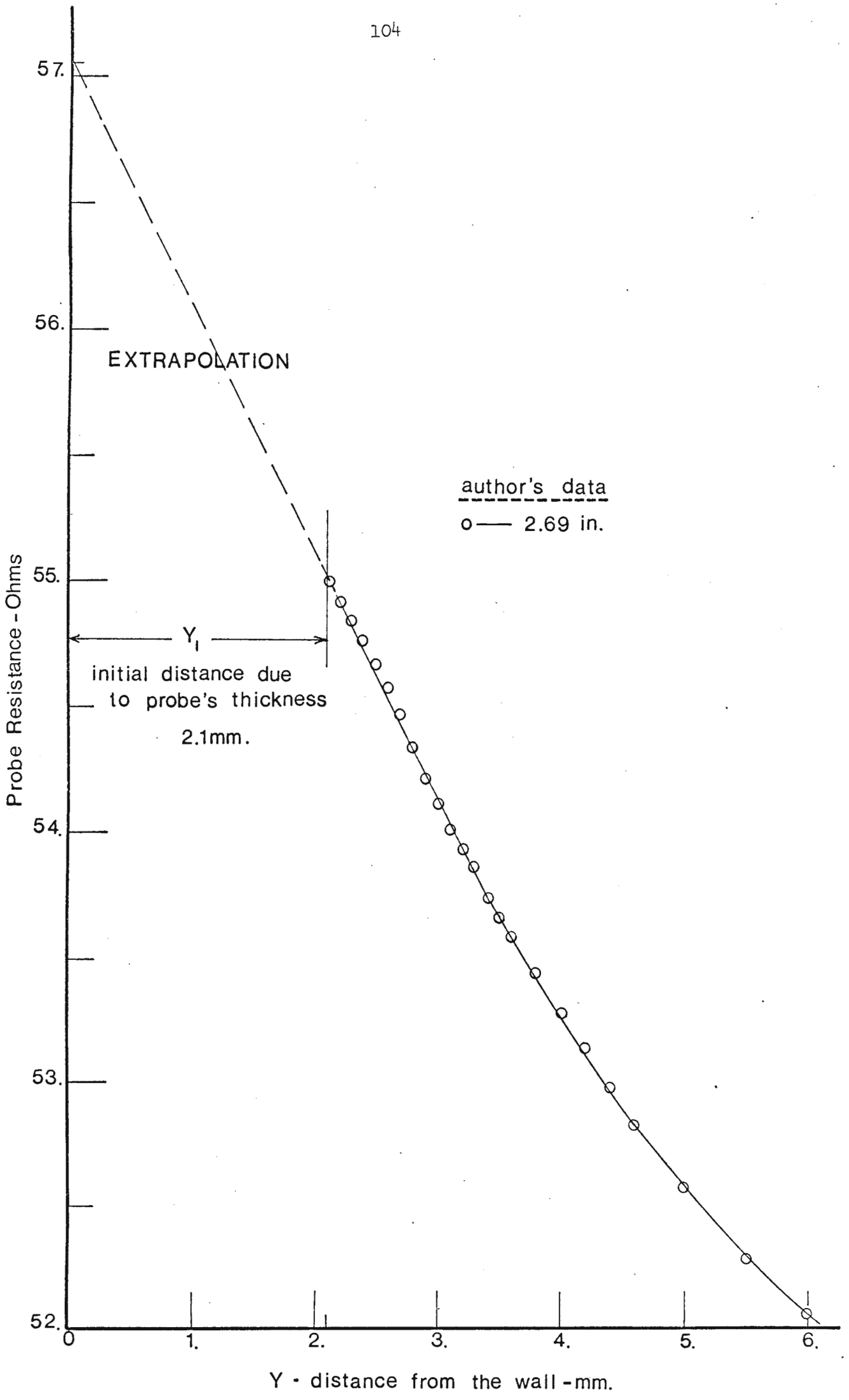
57.
56.
55.
54.
53.
52.
EXTRAPOLATION
author's data
o—— 2.69 in.
Y_1
initial distance due
to probe's thickness
2.1mm.
Probe Resistance - Ohms
0
1.
2.
3.
4.
5.
6.
Y - distance from the wall - mm.

FIGURE 6·4

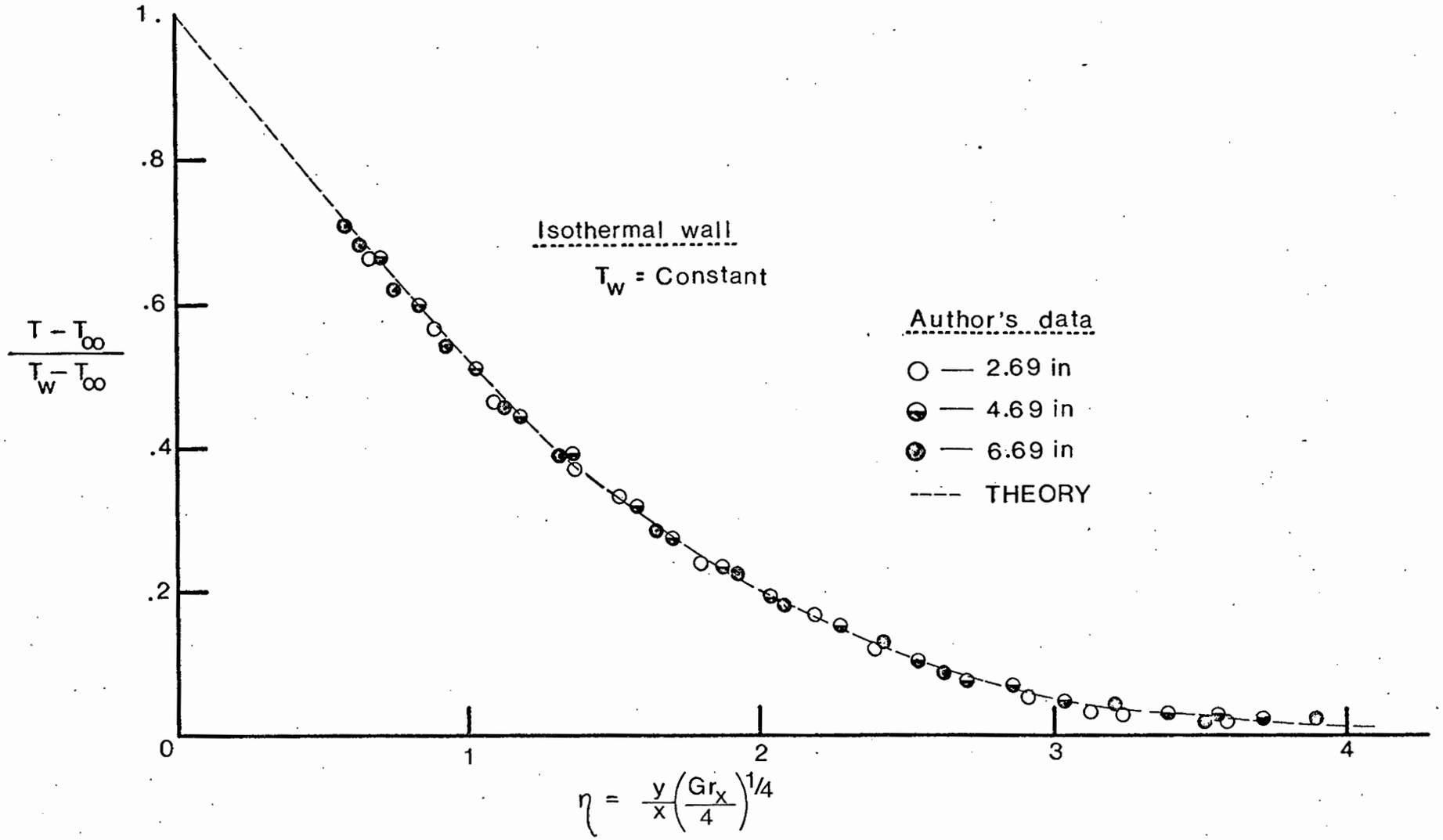
1.
.8
.6
.4
.2
0
1
2
3
4
$\frac{T - T_\infty}{T_w - T_\infty}$
Isothermal wall
T_w = Constant
Author's data
2.69 in
4.69 in
6.69 in
THEORY
$\eta = \frac{y}{x}\left(\frac{Gr_x}{4}\right)^{1/4}$

FIGURE 6·5

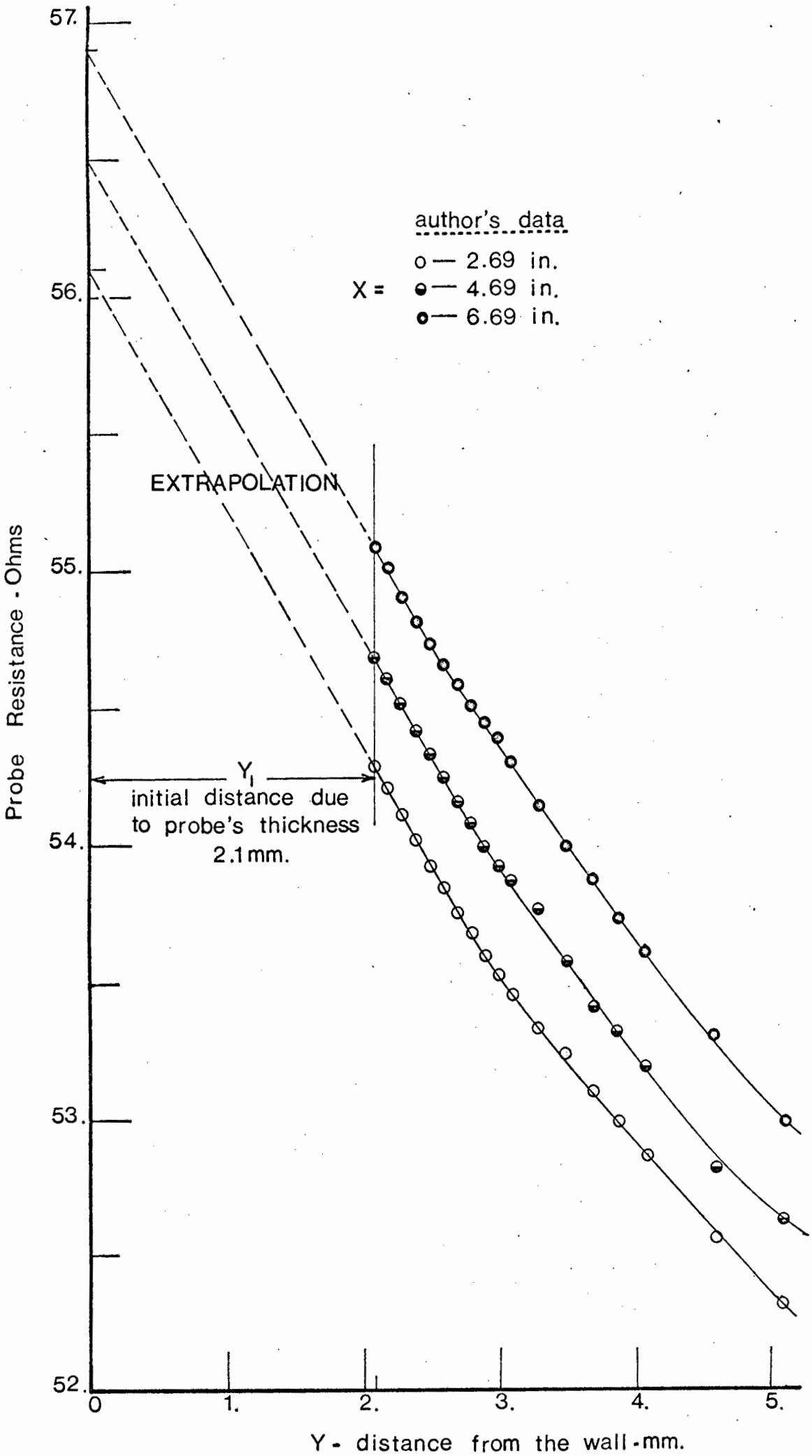
57.
56.
55.
54.
53.
52.
0
1.
2.
3.
4.
5.
Probe Resistance - Ohms
Y - distance from the wall - mm.
author's data
X = o — 2.69 in.
● — 4.69 in.
o — 6.69 in.
EXTRAPOLATION
Y_I
initial distance due to probe's thickness 2.1 mm.

FIGURE 6·7

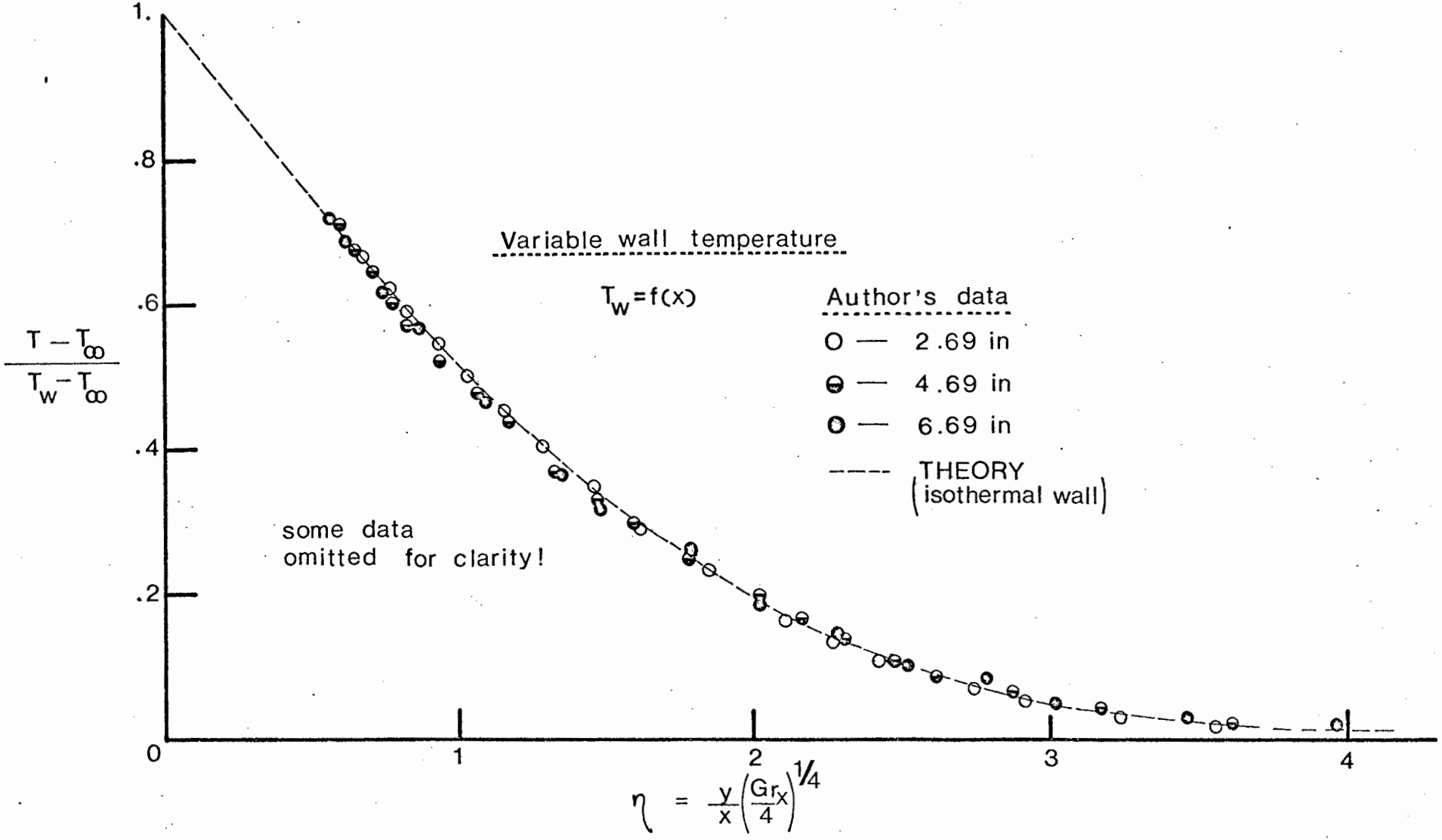
1.
.8
.6
.4
.2
0
1
2
3
4
$\frac{T-T_\infty}{T_w-T_\infty}$
Variable wall temperature
$T_w = f(x)$
Author's data
O — 2.69 in
⊖ — 4.69 in
O — 6.69 in
---- THEORY (isothermal wall)
some data omitted for clarity!
$\eta = \frac{y}{x}\left(\frac{Gr_x}{4}\right)^{1/4}$

FIGURE 6·8

CHAPTER VII

Application of the Buoyancy Diffusion Coefficient

Ideally an experiment should be devised to verify completely the validity of the Buoyancy Diffusion Coefficient, however, using a simple experiment of a flat plate in free convection, we will attempt to verify a simplified form of equation 2.35 derived in Chapter IIe. (page 45).

The heat transfer from a surface to a fluid may be calculated from the conduction equation provided the temperature profile in the boundary layer is known, however, we may also evaluate the heat transfer, formulating the following expression (keeping the notation of Chapter II section e)

$$q = -k\,\dot{c}\,(1+f/2)\,Db_w \left.\frac{dT}{dy}\right|_{y=o} \qquad (7.1)$$

where k is the Boltzman constant, $\dot{c}$ is the molecular density, f is the degree of freedom of the molecule, and Db_w is the Buoyancy Diffusion coefficient at the wall. In fact in equation (2.53) by letting $r = y = \ell$ (the first mean free path of the molecules), it is seen that the term $6\pi a\eta/m$ is zero (no collisions have taken place yet) and $T = T_w$. Consequently equation (2.53) reduces to

$$Db_w = \frac{\ell}{2}\,(2kT_w/m)^{\frac{1}{2}} \qquad (7.2)$$

Substitution of the above in equation (7.1) yields

$$q = k\,\dot{c}\,(1+f/2)\,\frac{\ell}{2}\sqrt{\frac{2kT_w}{m}}\cdot\left.\frac{dT}{dy}\right|_{y=o} \qquad (7.3)$$

Comparing/ .....

Comparing equation (7.3) with the conduction equation

$$q = -k\frac{dT}{dy}$$

it is seen that we are determining the validity of the proposed temperature profile inside the boundary layer (eq. 2.3), and obtaining an expression for the thermal conductivity of the fluid near the wall, in terms of molecular constants, absolute temperature mean free path, etc.

$$K = k\,\dot{c}(1 + f/2)\,\frac{\ell}{2}\sqrt{\frac{2kT_w}{m}} \qquad (7.4)$$

Equation (7.3) reduces after substituting the values for air at atmospheric pressure.

$$\dot{c} = p/kT_w \ \frac{\text{molecules}}{\text{cm}^3}\ , \quad \lambda = \pi(2a)^2 \ \text{cm}^2 \ \text{(collision area)}$$

$$\ell = 1/\dot{c}\,\lambda \ \text{cm}, \quad f = 5$$

$$k = 1.38 \times 10^{-16} \ \frac{\text{ergs}}{\text{molecule}}\ ^{o}K$$

$$\text{to} \quad q = \frac{7/2\ k}{8\pi a^2}\sqrt{\frac{2kT_w}{m}}\ \frac{dT}{dy} \qquad (7.5)$$

The mass of the air molecule is found by

$$m = \frac{M}{A_v} = \frac{28.97}{6.02 \times 10^{-23}} = 4.8 \times 10^{-23} \ \text{gm/molecule.}$$

where M is the molecular weight of the air and A_v is Avogadro's number.

The radius of the molecule is found as follows:

The molecular weight is divided by the density of the air at the liquid point giving us the molal volume; if we assume that the

molecules/ .....

molecules are cubic.

$$\frac{28.97}{\frac{54.56}{62.4}\times 1} = 33 \frac{cm^3}{mole} \quad \text{and} \quad \frac{33}{6.02 \times 10^{23}} = 5.49 \times 10^{-23} \frac{cm^3}{molecule}$$

However if we assume that the molecules are spherical (more nearly true) the actual volume is 0.655 of the volume of a molecule assumed cubical. Therefore

$$4/3\pi a^3 = 0.655\ (5.49 \times 10^{-23})$$

hence $a = 1.88 \times 10^{-8}$ cm or $1.88\ A^{o}$.

Equation (7.5) becomes after substitution for m, a and the other molecular constants

$$q = 1.3 \times 10^{2} \sqrt{T_w} \left.\frac{dT}{dy}\right|_{y=o} \frac{ergs}{cm^2\ sec} \qquad (7.6)$$

or

$$q = 4.14 \times 10^{-2} \sqrt{T_w} \left.\frac{dT}{dy}\right|_{y=o} \quad Btu/hr ft^2 \qquad (7.7)$$

where T_w is in ^{o}K and $\frac{dT}{dy}$ is $\frac{^{o}K}{cm}$

Experiment

It was decided to use the apparatus previously employed in the investigation described in Chapter V for the following reason:

In equation (7.6) we see that the temperature gradient must be known before we can evaluate the heat transfer rate. The optical technique, employing the Mach Zehnder interferometer gives this information.

The evaluation of the local heat transfer rates is quite simple, because one has only to obtain the temperature gradient at the wall as we have already seen in Chapter V. Problems of plate thermocouple monitoring and calorimetric techniques in determining

losses/ .....

losses by radiation and possibly conduction from the plate, just simply do not exist.

There was only one precaution taken. In view of the findings concerning the effects of the leading edge on the local Nusselt number, care was exercised to observe the phenomenon at a height on the plate where these effects are not present. (Beyond 0.5-in from the leading edge).

The procedure adopted was briefly as follows:
The interferometer was adjusted for wedge fringes and the plate was allowed to warm up. At intervals interferograms were obtained of the field surrounding the plate. Having recorded the ambient wet and dry bulb temperatures, and atmospheric pressure, from the interferograms, the temperature gradient was measured at a height of 1.5-in from the leading edge of the plate.

Using equation (5.2)

$$\Delta T = \frac{T_\infty \Delta N}{\frac{L}{\lambda}(n-1) - \Delta N}$$

The plate temperature was evaluated. With the abovementioned information, and employing equation 7.7, the local heat transfer rates were evaluated. From these results local Nusselt numbers were obtained and compared with the theoretical values given by equation (1.2)

$$Nu_x = 0.360\ (Gr_x)^{\frac{1}{4}} \qquad (1.2)$$

The results appear in table 7.1. Also see sample interferograms. Sample calsulations in appendix C page 147.

TABLE 7.1/ .....

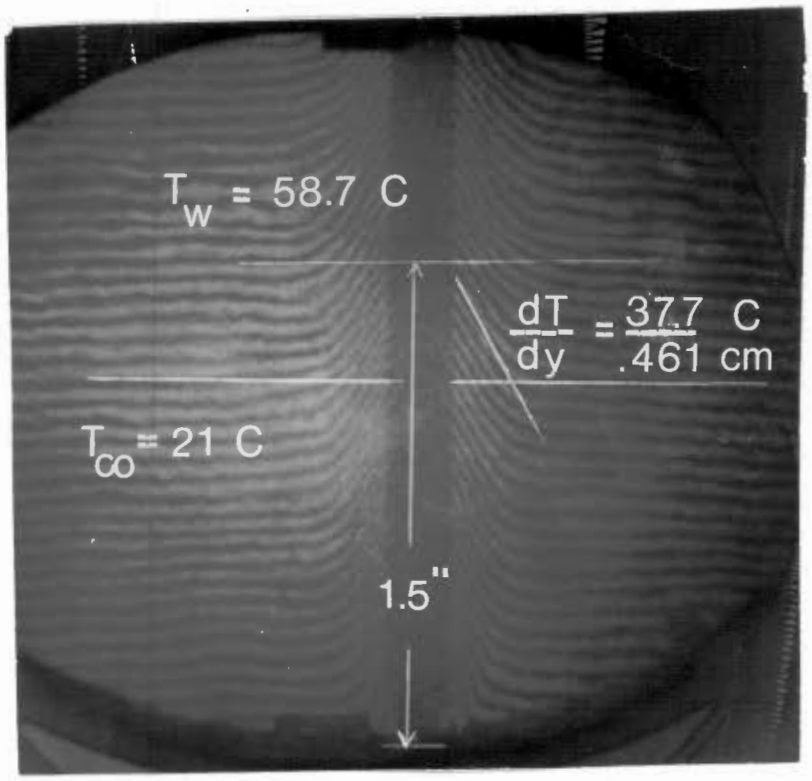

Interferogram no. 1

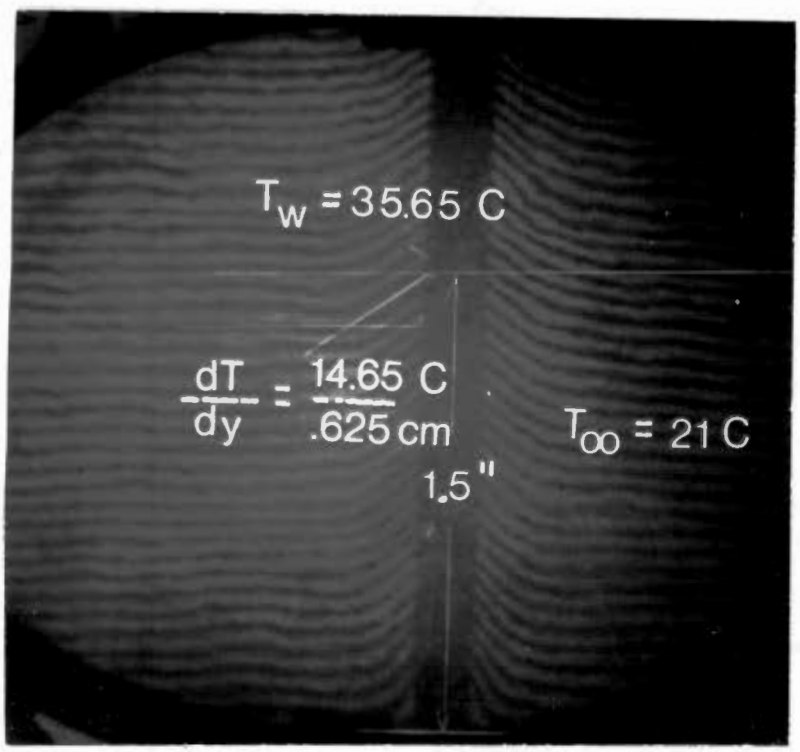

Interferogram no. 4

TABLE 7-1

Interferogram No.	T_w °C	Gr_x	q Btu/hr ft² (equation 1.2)	h Btu/hr ft² °F (equation 1.2)	q	h (equation 7.7)
1	58.7	2.40×10^5	63.7	0.962	61.5	0.92
2	53.0	2.06×10^5	51.6	0.921	50.2	0.897
3	47.4	1.77×10^5	40.6	0.883	38.2	0.83
4	35.7	9.85×10^4	18.85	0.735	17.1	0.685
5	31.5	7.34×10^4	12.1	0.691	11.7	0.67

T_∞ = 21 °C (constant).

CHAPTER VIII

- DISCUSSION AND CONCLUSIONS -

1. On the Order of Magnitude of δ and δ_T

The theoretical analysis, presented in Chapter II Section a, using integral methods, showed that for the phenomenon of laminar free convection from a vertical plate the hydrodynamic boundary layer is equal to the thermal boundary layer.[20]. The author chose the integral method because at the present time, of the four accepted methods utilized in dealing with convective phenomena, as discussed in the preface, this method is the only one that gives quantitative information about the boundary layer thickness.

The formal or similarity solutions although very attractive are inadequate for predicting the boundary layer and can only be applied if a similarity variable is found (which is not an easy task). These solutions being series solutions which converge very slowly, fail to define quantitatively the boundary layer.

One might argue that the integral methods are less exact than the similarity solutions, however, we must not overlook the excellent agreement of solutions that have been obtained by them when compared with experimental data. In this case, (free convection from a vertical plate) physical intuition tells one that the motion of the fluid is a result of the temperature differences which create the buoyancy effects. This induces a velocity in the boundary layer which is zero at the wall, increases to a maximum value within the boundary layer for a short distance away from the wall due to the large temperature gradients existing in this region, and decays to zero as the temperature gradients diminish. It is therefore perfectly valid to assume that the velocity will decay

to zero/ .....

to zero at the same distance away from the wall where the temperature gradient is zero. Hence $\delta = \delta_T$.

Returning to our analysis in Chapter II section a, one may wish from the outset to assume exponential functions for U_1, δ_T as well as δ

$$U_1 = Ax^m$$

$$\delta = Bx^n$$

$$\delta_T = Cx^r$$

Here making use of equation 2.2 as well as equation 2.1 we obtain after a rather lengthy computation

$$m = \tfrac{1}{2}, \quad n = r = \tfrac{1}{4}, \quad B = C.$$

hence again $\delta = \delta_T$.

It is worthwhile pointing out that this result is in accordance with Schlichting [2] who states that both the hydrodynamic and thermal boundary layer thicknesses are proportional to $x^{\frac{1}{4}}$. This is easily seen from figures 1.1 and 1.2 where the similarity variable η is the same for both temperature and velocity profiles.

2. On the Analogy with Forced Convection.

In Chapter II Section b, the author has shown that for laminar free convection from a vertical plate there exists an analogy with laminar forced convection phenomena. The idea that some characteristic velocity in free convection can be used to formulate a Reynolds number (and hence Nu = f(Re Pr)) stems from Schlichting [2 pg. 300] where it is shown that in the case of small velocities and considerable temperature differences

$$Re^2 \approx Gr.$$

The author/ .....

The author assumed that since the buoyancy forces account for the fluid's acceleration from rest at the wall, giving rise to a maximum velocity at approximately $y = \delta/3$, the use of this velocity in the forced convection equation should transform the Reynolds number to the Grashof number. This was shown to be true in equation (2.21). Further analysis, utilizing the maximum velocity from the formal solution for a vertical plate in free convection resulted in equation (2.23)

$$Re^2 = 0{,}325\ Gr.$$

which enabled the formulation of the analogy

$$Nu_x = 0{,}476\ Re_{Umax}^{\frac{1}{2}} = 0{,}36\ Gr_x^{\frac{1}{4}}$$

Essentially no new result has been obtained, however it has been shown conclusively that the condition of $Re^2 \approx Gr$ is satisfied.

3. On the Average Heat Transfer Rates at Low Grashof Numbers.

Chapters III and IV of the thesis were devoted to the presentation of the equipment, various techniques employed, and the results obtained in the investigation for the validity of the power law relationship (equation 1.1) $\overline{Nu} = 0{,}555\ (Gr\ Pr)^{\frac{1}{4}}$, at the low Grashof number region, i.e. $Gr < 10^5$.

For overall heat transfer rates, bearing in mind Saunders' [7] results, see figure 1.6, detailed experimental data were needed in order to ascertain the validity of the boundary layer concepts in the moderate and low Grashof number range. Saunders' [7] explanation for the lack of correlation below $Gr = 10^5$, that the convective currents become insignificant and the energy is predominently transferred by pure conduction is quite valid; however, the results obtained have shown conclusively that the influence of pure conduction is not felt at such high Grashof numbers. (See figures 4.5 and 4.7). Since the data reported by

Saunders/ .....

Saunders [7] are insufficient to perform an analysis, one may suggest that his departure from the power-law relationship is due to his failure to recognize that the boundary layer thickness increases rapidly at low Grashof numbers. Thus if his temperature measuring probe was within the boundary layer it would indicate smaller temperature differences between the plate and the bulk air, and hence higher free convective coefficients.

In figure 4.7 the lack of correlation with the "pure conduction limit" reported by Suriano and Yang [6] is also observed. It is unfortunate that lower Grashof numbers than Gr = 10 could not be obtained, so the most that can be said is that the pure conduction limit occurs at Grashof numbers well below 10 and that the limiting Nusselt number is less than 1.078.

Still looking into the problem more deeply one must examine the Grashof number.

$$Gr = \rho^2 \frac{\beta g \Delta T x^3}{\mu^2}$$

When performing experiments with vertical plates in air for all practical purposes low Grashof numbers may be obtained by (a) small temperature differences, (b) at low densities as it was done here, and (c) by observing the phenomenon at small heights (x's) from the leading edge. Physical intuition tells us that by letting $\Delta T \rightarrow 0$ the convective currents vanish and one might expect a pure conduction limit. By letting $\rho \rightarrow 0$ the convective currents also vanish but it is not so obvious that we are approaching a pure conduction limit. Finally, by observing the phenomenon at small x's one does not expect to encounter the conduction limit, but rather find that the boundary layer concepts do not apply because of the leading edge effects.

The author's/ .....

The author's data shows that the leading edge of the plate does not influence greatly the average heat transfer rates from the vertical plate. This is in accordance with Scherberg [28] who has shown that for the case of a constant temperature plate the leading edge only affects the relative vertical position of the boundary layer, and not its thermal or velocity form. Also, from the interference photographs by Brodowicz [18] it is seen that the flow ahead of the leading edge might depend on the physical thickness of the plate under consideration, and will only become important if the plate's height is reduced to such an extent that the portion of the boundary layer ahead of the plate is of noticeable percentage of the overall boundary layer exhibited around it. It is worth mentioning along the same lines, that Saunder's [7] results in the lower Grashof range were obtained by using plates having extremely small heights. (2.5 and 0.325 cm). In view of the results obtained in this investigation, it is suggested that the power law relationship (equation 1.1) can be used with sufficient accuracy in the laminar region and its limits may be increased from $10^5 < Gr\ Pr < 10^8$ to $10 < Gr\ Pr < 10^8$ [29].

4. On the Local Heat Transfer Rates near the Leading Edge.

The results of this investigation (see Chapter V) show excellent agreement with equations 1.2 and 2.12, away from the leading edge, i.e. at high Grashof numbers, and confirm the data reported by Cheesewright [17]. However as expected, the results show conclusively that the range of applicability of boundary layer concepts, as far as local values are concerned, is for Grashof numbers greater than 10^4. In figure 5.1 it is seen that below $Gr \simeq 5 \times 10^3$ there is a marked departure from the accepted relationship, thus showing that the local Grashof-Nusselt number expression is not universal at low Grashof numbers obtained by decreasing co-ordinate along the plate towards the leading edge.

It is worth pointing out that the phenomenon of free convection at low Grashof numbers falls into the area where the fluid kinematic viscosity does not approach zero, as characterized by moderate Reynolds or Grashof numbers, and is therefore in an area which has not been fully explored.

In the past, investigators have recognized the need of refining the boundary layer solution in order to describe this phenomenon more accurately. To the knowledge of this writer the first attempt was presented by Yang and Jerger [4], however, their results are at variance (see figure 1.3) with the data presented in Chapter V fig 5.1. This is because, in their first order perturbation analysis, they failed to take into account the leading edge effects. It appears that the effects are quite significant and they are due mainly to the induced flow ahead of the leading edge. This induced flow is a result of the non-zero normal component of velocity at the leading edge.

Suriano / .....

Suriano, Yang and Donlon [5] presented a paper where they have shown that the corrections on the boundary layer, due to the leading edge effects, are much more significant than those due to the boundary layer perturbations. Unfortunately their results are presented as average values starting about $Gr \approx 10^4$ and do not permit direct comparison with the present data, however they do indicate similar departure from the accepted solution (see figure 1.3). An interesting fact comes to light when examining the points of departure in figure 5.1. The departure occurred at approximately the same distance from the leading edge (0.5 "), but due to different temperature differences, at different Grashof numbers. In other words as the overall temperature difference ΔT , decreased for the same distance from the leading edge, the Grashof number became smaller and the agreement with the theory was extended! This may be explained by the magnitude of the normal component of the velocity at the leading edge, which is the result of the buoyancy induced flow. At higher temperature differences the greater is the buoyancy induced flow, hence the larger normal component of velocity. This will increase the leading edge effects, making them more significant in the region under question.

It appears then, from the data reported here, that there is a surprising influence of the temperature difference on the Nusselt number for fixed Grashof numbers in the range below 5×10^3 (see figure 5.1). This to the knowledge of the author is new data [30].

5. On the Effects of Variable Wall Temperature on the Boundary Layer.

Chapter VI dealt with the apparatus, procedure and results which served to verify the analysis presented in Chapter II section d.

The integral methods analysis indicated that the temperature profiles from a variable wall temperature are identical to those for a uniform wall temperature and that the boundary layer is still

proportional/ .....

proportional to $x^{\frac{1}{4}}$. The results presented in figure 6.8 substantiate the analysis which is at variance with Sparrow and Gregg [22]. The author has pointed out that the results by Sparrow and Gregg [22] are questionable since the surface temperature in their paper: $T_w - T_\infty = Nx^n$, has a singularity point, requiring $T_w = T_\infty$ at $x = 0$, which is hardly the case in a real situation. Furthermore for a linear wall temperature distribution, i.e. $n = 1$, their similarity variable $\eta = C_1 y x^{\frac{n-1}{4}}$, becomes independent of x indicating that δ is a constant!

The results by Sparrow and Gregg [22] are only qualitatively correct for the case where there exists a vertical temperature gradient for the bulk fluid temperature T_∞, in which case the formulation of $T_w - T_\infty = Nx^n$ is partly correct. This can be seen from the data reported by Cheesewright [17] which fall below the theoretical isothermal plate solution, and the discrepancy is explained by the small vertical temperature gradients in the laboratory during his experiments. In the experiment performed by the author T_∞ was constant and the proposed equation for the plate's temperature, $T_w(x) = Tw_{x=0} + C(\frac{x}{L})^p$ was fully simulated. (See figure 6.6).

In particular a linear wall temperature distribution ($p = 1$) was established so that direct comparison with Sparrow's and Gregg's [22] results could be made. It is seen from the results presented in figure 6.8 and table 6.1 that the boundary layer is proportional to $x^{\frac{1}{4}}$, and <u>not</u> independent of x. i.e. at variance with [22]. It should be pointed out that the proposed equation for the variable wall temperature distribution, in the author's analysis (eq. 2.32), has no singularity points and may be used to represent real situations, and furthermore, the solution holds for a finite length plate in free convection with T_∞ truly a constant. It appears that the prediction of the boundary layer from a non-isothermal finite plate can be made

using/ .....

using equation 2.38, which is qualitatively identical to equation 2.9, provided the wall temperature at x = 0 is known as well as the constant C.

The local Nusselt number can be evaluated using the following expression

$$Nu_x = 0.376 \left(\frac{\rho^2 \beta g x^3}{\mu^2}\left[(T_w - T_\infty)_{x=0} + C\right]\right)^{\frac{1}{4}} \qquad (8.1)$$

where the term in parenthesis is a modified Grashof number because it involves the peculiar ΔT terms.

Looking deeper into this problem, it is seen that the more rigorous approach (similarity solution), because of the difficulties involved in finding similarity variables to transform the pertinent partial differential equations into ordinary differential equations, and the use of the particular surface temperature equation (2.30), has changed the phenomenon. The similarity solution presented by Sparrow and Gregg [22] is not for a non-isothermal vertical plate, but rather for a plate exposed to a surrounding fluid whose temperature T_∞ varies along the height parallel to the plate.

A less elegant and simpler solution such as the integral methods, gave the solution for a non-isothermal wall exposed to a fluid with constant T_∞, and this solution was proven conclusively with experimental data.

6. On the Buoyancy Diffusion Coefficient

The analysis presented in Chapter II section e is a radical departure from the conventional methods used so far in solving convective heat transfer phenomena.

The model proposed is really quite simple. It uses basically Brownian motion theory to describe the motion of the fluid particles which act as carriers of the energy from a surface. For example, a particle of dust behaves as if it were a very large molecule. In air it has the same average translational kinetic energy as the gas molecule and repeatedly is interchanging energy with the air molecules that collide with it. This is Brownian motion which furnishes the most direct and convincing check of the validity of the kinetic theory. The author simply reduced the dust particle to the size of the air molecules; in fact, he made it an air molecule. From then on he used probability functions to determine its position and velocity after colliding with the wall and exchanging energy. Through the so called boundary layer the molecule continuously exchanges energy until it reaches the level of the "undisturbed" fluid. The analysis yielded the Buoyancy Diffusion Coefficient which looks very promising, but it can not be claimed that the theory replaces the conventional methods. At present it seems that the theory is not rich enough to yield information concerning the temperature profile or the boundary layer thickness. The experiment performed verified the validity of the Buoyancy Diffusion Coefficient at the wall yielding heat transfer rates, which are in good agreement with the classical solution, (See table 7.1), therefore it can be claimed that both qualitatively and quantitatively, at least near the wall, the Buoyancy Diffusion Coefficient must be accepted.

It is/ .....

It is seen that the thermal conductivity of the fluid can be expressed as a function of the absolute temperature at the wall and molecular constants if equation (7.3) is compared with the conduction equation.

Also, the validity of the temperature profile equation (2.3) which has been proposed as a good approximation for this phenomenon, is established in view of the good agreement for the heat rates that were observed.

A number of additional points of information concerning the phenomenon of free convection from a vertical plate can be drawn when it is examined through our proposed theory.

Firstly, it appears that the local heat rates are independent of x and depend mainly on the wall temperature at any height. However, observing the interferograms, one sees that the temperature gradient varies along x. So in equation (7.7) the dependence of the heat rates in $\dot{x}$ is hidden in the temperature gradients.

Secondly, the theory substantiates the results obtained in the investigation for the Nusselt numbers at low Grashof numbers obtained in Chapters III and IV when the pressure inside the chamber was reduced below atmospheric. We can safely draw the conclusion that the heat rates are independent of pressure, both in view of the results of chapter IV and of our proposed theory. In the theory the molecular density($\dot{c}$) which depends on pressure cancels out (see page 111).

Finally the proposed theory fully explains the phenomenon at the leading edge, where so much speculation exists for the reason of the boundary layer starting ahead of it. Since the leading edge has physical dimensions and is also heated, the molecules diffuse normally in relation to it, thus giving rise

to a / .....

to a boundary layer ahead of the leading surface.

In conclusion, if appears that local heat rates can be predicted from equation (7.7) once the wall temperature and the temperature gradients are known; an easy task when using our interferometer. We no longer have to contend with Nusselt, Grashof or Prandtl numbers, so problems such as at what temperature to evaluate the properties involved in these dimensionless groups, or their dependence on each other, simply fall away.

GENERAL COMMENTS

The author has chosen to present his work in the chronological order in which it was accomplished, the reason being, that in this manner the refinements in the techniques employed are brought out. It is a relatively easy task, at this stage, to look upon the past and make recommendations.

Experimental Techniques.

The first investigation undertaken was to determine the validity of the accepted power-law relationship, equation 1.1 for Grashof numbers below 10^5. At the time, the calorimetric methods appeared attractive because they are basically of the standard type, however before any results could be presented, they were checked by independent means, such as we saw in the case of emissivity measurements. During this investigation the author acquired invaluable experience in the construction of the vertical plates, the enclosures, and general handling of the hardware. The information obtained through this technique is limited, in a sense, if one examines the phenomenon on a broader basis; however, judging from the response received following the publication of the results [29], the author feels that the time and labour spent were well rewarded. The calorimetric technique does not yield information on local values, the influence of the leading edge or the case of a non-uniform temperature plate. The author, guided by the literature survey, decided on the construction of a Mach-Zehnder Interferometer which would be used to observe and take measurements of the phenomenon near the leading edge. The advantages of the interferometric technique over the previous one are innumerable. For example the ease, simplicity, and accuracy of measurements obtained, as well as the information that is available, over-shadow the calorimetric method.

The construction/ .....

The construction of the instrument was accomplished at a great cost and with considerable labour, however, its use for the investigations that followed was invaluable. Using the instrument, the data collected showed conclusively that the phenomenon near the leading edge of a flat plate can not be described with a universal Nusselt-Grashof number relationship. [30].

The apparent dependance on the temperature difference is, to the knowledge of this author, new data.

Following the conclusion of the above project, the next aspect was undertaken. The investigation of the effects of a non-isothermal vertical plate. Here the use of the interferometer was considered; however, it was precluded because of the physical sizes involved. The author used a new plate which was constructed in a manner as to enable the control of the heat input at different heights, thus establishing any required temperature distribution on the plate. Using hot wire anemometry, the temperature profiles were obtained. To the knowledge of the author, these data are new, or the first to be reported. (that is, temperature profiles from a non-isothermal plate).

Finally, the last project undertaken was to establish the validity of the Buoyancy Diffusion Coefficient. Here again the versatility of the interferometer enabled the author to obtain the necessary data. In our opinion the interferometer is to be highly recommended for use in experimental investigations.

Analytical Methods

It appears that the analytical methods that have been employed up to present times in investigating convective phemomena , are best applied depending on the nature of each project. For example, when restricted information such as heat rates is required, dimensional analysis coupled with experiment should be adequate.

Without doubt considerable information can be obtained through

classical/ .....

classical solutions, the only draw-back being that not always is it possible to obtain such solutions. In the search for a similarity variable, care should be exercised that the problem is not distorted from its original postulation just for the sake of obtaining a solution. As it was pointed out, quantitative information of the boundary layer cannot be obtained, nor the phenomenon at the leading edge explained through a similarity solution.

The integral methods are more flexible and simpler and yield information concerning the boundary layer and solutions such as for a non-isothermal wall. Admittedly, before such methods can be used to obtain a complete solution, the temperature and velocity profiles must be known. This is not such a major task if one is prepared to obtain the necessary data with an interferometer, or a hot wire anemometer. Using this method we were able to show that $\delta = \delta_T$[20]. The author's proposed theory, which yielded the Buoyancy Diffusion Coefficient, looks very promising. Although not replacing the above mentioned methods, it did yield additional information on the nature of the flow. Furthermore the phenomenon at the leading edge can be explained, something that all other methods have failed to do. In all, the most that can be said concerning analytical methods of attacking a problem, is that investigators should be familiar with all of them, and choose the one that gives the required information in the most direct manner.

A P P E N D I X A

Dimensional Analysis and Properties.

Fig - A Viscosity and Thermal Conductivity of Air. [31]

Fig - B Viscosity and Thermal Conductivity of Argon and Helium. [31]

APPENDIX A

Dimensional Analysis of Properties

In practice the convective heat transfer coefficients are generally calculated from empirical equations obtained by correlating experimental data with dimensional analysis. Dimensional analysis differs from other methods of approach in that it does not yield equations that are readily solveable. It combines the many variables in any problem into dimensionless groups which facilitate the interpretation.

The first step is to select a system of fundamental dimensions. This choice is arbitrary and the dimensions selected here were mass M, length L, time θ, and temperature T.

Next the list of the important variables influencing the phenomenon of free-convection was compiled.

Variable	Symbol	Dimensions
Free convective heat transfer coefficient	h_c	$\frac{M}{\theta^3 T}$
Characteristic dimension of the system	L	L
Thermal conductivity of the fluid	k	$\frac{ML}{\theta^3 T}$
Absolute viscosity of the fluid	μ	$\frac{M}{L\theta}$
Specific heat of the fluid	C_p	$\frac{L^2}{\theta^2 T}$
Density of the fluid	ρ	$\frac{M}{L^3}$
* Coefficient of thermal expansion of the fluid	β	T^{-1}
* Gravitational acceleration	g	$\frac{L}{\theta^2}$
* Temperature difference between the fluid and the surface	ΔT	T

From the physical knowledge of the phenomenon it is

recognised/ .....

recognised that the three last variables (denoted by asterisks) account for the buoyancy force, so they are grouped together and replaced by a single variable. $(g\beta\Delta T)$ with the dimensions of $\frac{L}{\theta^2}$.

Since a solution for h_c is required the following equation can be assumed.

$$h_c = C\left[L^a\ k^b\ \mu^c\ C_p^{\ d}\ \rho^e\ (g\beta\Delta T)^f\right] \qquad (a)$$

The variables in equation (a) are replaced by their dimensions

$$M\theta^3 T^{-1} = L^a\ (ML\theta^{-3} T^{-1})^b (ML^{-1}\theta^{-1})^c (L^2\theta^{-2}T^{-1})^d$$

$$(ML^{-3})^e (L\theta^{-2})^f$$

Equating the exponents for each side yields:

for M $\quad 1 = b + c + e$

for L $\quad 0 = a + b - c + 2d - 3e + f$

for θ $\quad -3 = -3v - c - 2d - 2f$

for T $\quad -1 = -b - d.$

With six independent variables and four equations, any four can be solved in terms of the other two, provided the four selected contain all the fundamental dimensions between them.

Solving for a, b, c and f in terms of d and e.

$$a = \frac{2}{3}e - 1, \quad b = 1 - d, \quad c = d - e, \quad f = \frac{e}{2}$$

Substituting these values into equation (a)

$$h_c = C(L^{\frac{3}{2}e-1}\ k^{1-d}\ \mu^{d-e}\ C_p^{\ d}\ \rho^e\ (g\beta\Delta T)^{\frac{e}{2}})$$

which reduces to

$$h_c = C\ (\frac{L^{\frac{3}{2}}(g\beta\Delta T)^{\frac{1}{2}}\rho}{\mu})^e\ (\frac{C_p\ \mu}{k})^d\ \frac{k}{L} \qquad (b)$$

after rearrangement

$$\frac{h_c L}{k}/ \ \ldots\ldots\ldots\ldots$$

$$\frac{h_c L}{k} = C\left(\frac{L^3 \, g\beta\Delta T\rho^2}{\mu^2}\right)^e \left(\frac{Cp\mu}{k}\right)^d \qquad (c)$$

which is recognised as

$$\overline{Nu} = C(Gr)^e(Pr)^d \qquad (d)$$

The above expression can be further simplified if the Prandtl number is assumed to be a constant,

$$Nu = C_1(Gr)^e \qquad (e)$$

where C_1 is a constant and e an exponent both to be determined from correlation with experimental data.

In equation (c) it is shown that the free convective heat transfer rate can be correlated by the dimensionless groups, namely the Nusselt, Grashof and Prandtl numbers.

These groups are composed of either constants like gravity (g) or characteristic length (L) or fluid properties such as specific heat at constant pressure(Cp), absolute viscosity (μ), thermal conductivity (k), etc., with the exception of the Nusselt number which involves the convective heat transfer coefficient (h_c).

The fluid properties such as Cp, μ or k cannot be measured or observed directly.

The absolute viscosity (μ) is a property that depends only on temperature, as stated by the kinetic theory of gases, a fact also verified by experiment. The same can be said for the thermal conductivity of gases. Here it must be pointed out that a recent publication of the American Bureau of Standards [31] shows that both viscosity and thermal conductivity of Air, Argon and Helium are pressure dependent below 5 mm Hg abs. pressure; however, the variation is so minute that it was decided to treat these properties as being temperature dependent alone.

Values/ .....

Values of the specific heat at constant pressure have been calculated for a great many gases and for a wide range of temperatures [3].

The density (ρ) can be calculated from the equation of an ideal gas

$$\rho = \frac{P}{RT}$$

The coefficient of thermal expansion for an ideal gas is a function of the absolute temperature alone

$$\beta = \frac{1}{T}$$

So it is seen that all properties can be evaluated by temperature and pressure measurements alone.

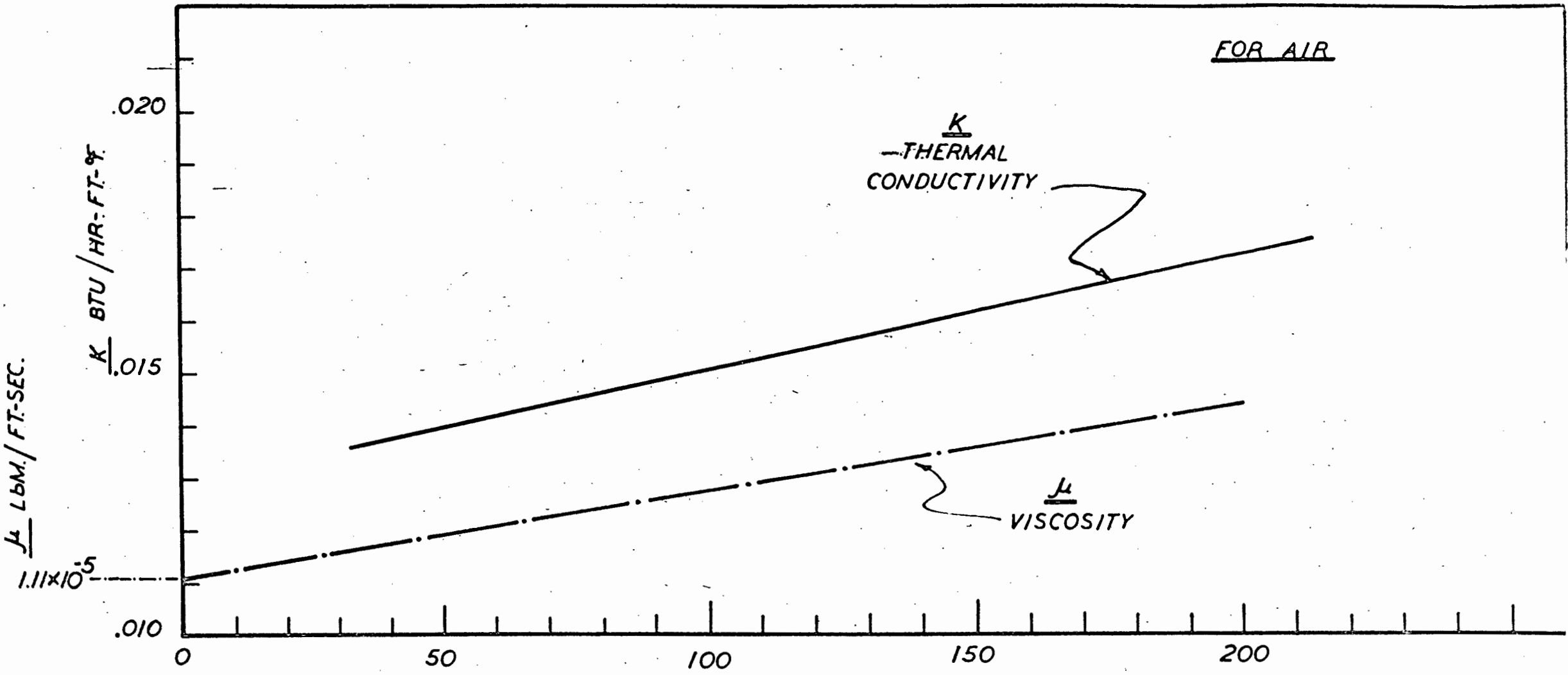
FOR AIR
K
—THERMAL
CONDUCTIVITY
μ
VISCOSITY
.020
.015
.010
K BTU/HR-FT-°F
μ LBM./FT-SEC.
1.11×10⁻⁵
0
50
100
150
200
TEMPERATURE —°F

FIGURE — A

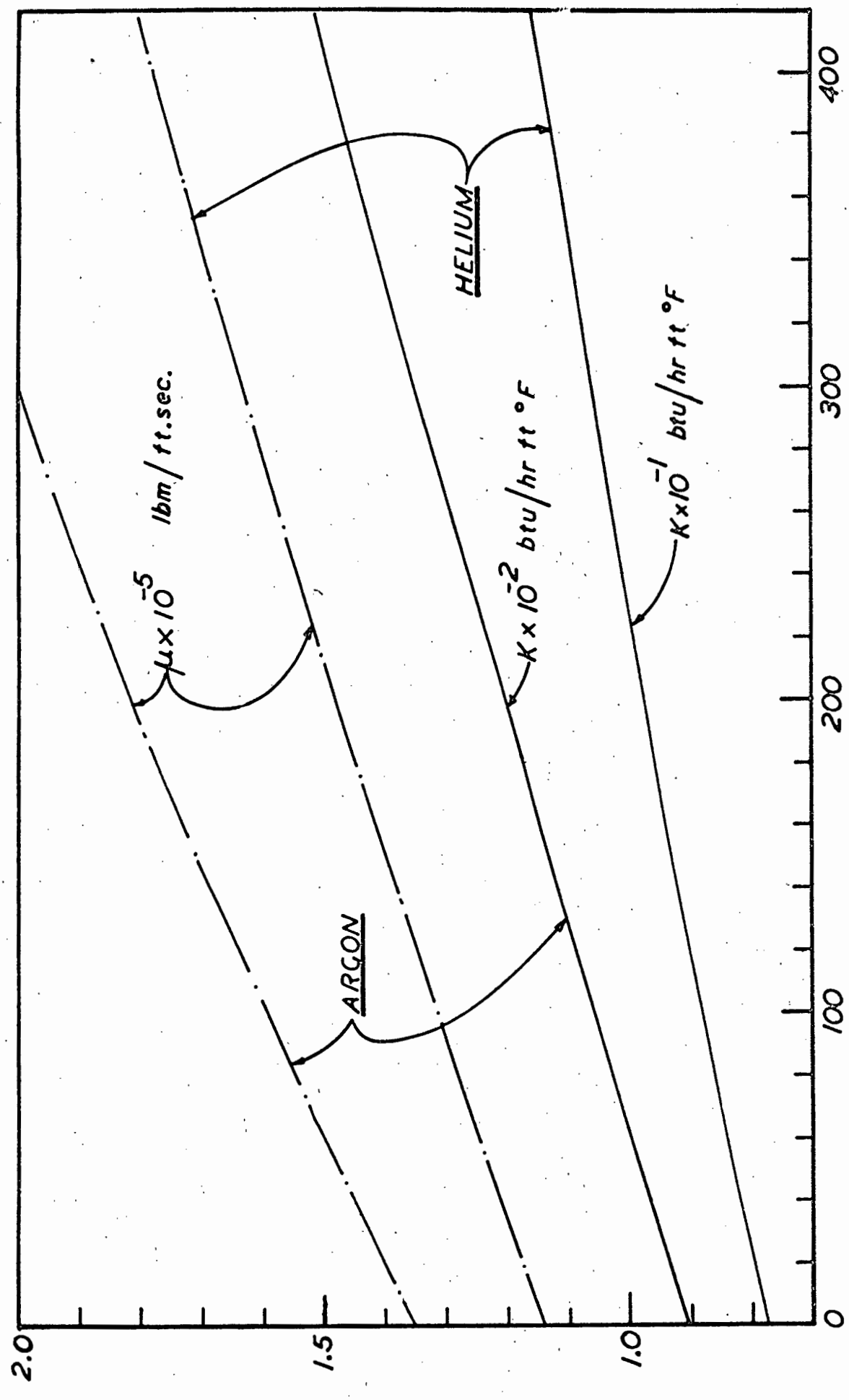
2.0
1.5
1.0
0
100
200
300
400
TEMPERATURE – °F
HELIUM
ARGON
μ × 10^-5 lbm/ft.sec.
K × 10^-2 btu/hr ft °F
K × 10^-1 btu/hr ft °F

FIGURE – B

A P P E N D I X B

Emissivity measurements.

APPENDIX B

Emissivity

Calorimetric Method.

Using the following expression

$$Q = (3.413)(I)(V) = \sigma\varepsilon_1 A.(T_1^4 - T_2^4) \qquad (a)$$

an energy balance was made as heat input to the plate must equal the heat lost by radiation (neglecting convection effects at low pressures).

In equation (a) I is the current in amperes and V is the voltage in volts. T_1 is the temperature of the plate and T_2 is the temperature of the chamber's walls.

The following table gives the results obtained:

Table 1

Abs. Press. mm. Hg.	Power Input	Plate Temp.	Wall Temp.	Emissivity
0.2	17.79 Btu/hr	619.5°R	547.5°R	0.542
0.45	26.60	655.0°R	560°R	0.543
0.65	38.67	695.0°R	574°R	0.543

In view of the above results, since the emissivity remained constant in the range of temperatures that the tests were to be carried out, the value of 0.543 was taken for the emissivity of plate no. 1 as being a very good approximation.

Using a Compensating Thermopile.

Using the compensating thermopile the following procedure was carried out to determine the emissivity of the gold plated surface of plate no. 5.

Since the thermopile was calibrated for a point source it was necessary first to obtain a new factor applicable to a plane

surface/ .....

surface. This was done by taking a copper container where water was slowly being heated, until it reached its boiling point. One of the surfaces of the container was blackened with acetylene soot (emissivity 0.99). The thermopile with a suitable receiving cone was placed in front of the darkened surface and the millivolts deflection of the thermopile was recorded. Then using the following expression.

$$\frac{Q}{A} = \sigma\varepsilon\ (T_1^4 - T_2^4) = \text{deflection.}$$

∴ The heat transfer rate factor per millivolt was obtained.

For example

The deflection was 0.85 mv.
Temp. of the surface 660.0°R.
Temp. of the ambient 530.0°R.

$$\therefore\ 0.85 = (0.1714)(0.99)\ (6.6^4 - 5.3^4),$$

$$f = \frac{187}{0.85} = 221 \text{ Btu/hr ft}^2 \text{ mv.}$$

The average of various readings yielded a factor of 220 Btu/hr.ft^2 mv. for the thermopile, viewing a plane surface.

Having obtained this calibration factor, the emissivity of the gold plated surface was evaluated as follows:

The power input to the plate was controlled by the variable transformer, the temperature of the plate was recorded through the potentiometer, the thermopile was connected to the recorder where its deflection was noted., The tests were carried out in a darkened room and numerous readings yielded an average of 0.071 as the value for the emissivity of the gold plated surface. An example of typical values follows:

Deflection 0.032 mv.
Temp. of the plate 608.5°R.
Temp. of the ambient 530°R.

from/ .....

from

$$\sigma\varepsilon_1 (T_1^4 - T_2^4) = f \times \text{deflection}$$

$$\varepsilon = (220)(0.032)/(0.1714)(582) = 0.0706.$$

The figures given for electrolytically deposited gold, range between 0.02 and 0.03. Hutte [3] gives a figure of 0.049. Taking into account the scratched surface of the plate, the figure 0.071 arrived at is acceptable.

APPENDIX C

i. Sample calculations for average heat transfer rates at low Grashof numbers.

ii. Selected data.

iii. Evaluation of a typical interferogram.

A P P E N D I X C

i. Sample Calculations.

Consider figure 4.7 page 79.

Coordinates $\text{Log}_{10}\text{Gr.Pr.} \approx 3.3$

$$\overline{Nu} \simeq 4.0$$

The data collected for this point were

$T_w = 168^\circ F = 628^\circ R$ $\quad$ I = .287 amperes

$T_\infty = 73.5^\circ F = 535.5^\circ R$ $\quad$ V = 3.7 volts

$T_c = 73.5^\circ F = 533.5^\circ R$ $\quad$ Plate No. 5, 2-in × 3-in.

P = 48 mm.Hg.abs. (air) $\quad \varepsilon = 0.071$

$Q_{in} = (.287)(3.7)(3.413) = 3.625$ Btu/hr. $\quad$ eq (3.1)

$$Q/A = \frac{3.625(144)}{(2\times3)(2)} = 43.5 \text{ Btu/hr.ft}^2.$$

$\Delta T = 628 - 533.5 = 94.5^\circ F$ or $^\circ R$.

Using equation (3.2)

$$u = \frac{Q/A}{\Delta T} = \frac{43.5}{94.5} = 0.46 \text{ Btu/hr.ft}^2\,^\circ F.$$

Using equation (3.6)

$$h_r = \frac{\sigma\varepsilon(T_w^4 - T_c^4)}{(T_w - T_\infty)} = \frac{(.1714)(0.071)}{94.5}\left[6.28^4 - 5.335^4\right]$$

$$h_r = 0.096 \text{ Btu/hr ft}^2\,^\circ F.$$

Using equation (3.3)

$$h_c = u - h_r = 0.46 - 0.096 = 0.364 \text{ Btu/hr.ft}^2\,^\circ F.$$

$$\beta = \frac{1}{T_\infty} = \frac{1}{533.5} = 1.87 \times 10^{-3}\ 1/^\circ R$$

Using equation (1.5)

$$T_r = T_w - 0.38\,(T_w - T_\infty)$$

T_r = / .....

$T_r = 628 - 0.38\ (94.5) = 592^{\circ}R$ or $132^{\circ}F$.

From Appendix A.

$\mu = 1.33 \times 10^{-5}$ lbm/ft.sec.

$k = 0.0158$ Btu/hr.ft$^{\circ}$F

$$\rho = \frac{P}{RT_r} = \frac{(48)(2.785)}{(53.3)(592)} = 0.00425 \text{ lbm/ft}^3$$

$$\overline{Nu} = \frac{hL}{k} = \frac{(0.364)(2/12)}{.0158} = 3.85$$

$$Gr_L = \rho^2 \frac{\beta g \Delta T L^3}{\mu^2} = \frac{(0.00425)^2\ (1.87 \times 10^{-3})(32.2)(94.5)(4.61 \times 10^{-3})}{(1.32 \times 10^{-5})^2}$$

$$Gr_L = 2680 \quad : \quad Pr = \frac{(.24)(1.33 \times 10^{-5})}{(.0158)} \times 3600 = 0.726$$

$$Gr_L.Pr. = (2680)(0.726) = 1930$$

$$\text{Log}_{10}\ Gr_L Pr. = 3.286$$

Actual coordinates. $\overline{Nu} = 3.85$

$$\text{Log}_{10}\overline{Gr}.Pr. = 3.286$$

If the edge areas were included as mentioned on page 80 using the same sample calculations as above

$Q = 3.625$ Btu/hr

$A \simeq 2(2 \times 3) + (2)(2)(1/4) \simeq 13$ in^2

$$Q/A = \frac{3.625\ (144)}{13} = 40.3 \text{ Btu/hr.ft}^2$$

$$u = \frac{40.3}{94.5} = 0.427 \text{ Btu/hr.ft}^2\ ^{\circ}F$$

$$h_c = 0.427 - 0.096 = 0.331 \text{ Btu/hr.ft}^2\ ^{\circ}F$$

$$\overline{Nu} = \frac{(0.331)(2/12)}{0.0158} = 3.5$$

as compared to 3.85 previously calculated.

NOTE:/ .....

NOTE:

Using the film temperature (Eq. 1.4) as the representative temperature for the evaluation of the dimensional groups the coordinates are:

$\overline{Nu}$ = 3.92 which represents an error of 1.82% over the previous value of $\overline{Nu}$ = 3.85

Log_{10} Gr. Pr. = 3.280

---

ii. Due to the vast amount of data collected the author presents a selected quantity of data pertaining to figure 4.7.

Data for Plate No. 4 (3" x 2") Chamber No. 2.

In Air

Constant Heat Input = 173 Btu/hr ft^2

e = 0.99.

T_w	T_∞	Press mm.Hg	h_r (Btu/hr ft^2	h_c ^oF)	Log_{10}Gr.Pr. (Dimensionless	$\overline{Nu}$)
147	70.5	483	1.270	0.990	5.242	10.6
151	71.5	353	1.285	0.890	4.980	9.54
155	71.5	253	1.300	0.770	4.742	8.23
160	69	131	1.315	0.585	4.165	6.20
168	71	63	1.335	0.450	3.550	4.75
174	71	33	1.350	0.325	2.995	3.42
178	73	22	1.370	0.277	2.650	2.89
180.5	73	15	1.385	0.225	2.316	2.35
180.5	71	13	1.375	0.214	2.200	2.14
182.5	71.5	12	1.386	0.173	2.135	1.810
183	71	9	1.385	0.160	1.890	1.665
184.5	73	8	1.400	0.150	1.795	1.560
186	74	7	1.405	0.140	1.662	1.450
182.5	70	7	1.380	0.160	1.675	1.670
186	73	6	1.400	0.130	1.435	1.345
185	71.5	5	1.392	0.133	1.390	1.385
186.5	73	4.3	1.405	0.120	1.278	1.240
185	70	4	1.390	0.115	1.890	1.665
182.5	70	4	1.412	0.120	1.675	1.670

Note In all cases the temperature of the chamber's walls was the same as the bulk fluid temperature.

Data for Plate No. 5 (2" x 3") Chamber No. 3.

In Air

Constant Heat Input = 43.5 Btu/hr ft^2

e = 0.071

T_w ^oF	T_∞ ^oF	Press mm.Hg.	h_r (Btu/hr	h_c ft^2 ^oF)	Log_{10} Gr.Pr. (Dimensionless)	$\overline{Nu}$
107	74.5	754	0.0815	1.259	5.312	13.9
109	72	665	0.0812	1.0938	5.235	12.0
113	74.5	582	0.0836	1.0464	5.142	11.5
114	73.5	482	0.0825	0.9920	5.015	11.0
117	73.5	421	0.0830	0.9170	4.920	10.1
118	72	324	0.0835	0.8610	4.716	9.5
126	73.5	217	0.0880	0.7420	4.410	8.1
134.5	73.5	155	0.0876	0.6254	4.170	6.8
143	72	83	0.0894	0.5226	3.840	5.63
153	72	69	0.0920	0.4440	3.560	4.73
168	73.5	48	0.0960	0.3640	3.288	3.86
180.5	75.5	29	0.0997	0.3153	2.850	3.28
192	71	17	0.1019	0.2550	2.462	2.63
205	71	12	0.1055	0.2185	2.150	2.22
225	73	8	0.1120	0.1720	1.856	1.72
240	73.5	5	0.1160	0.1450	1.460	1.44
261	74	3	0.1235	0.1120	1.038	1.09

iii. The following is a typical interferogram and the method used in evaluating

(a) the plate temperature - T_w -

(b) the local heat transfer by convection

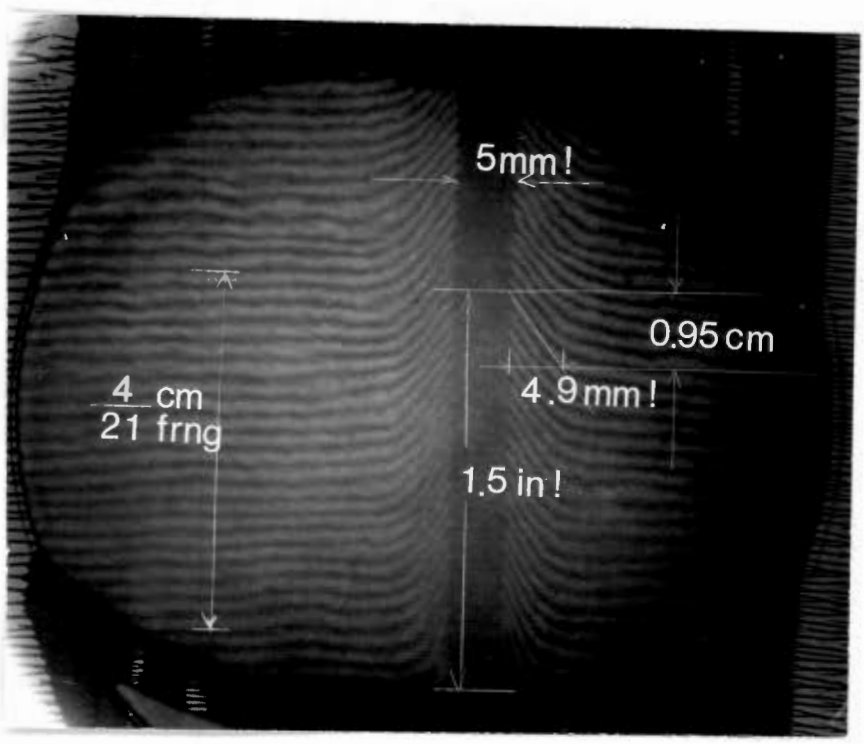

Typical Interferogram.

Note: The values without (!) do not need correction for the magnification of the photo -

Data relating to the above interferogram

P_∞ = 757 mm Hg

T_∞ = 21°C

T_∞ wet bulb = 16° C

Plate L = 10.15 cm

λ = 5 482°A (green light)

T_w (thermocouple) (copper const.) 2.167 mv = 53$^+$ °C.

x = 1.5 inches.

(a) From [27] for the above conditions the refractive index of air n, is 1.00033065

From the interferogram ΔN (fringe shift) is evaluated dividing the distance that a fringe has shifted by the fringe spacing (see photograph).

$\frac{4}{21}$ / .....

$$\frac{4}{21} = .19 \frac{cm}{fringe} \qquad \therefore \Delta N \frac{.95}{.19} = 5.0$$

Using equation (5.2)

$$\Delta T = \frac{(273 + 21)\ 5}{(1.85 \times 10^{5})(.33065) \times 10^{-3}-5} = 32^{o}C.$$

$\therefore T_w$ 21 + 32 = 53°C

which checks with the thermocouple reading.

(b) Using the conduction equation

$$q = -k\frac{dT}{dy}$$

where k, the thermal conductivity, is evaluated at the wall temperature $k_{127^{o}F}$ = 0.01560 Btu/hr ft °F

and $\frac{dT}{dy}$ evaluated from the interferogram

$$\frac{dT}{dy} = \frac{32}{49} \frac{^{o}C}{mm} = \frac{56.5}{0.01605} \frac{^{o}F}{ft}$$

$$q = (0.01560 \times \frac{56.5}{0.01605} = 54.9 \text{ Btu/hr ft}^2$$

$$h = \frac{54.9}{56.5} = .97 \frac{Btu}{hr\ ft^2\ ^{o}F}$$

Checking the above, using equation (2.12)

$$h = \frac{k}{x}\ 0.376\ Gr_x^{\frac{1}{4}}$$

$T_f = 99^{o}F$, $\mu = 1.27 \times 10^{-5}$, k = 0.0150, x = .125 ft.

$Gr_x = 21.0 \times 10^{4}$.

$$h = \frac{0.0150}{.125} \times 0.376\ (21.0 \times 10^{4})^{\frac{1}{4}} = 0.968 \frac{Btu}{hr\ ft^2\ ^{o}F}$$

which checks with the previous calculated value.

REFERENCES / .....

REFERENCES.

1. F. KREITH.
"Principles of Heat Transfer". International Textbook Co. 1965 pg. 335.

2. H. SCHLICHTING.
"Boundary Layer Theory". McGraw Hill Co. 1960 pg. 334.

3. L.M.K. BOELTER and OTHERS.
"Heat Transfer Notes". McGraw Hill Co. 1964 pg. 494.

4. K.T. YANG and E.W. JERGER.
"First order Perturbations of Laminar Free-Convection Boundary Layers on a Vertical Plate". J. Heat Transfer 86, 1964 pg. 107.

5. F.J. SURIANO, K.T. YANG and J.A. DONLON.
"Laminar Free Convection Along a Vertical Plate of Extremely Small Grashof Numbers". Int. J. Heat and Mass Transfer 8, 1965 pg. 815.

6. F.J. SURIANO and K.T. YANG.
"Laminar Free Convection about Vertical and Horizontal Plates at Small and Moderate Grashof Numbers". Int. J. Heat and Mass Transfer, 11, 1968 pg. 473.

7. O.A. SAUNDERS.
"The Effects of Pressure upon Natural Convection in Air". Proc. Roy. Soc. 157, 1936 pg. 278.

8. E. POHLHAUSEN.
"Der Wärmeaustausch zwischen festen Körpern und Flüssigkeiten mit kleiner Reibung und kleiner Wärmeleitung. ZAMM 1, 1921 pg. 115.

9. E.SCHMIDT and W. BECKMANN.
"Das Temperatur- und Geschwindigkeitsfeld von einer wärme-abgebenden senkrechten Platte bei natürlicher Konvektion" Tech. Mech. u. Thermodynamik Bd. 1 Nr. 10, 1930 pg. 341; cont. Bd. 1, Nr. 11, 1930 pg. 391.

10. E.M. SPARROW/ .....

10. E.M. SPARROW and J.L. GREGG.
"Laminar Free Convection from a Vertical Plate with Uniform Surface Heat Flux." Trans. ASME, 78 1956, pg. 435.

11. E.M. SPARROW and J.L. GREGG.
"The Variable Fluid-Property Problem in Free Convection." Trans. ASME, 80, 1958 pg. 879.

12. J.J. MAHONEY
"Heat Transfer at Small Grashof Numbers." Proc. Roy. Soc. A238, 1956, pg. 412.

13. P.H. OOSTHUIZEN
"The Effect of Surface Slip on Laminar Free-Convection Heat Transfer from an Isothermal Vertical Plate." Appl. Sci. Res. 16, 1965 pg. 121.

14. W.T. KIERKUS.
"An Analysis of Laminar Free Convection Flow and Heat Transfer about an inclined isothermal Plate." Int. J. Heat and Mass Transfer, 11, 1968, pg. 241.

15. R.J. GOLDSTEIN and E.R.G. ECKERT.
"The Steady and Transient Free Convection Boundary Layer on a uniformly heated Vertical Plate." Int. J. Heat and Mass Transfer 1, 1960, pg. 208.

16. A.K. REBROV and N.V. MUKHINA.
"The Natural Convection Boundary Layer in Rarefied Gas". Int. J. Heat and Mass Transfer, 9, 1966, pg. 822.

17. R. CHEESWRIGHT.
"Turbulent Natural Convection from a Vertical Plane Surface". J. Heat Transfer. 90, 1968, pg. 1.

18. K. BRODOWICZ.
"An Analysis of Laminar Free Convection around Isothermal Vertical Plate". Int. J. Heat and Mass Transfer, 11, 1968, pg. 201.

19. Th. von KÁRMÁN.
"Über laminare und turbulente Reibung". ZAMM 1, 1921 pg. 233.

20. J. GRYZAGORIDIS/ .....

20. J. GRYZAGORIDIS.
"A note on the Thermal Boundary Layer thickness in Free Convection". Bull, Mech. Engng. Educ. 9, 1970, pg. 141.

21. J.P. HOLMAN.
"Heat Transfer" McGraw Hill Co. 1968, pg. 134.

22. E.M. SPARROW & J.L. GREGG.
"Similar Solutions for Free-Convection from a Non-isothermal Vertical Plate". Trans. ASME, 80, 1958 pg. 379.

23. S. CHANDRASEKHAR.
"Stochastic Problems in Physics and Astronomy" Reviews of Modern Physics. 15, 1943.

24. LEEDS AND NORTRUP CO.
"Conversion Tables for Thermocouples" - 007789 pg. 18-20.

25. J.A. WIEBELT.
"Engineering Radiation Heat Transfer" Holt Rinehart and Winston Inc. 1966 pg. 213.

26. S.T. HSU.
"Engineering Heat Transfer" van Nostrand 1963, pg. 583.

27. NATIONAL PHYSICAL LABORATORY.
"The Refractive Index of Air for Radio Waves and Microwaves" Dept. of Scientific Research (65498).

28. M.G. SCHERBERG.
"Natural Convection near and above thermal leading edges on Vertical Walls". Int. J. Heat Mass Transfer., 5, 1962 pg. 1001.

29. J. GRYZAGORIDIS.
"Natural Convection from a vertical flat plate in the low Grashof number range". Int. J. Heat and Mass Transfer, 14, 1971, pg. 162.

30. J. GRYZAGORIDIS.
"Leading Edge Effects on the Nusselt number for a vertical Plate in Free-Convection". To be published in the Int. J. Heat and Mass Transfer. (Accepted for publication in June 1972)

31.NATIONAL/ .....

31. NATIONAL BUREAU OF STANDARDS.
"Tables of Thermal Properties of Gases". Circular No. 564 November, 1955.

32. H. HANSEN.
"Neue Gleichungen für die Wärmeübertragung bei freier oder erzwungener Strömung". Allg. Warmetech 9, 75, 1959.

33 H.W. McADAMS.
"Heat Transmission". Third edition. Chapt. 7. McGraw Hill New York, 1954.

34. M. JAKOB.
"Heat Transfer". Chapt. 25, Willey New York 1949.

Reprinted from

International Journal of Heat and Mass Transfer

PERGAMON PRESS
OXFORD NEW YORK LONDON PARIS

LEADING EDGE EFFECTS ON THE NUSSELT NUMBER FOR A VERTICAL PLATE IN FREE CONVECTION

J. GRYZAGORIDIS

Mechanical Engineering Department, University of Cape Town, Cape Town, S. Africa

(*Received* 8 *December* 1971 *and in revised form* 12 *June* 1972)

NOMENCLATURE

- C_p, specific heat of the fluid;
- g, acceleration due to gravity;
- Gr_x, local Grashof number $\rho^2\beta g(T_w - T_\infty)x^3/\mu^2$;
- h, free convective coefficient;
- k, thermal conductivity of the fluid;
- L, width of the plate;
- Nu_x, local Nusselt number $h_x x/k$;
- Pr, Prandtl number $C_p\mu/k$;
- q, heat transfer per unit area;
- T, temperature;
- ΔT, temperature difference;
- ΔN, fringe shift;
- n, refractive index of fluid;
- x, distance along the length of the plate;
- y, distance perpendicular to the plate.

Greek symbols

- β, coefficient of thermal expansion of the fluid;
- λ, wavelength of light;
- μ, absolute viscosity of the fluid;
- ρ, density of the fluid.

Subscripts

- w, wall conditions;
- ∞, undisturbed fluid;
- L, based on overall height of the plate.

INTRODUCTION

It is to be expected that the classical boundary layer solution by Schmidt and Beckmann [1] for local heat transfer rates from a vertical plate in free convection

$$Nu_x = 0{\cdot}360\,(Gr_x)^{\frac{1}{4}} \tag{1}$$

and the integral method by Eckert and Drake [2] which yielded

$$Nu_x = 0{\cdot}378\,(Gr_x)^{\frac{1}{4}} \tag{2}$$

are not adequate to explain the phenomenon of free convection from a vertical plate, near the leading edge, since they do not account for the flow that starts ahead of the plate which some investigators call induced flow.

Previous papers by Suriano and Yang [3], Yang and Jerger [4], and Suriano Young and Donlon [5], have dealt with this aspect using perturbation techniques or finite difference schemes and they have shown departure from the classical solution approximately below $Gr \simeq 10^3$.

More recently Cheesewright [6], has shown experimental results in agreement with the classical solution as low as $Gr_x = 10^3$. The author [7], has shown that when average heat transfer rates are calculated, the empirical power law relationship

$$Nu_L = 0{\cdot}555\,(Gr_L Pr)^{\frac{1}{4}} \tag{3}$$

holds as low as $Gr \simeq 10$, the reason being that the leading edge effects which take place in a relatively small percentage of the boundary layer exhibited around the whole plate, are lost in the integration over the entire length of the plate. It appears that detailed experimental data near the leading edge of a vertical plate are very much needed as far as local values are concerned.

Heat and Mass MS 179 327-8-9 IC 6-7-72 C-CH
(F11)

EXPERIMENTAL TECHNIQUE

In order to obtain local Nusselt numbers near the leading edge of a verical plate, the author constructed a 10 cm field Mach Zehnder Interferometer, where an electrically heated plate, having the dimensions: 6·35 cm height, 10·15 cm width, 0·5 cm thickness, was placed for observation. From the interferograms taken local Nusselt numbers were evaluated using the following technique.

The interferometer was adjusted for wedge fringes field and when steady state conditions were established for the plate, a photographic record was taken. The temperature of the plate was evaluated using the following equation which relates the fluid temperature change ΔT to the fringe shift ΔN, length of the model L, wavelength of light λ, refractive index of air n, and the undisturbed fluid temperature T_∞.

$$\Delta T = \frac{T_\infty \Delta N}{(L/\lambda)(n-1) - \Delta N}. \tag{4}$$

As a check measure the plate was equipped with six thermocouples spaced 1·0 cm apart from the leading edge. In each case the temperature of the plate calculated from equation (4) was identical to the one indicated by the corresponding thermocouple. With the wedge fringes oriented perpendicular to the plate, the plate temperature was indicated by the displacement of the fringe from its initial undisturbed position to where it met the surface. The slope of the fringe near the surface is directly related to the heat loss from the surface by convection thus there is no need to account for radiation losses, and since the plate was suspended by thin wires there were negligible conduction losses. The heat flow from the surface was calculated using the conduction equation

$$q = -k \left.\frac{\mathrm{d}T}{\mathrm{d}y}\right|_{y=0}. \tag{5}$$

The values of the temperature gradients at the surface were obtained from the interferograms for any desired distance from the leading edge and the thermal conductivity of the fluid was evaluated at the surface temperature.

The heat loss from a surface by convection is usually expressed by the relation,

$$q = h_c(T_w - T_\infty) \tag{6}$$

and from the above the local free convective coefficients were evaluated and subsequently the local Nusselt numbers. The corresponding Grashof numbers were evaluated at the film temperature,

$$T_f = \frac{T_w + T_\infty}{2}. \tag{7}$$

DISCUSSION

The results of this investigation show excellent agreement with equations (1) and (2) away from the leading edge, i.e. at high Grashof numbers, and confirm previous data reported by Cheesewright [6]. However as expected, the results show conclusively that the range of applicability of boundary layer concepts, as far as *local* values are concerned, is for Grashof numbers greater than 10^4. In Fig. 1 it is seen that below $Gr_x \simeq 5 \times 10^3$ there is a marked departure from the accepted expressions thus showing that the *local* Grashof-Nusselt number relationship is not universal at low Grashof numbers obtained by decreasing coordinate along the plate toward the leading edge.

When performing experiments on a vertical plate in air, for all practical purposes low Grashof numbers may be obtained, by small ΔT's, reduced densities, or using small plates. With the first two methods i.e. $\Delta T \to 0$ and $\rho \to 0$, the convection currents decay thus approaching the pure conduction limit, however when small Grashof numbers are approached by decreasing coordinate toward the leading edge, the pure conduction limit is not approached, the reason being that the boundary layer starts ahead of the leading edge.

The author has reported data in [7] for *average* heat transfer values for similar size plates with the one used in the present investigation, obtained by letting $\rho \to 0$, showing that the accepted power law relationship

$$\overline{Nu}_L = 0{\cdot}555\,(\overline{Gr}_L Pr)^{\frac{1}{4}}$$

is adequate for the range of Grashof numbers between 10 and 10^8. For *average* values the leading edge effects which take place in a relatively small percentage of the plate are not significant because they are lost in the integration process.

In the past, investigators have recognized the need of refining the boundary layer solution in order to describe the phenomenon more accurately in the region of finite Grashof numbers. To the knowledge of this writer the first

attempt was presented by Yang and Jerger [4]. Their results however are in variance with the data reported in this investigation. This is because, in their first order perturbation analysis, they have failed to take into account the leading edge effects. It appears that these are quite significant, and they are mainly due to the induced flow ahead of the leading edge.

Suriano Yang and Donlon [5] presented a paper where they have shown that the corrections on the boundary layer values due to the leading edge effects are much more significant than due to the boundary layer perturbations. Unfortunately their results are presented as average values starting about $Gr_L = 10^4$ and do not permit direct comparison with the present data, reported in Fig. 1, however they do indicate similar departure from the accepted solution.

An interesting fact comes to light examining the points of departure in Fig. 1. The departure occured at approximately the same distance from the leading edge (12·7 mm), but due to different temperature differences, at different Grashof numbers. In other words as the overall temperature difference ΔT, decreased for the same distance from the leading edge, the Grashof number became smaller and the agreement with the theory was extended!

The exact mechanism of how the flow starts ahead of the leading edge is not known, however professor Gebhart's discussion in [4] on the behavior of the flow in the immediate neighborhood of the leading edge is well taken and worthwhile quoting here. "This flow is induced by lower pressures which are found near the leading edge due to the presence of the normal component of velocity v_∞ resulting from the buoyancy induced flow. Since v_∞ decreases toward zero with increasing x, the pressure outside the boundary region (excepting hydrostatic effects) increases with x toward the limiting value in the completely undisturbed fluid, say p_∞, thus inducing a flow field outside of the boundary region."

Bearing in mind the above mentioned the tendency of the author's data to agree with the theory at lower temperature differences may be explained. Because the temperature differences are smaller, the buoyancy induced flow is less, and consequently the effects of the induced flow ahead of the leading edge are reduced. It appears from the data reported here, that there is a surprising influence of the temperature difference on the Nusselt number for fixed Grashof numbers, in the region below 5×10^3. This to the knowledge of the author is new data which lead to a new set of questions. If the temperature difference is a new parameter as shown in Fig. 1, then there must be a dimensionless parameter associated with this temperature difference. What could that be? Can this parameter be extracted out of the complete differential equations? In the table below some of the experimental data is provided so that interested readers may draw their own conclusions.

Table 1.

x, mm	Nu_x	Gr_x	ΔT, °C
25·4	4·8	$2{\cdot}98 \times 10^4$	14·0
12·7	3·1	$3{\cdot}72 \times 10^3$	14·0
8·75	2·66	$1{\cdot}2 \times 10^3$	14·0
4·60	2·22	$1{\cdot}66 \times 10^2$	14·0
12·7	3·2	$5{\cdot}2 \times 10^3$	19·5
11·1	2·95	$2{\cdot}76 \times 10^3$	19·5
6·8	2·77	$8{\cdot}0 \times 10^2$	19·5
3·95	2·62	$1{\cdot}58 \times 10^2$	19·5
12·7	3·5	$6{\cdot}46 \times 10^3$	25·8
8·75	3·1	$2{\cdot}1 \times 10^3$	25·8
4·75	2·82	$3{\cdot}42 \times 10^2$	25·8

REFERENCES

1. E. SCHMIDT and W. BECKMANN. Das temperature und geschwindigkeitsfeld von einer warme abgebenden senkrechten platte bei naturlicher konvection. *Tech. Mech. Thermodynamik* **1**. 341 (1930).
2. E. R. G. ECKERT and R. M. DRAKE. *Heat and Mass Transfer*. 315 pp. McGraw-Hill. New York (1959).
3. F. J. SURIANO and K. T. YANG. Laminar free convection about vertical and horizontal plates at small and moderate Grashof numbers. *Int. J. Heat Mass Transfer* **11**. 473 (1968).
4. K. T. YANG and E. W. JERGER. First order perturbations of laminar frec convection boundary layers on a vertical plate. *J. Heat Transfer* **86**. 107 (1964).
5. F. J. SURIANO, K. T. YANG and J. A. DONLON. Laminar free convection along a vertical plate of extremely small Grashof numbers. *Int. J. Heat Mass Transfer* **8**. 815 (1965).
6. R. CHEESEWRIGHT. Turbulent natural convection from a vertical plane surface. *J. Heat Transfer* **90**. 1 (1968).
7. J. GRYZAGORIDIS. Natural convection from a verical flat plate in the low Grashof number range. *Int. J. Heat Mass Transfer* **14**. 162 (1971).

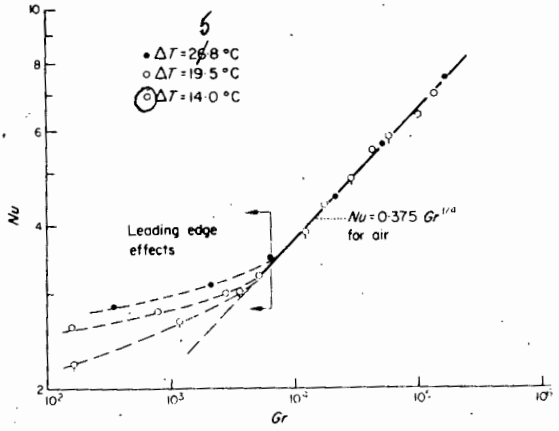

FIG. 1. Local heat transfer rates from a vertical plate in free convection showing the effects of leading edge.

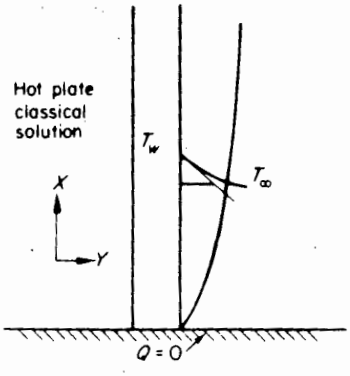

FIG. 2.

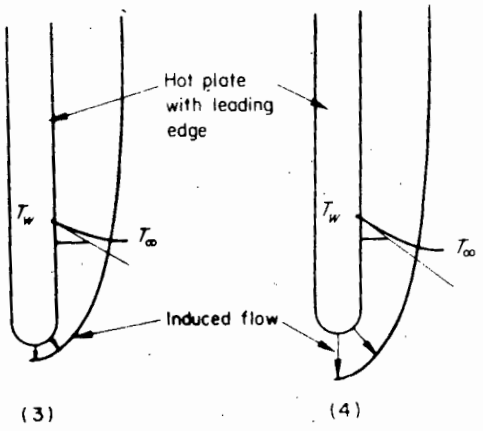

FIG. 3.

FIG. 4.

Reprinted from

International Journal of Heat and Mass Transfer

PERGAMON PRESS
OXFORD NEW YORK LONDON PARIS

LEADING EDGE EFFECTS ON THE NUSSELT NUMBER FOR A VERTICAL PLATE IN FREE CONVECTION

J. GRYZAGORIDIS

Mechanical Engineering Department, University of Cape Town, Cape Town, S. Africa

(*Received* 8 *December* 1971 *and in revised form* 12 *June* 1972)

NOMENCLATURE

C_p, specific heat of the fluid;
g, acceleration due to gravity;
Gr_x, local Grashof number $\rho^2\beta g(T_w - T_\infty)x^3/\mu^2$;
h, free convective coefficient;
k, thermal conductivity of the fluid;
L, width of the plate;
Nu_x, local Nusselt number $h_c x/k$;
Pr, Prandtl number $C_p\mu/k$;
q, heat transfer per unit area;
T, temperature;
ΔT, temperature difference;
ΔN, fringe shift;
n, refractive index of fluid;
x, distance along the length of the plate;
y, distance perpendicular to the plate.

Greek symbols

β, coefficient of thermal expansion of the fluid;
λ, wavelength of light;
μ, absolute viscosity of the fluid;
ρ, density of the fluid.

Subscripts

w, wall conditions;
∞, undisturbed fluid;
L, based on overall height of the plate.

INTRODUCTION

It is to be expected that the classical boundary layer solution by Schmidt and Beckmann [1] for local heat transfer rates from a vertical plate in free convection

$$Nu_x = 0{\cdot}360\,(Gr_x)^{\frac{1}{4}} \tag{1}$$

and the integral method by Eckert and Drake [2] which yielded

$$Nu_x = 0{\cdot}378\,(Gr_x)^{\frac{1}{4}} \tag{2}$$

are not adequate to explain the phenomenon of free convection from a vertical plate, near the leading edge, since they do not account for the flow that starts ahead of the plate which some investigators call induced flow.

Previous papers by Suriano and Yang [3], Yang and Jerger [4], and Suriano Young and Donlon [5], have dealt with this aspect using perturbation techniques or finite difference schemes and they have shown departure from the classical solution approximately below $Gr \simeq 10^3$.

More recently Cheesewright [6], has shown experimental results in agreement with the classical solution as low as $Gr_x = 10^3$. The author [7], has shown that when average heat transfer rates are calculated, the empirical power law relationship

$$Nu_L = 0{\cdot}555\,(Gr_L Pr)^{\frac{1}{4}} \tag{3}$$

holds as low as $Gr \simeq 10$, the reason being that the leading edge effects which take place in a relatively small percentage of the boundary layer exhibited around the whole plate, are lost in the integration over the entire length of the plate. It appears that detailed experimental data near the leading edge of a vertical plate are very much needed as far as local values are concerned.

Heat and Mass MS 179 327-8 9 1C 6 7 72 C-CH
(F11)

EXPERIMENTAL TECHNIQUE

In order to obtain local Nusselt numbers near the leading edge of a verical plate, the author constructed a 10 cm field Mach Zehnder Interferometer, where an electrically heated plate, having the dimensions: 6·35 cm height, 10·15 cm width, 0·5 cm thickness, was placed for observation. From the interferograms taken local Nusselt numbers were evaluated using the following technique.

The interferometer was adjusted for wedge fringes field and when steady state conditions were established for the plate, a photographic record was taken. The temperature of the plate was evaluated using the following equation which relates the fluid temperature change ΔT to the fringe shift ΔN, length of the model L, wavelength of light λ, refractive index of air n, and the undisturbed fluid temperature T_∞,

$$\Delta T = \frac{T_\infty \Delta N}{(L/\lambda)(n-1) - \Delta N}. \tag{4}$$

As a check measure the plate was equipped with six thermocouples spaced 1·0 cm apart from the leading edge. In each case the temperature of the plate calculated from equation (4) was identical to the one indicated by the corresponding thermocouple. With the wedge fringes oriented perpendicular to the plate, the plate temperature was indicated by the displacement of the fringe from its initial undisturbed position to where it met the surface. The slope of the fringe near the surface is directly related to the heat loss from the surface by convection thus there is no need to account for radiation losses, and since the plate was suspended by thin wires there were negligible conduction losses. The heat flow from the surface was calculated using the conduction equation

$$q = -k \left.\frac{\mathrm{d}T}{\mathrm{d}y}\right|_{y=0}. \tag{5}$$

The values of the temperature gradients at the surface were obtained from the interferograms for any desired distance from the leading edge and the thermal conductivity of the fluid was evaluated at the surface temperature.

The heat loss from a surface by convection is usually expressed by the relation,

$$q = h_c(T_w - T_\infty) \tag{6}$$

and from the above the local free convective coefficients were evaluated and subsequently the local Nusselt numbers. The corresponding Grashof numbers were evaluated at the film temperature,

$$T_f = \frac{T_w + T_\infty}{2}. \tag{7}$$

DISCUSSION

The results of this investigation show excellent agreement with equations (1) and (2) away from the leading edge, i.e. at high Grashof numbers, and confirm previous data reported by Cheesewright [6]. However as expected, the results show conclusively that the range of applicability of boundary layer concepts, as far as *local* values are concerned, is for Grashof numbers greater than 10^4. In Fig. 1 it is seen that below $Gr_x \simeq 5 \times 10^3$ there is a marked departure from the accepted expressions thus showing that the *local* Grashof-Nusselt number relationship is not universal at low Grashof numbers obtained by decreasing coordinate along the plate toward the leading edge.

When performing experiments on a vertical plate in air, for all practical purposes low Grashof numbers may be obtained, by small ΔT's, reduced densities, or using small plates. With the first two methods i.e. $\Delta T \to 0$ and $\rho \to 0$, the convection currents decay thus approaching the pure conduction limit, however when small Grashof numbers are approached by decreasing coordinate toward the leading edge, the pure conduction limit is not approached, the reason being that the boundary layer starts ahead of the leading edge.

The author has reported data in [7] for *average* heat transfer values for similar size plates with the one used in the present investigation, obtained by letting $\rho \to 0$, showing that the accepted power law relationship

$$Nu_L = 0{\cdot}555\,(Gr_L Pr)^{\frac{1}{4}}$$

is adequate for the range of Grashof numbers between 10 and 10^8. For *average* values the leading edge effects which take place in a relatively small percentage of the plate are not significant because they are lost in the integration process.

In the past, investigators have recognized the need of refining the boundary layer solution in order to describe the phenomenon more accurately in the region of finite Grashof numbers. To the knowledge of this writer the first

attempt was presented by Yang and Jerger [4]. Their results however are in variance with the data reported in this investigation. This is because, in their first order perturbation analysis, they have failed to take into account the leading edge effects. It appears that these are quite significant, and they are mainly due to the induced flow ahead of the leading edge.

Suriano Yang and Donlon [5] presented a paper where they have shown that the corrections on the boundary layer values due to the leading edge effects are much more significant than due to the boundary layer perturbations. Unfortunately their results are presented as average values starting about $Gr_L = 10^4$ and do not permit direct comparison with the present data, reported in Fig. 1, however they do indicate similar departure from the accepted solution.

An interesting fact comes to light examining the points of departure in Fig. 1. The departure occured at approximately the same distance from the leading edge (12·7 mm), but due to different temperature differences, at different Grashof numbers. In other words as the overall temperature difference ΔT, decreased for the same distance from the leading edge, the Grashof number became smaller and the agreement with the theory was extended!

The exact mechanism of how the flow starts ahead of the leading edge is not known, however professor Gebhart's discussion in [4] on the behavior of the flow in the immediate neighborhood of the leading edge is well taken and worthwhile quoting here. "This flow is induced by lower pressures which are found near the leading edge due to the presence of the normal component of velocity v_∞ resulting from the buoyancy induced flow. Since v_∞ decreases toward zero with increasing x, the pressure outside the boundary region (excepting hydrostatic effects) increases with x toward the limiting value in the completely undisturbed fluid, say p_∞, thus inducing a flow field outside of the boundary region."

Bearing in mind the above mentioned the tendency of the author's data to agree with the theory at lower temperature differences may be explained. Because the temperature differences are smaller, the buoyancy induced flow is less, and consequently the effects of the induced flow ahead of the leading edge are reduced. It appears from the data reported here, that there is a surprising influence of the temperature difference on the Nusselt number for fixed Grashof numbers, in the region below 5×10^3. This to the knowledge of the author is new data which lead to a new set of questions. If the temperature difference is a new parameter as shown in Fig. 1, then there must be a dimensionless parameter associated with this temperature difference. What could that be? Can this parameter be extracted out of the complete differential equations? In the table below some of the experimental data is provided so that interested readers may draw their own conclusions.

Table 1.

x, mm	Nu_x	Gr_x	ΔT, °C
25·4	4·8	$2{\cdot}98 \times 10^4$	14·0
12·7	3·1	$3{\cdot}72 \times 10^3$	14·0
8·75	2·66	$1{\cdot}2 \times 10^3$	14·0
4·60	2·22	$1{\cdot}66 \times 10^2$	14·0
12·7	3·2	$5{\cdot}2 \times 10^3$	19·5
11·1	2·95	$2{\cdot}76 \times 10^3$	19·5
6·8	2·77	$8{\cdot}0 \times 10^2$	19·5
3·95	2·62	$1{\cdot}58 \times 10^2$	19·5
12·7	3·5	$6{\cdot}46 \times 10^3$	25·8
8·75	3·1	$2{\cdot}1 \times 10^3$	25·8
4·75	2·82	$3{\cdot}42 \times 10^2$	25·8

REFERENCES

1. E. Schmidt and W. Beckmann. Das temperature und geschwindigkeitsfeld von einer warme abgebenden senkrechten platte bei naturlicher konvection. *Tech. Mech. Thermodynamik* **1**, 341 (1930).
2. E. R. G. Eckert and R. M. Drake. *Heat and Mass Transfer*. 315 pp. McGraw-Hill, New York (1959).
3. F. J. Suriano and K. T. Yang. Laminar free convection about vertical and horizontal plates at small and moderate Grashof numbers. *Int. J. Heat Mass Transfer* **11**, 473 (1968).
4. K. T. Yang and E. W. Jerger. First order perturbations of laminar free convection boundary layers on a vertical plate. *J. Heat Transfer* **86**, 107 (1964).
5. F. J. Suriano, K. T. Yang and J. A. Donlon. Laminar free convection along a vertical plate of extremely small Grashof numbers. *Int. J. Heat Mass Transfer* **8**, 815 (1965).
6. R. Cheesewright. Turbulent natural convection from a vertical plane surface. *J. Heat Transfer* **90**, 1 (1968).
7. J. Gryzagoridis. Natural convection from a verical flat plate in the low Grashof number range. *Int. J. Heat Mass Transfer* **14**, 162 (1971).

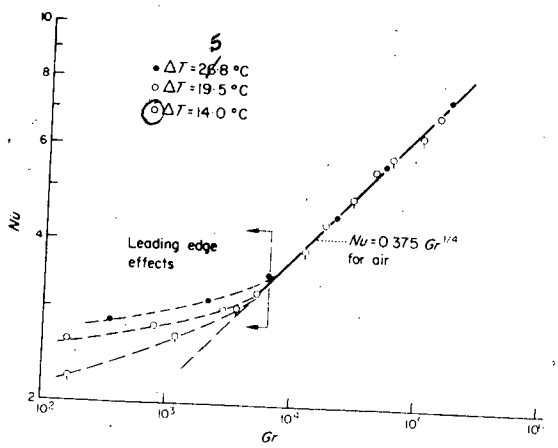

FIG. 1. Local heat transfer rates from a vertical plate in free convection showing the effects of leading edge.

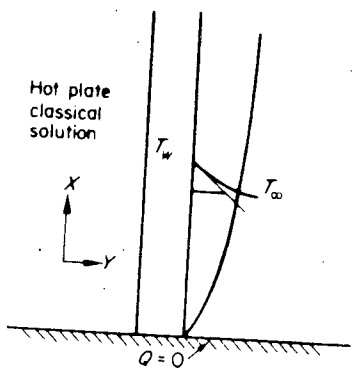

FIG. 2.

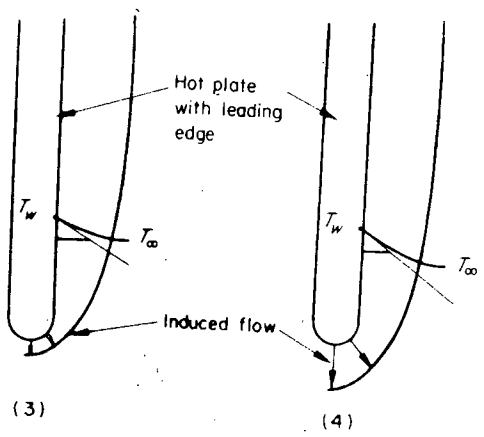

FIG. 3.

FIG. 4.